Synthetic Studies on Palladium-Catalyzed Olefin Dioxygenation, Indole Functionalization, and Helical Ligands

by

Marija Antonic

A thesis submitted in conformity with the requirements
for the degree of Masters of Science

Department of Chemistry
University of Toronto

Your file Votre référence
ISBN: 978-0-494-59280-9
Our file Notre référence
ISBN: 978-0-494-59280-9

Synthetic Studies on Palladium-Catalyzed Olefin Dioxygenation, Indole Functionalization, and Helical Ligands

Marija Antonic

Masters of Science

Department of Chemistry
University of Toronto

2009

Abstract

Palladium-catalyzed olefin dioxygenation is a powerful tool in the generation of complex and valuable substrates, one which may become complimentary to the well known Sharpless dihydroxylation. In this work the mechanism of this transformation is examined via reaction kinetics and Hammett studies, which corroborate a $Pd^{II/IV}$ catalytic cycle and suggest that the rate determining step is the oxidation of Pd^{II} to Pd^{IV}. Olefin dioxygenation was also found to proceed in the presence of catalytic quantities of BF_3•OEt_2 or triflic acid, with stoichiometric hypervalent iodine oxidant and an acetic acid solvent. Furthermore, asymmetric variants of intramolecular palladium-catalyzed olefin dioxygenation were also investigated, which resulted in the formation of tetrahydrofuran products in up to 36% ee.

Next, chelate-assisted C–H bond functionalization of indoles at the C7 position and of carbazoles at the C1 position was investigated with a variety of arylation, halogenation and oxygenation techniques. Lastly, our efforts towards the synthesis of a mono-phosphine based [5]helicene ligand via olefin metathesis and photocyclization strategies will be discussed.

Acknowledgments

This thesis is a direct product of the guidance and support that I received from my supervisor, Prof. Vy Dong. I would like to thank her for allowing me to join her research group and for giving me the opportunity to expand my knowledge and challenge myself as a chemist.

I am also indebted to Dr. Yang Li who initiated the olefin dioxygenation project and was an unforgettable mentor. Also, a sincere thank you goes to Prof. Datong Song for his helpful insight. To Peter Dornan: you will forever remain of my chemistry heroes; thank you for collaborating and sharing your knowledge with me.

To the entire Dong group, thank you for the laughs, discussions, and many memories – you will be terribly missed. More specifically, I would like to acknowledge Tom Hsieh, Thi Phan, Boni Kim, and Wilmer Alkhas for always keeping a smile on my face.

Lastly, to my friends, Antonic family, and Dilliott family, thank you for your constant encouragement and faith. Most importantly, to the two people that none of this would have happened without: Michael Dilliott and Elena Dimitrijević; to you I owe more than the world itself and I love you.

Table of Contents

Acknowledgments iii

Table of Contents iv

List of Abbreviations viii

List of Tables xi

List of Schemes xii

List of Figures xiii

Chapter 1 Palladium-Catalyzed Olefin Dioxygenation 1

1.1 Introduction 1

1.1.1 Olefin Dioxygenation via Osmium Catalysis 1

1.1.2 Vicinal Olefin Oxidations via Palladium Catalysis 1

1.1.3 $Pd^{II/IV}$ Catalyst Cycles 4

1.1.4 Enantioselective $Pd^{II/IV}$ Catalyst Cycles 6

1.1.5 Palladium-Catalyzed Olefin Dioxygenation 6

1.1.5.1 Intermolecular Palladium-Catalyzed Olefin Dioxygenation 8

1.1.5.2 Intramolecular Palladium-Catalyzed Olefin Dioxygenation 9

1.1.5.3 Recent Advances in Palladium-Catalyzed Olefin Dioxygenation 10

1.1.6 Research Goals 11

1.2 Results and Discussion 12

1.2.1 Mechanism of Palladium-Catalyzed Olefin Dioxygenation 12

1.2.1.1 Kinetic Studies 12

1.2.1.2 Hammett Study 16

1.2.1.3 Proposed Catalytic Cycle: A $Pd^{II/IV}$ Mechanism 19

1.2.1.4 Olefin Dioxygenation via Other Modes of Catalysis 21

1.2.1.5 Alternate Mechanistic Proposal for Olefin Dioxygenation 24

1.2.2 Enantioselective Palladium-Catalyzed Olefin Dioxygenation 26

1.3 Conclusion 29

1.4 Experimental Procedures 30

1.4.1 General Experimental 30

1.4.2 Materials 30

1.4.3 Instrumentation 31

1.4.4 Experimental Procedures and Characterizations 31

1.4.4.1 General Procedure for the Synthesis of 1-Phenyl-1-cyclohexanol Derivatives 31

1.4.4.2 General Procedure for the Synthesis of 1-Phenyl-1-cyclohexene Derivatives 34

1.4.4.3 General Procedure for the Synthesis of 1-Phenyl-1-cylohexyl hydroxyacetate Derivatives 37

1.4.4.4 General Procedure for Reaction Kinetics Experiments 41

1.4.4.5 General Procedure for Hammett Plot Kinetic Experiments 41

1.4.4.6 General Procedure for ^{18}O Labelling in the Dioxygenation of 1-Phenyl-1-cyclohexene 42

1.4.4.7 General Procedure for the Synthesis of 5-Arylpent-4-yn-1-ol Derivatives 43

1.4.4.8 General Procedure for the Synthesis of (*E*)-5-Arylpent-4-en-1-ol Derivatives 44

1.4.4.9 General Procedure for Intramolecular Pd-Catalyzed Olefin Dioxygenation 46

Chapter 2 Indole Functionalization 50

2.1 Introduction 50

2.1.1 C–H Bond Activation 50

2.1.2 Chelate-Assisted C–H Bond Activation 50

2.1.2.1 Amide Directed C–H Bond Activation 51

2.1.2.2 Urea Directed C–H Bond Activation 53

2.1.2.3 Directing Group-Assisted C–H Bond Halogenation 53
2.1.2.4 Directing Group-Assisted C–H Bond Oxygenation 54
2.1.3 C–H Bond Activation of Indoles 55
2.1.3.1 Indole C2 C–H Bond Activation 55
2.1.3.2 Indole C3 C–H Bond Activation 57
2.1.3.3 Indole C7 C–H Bond Activation 58
2.1.4 Research Goals 59
2.2 Results and Discussion 60
2.2.1 C–H Activation of the Indole C7 Position 60
2.2.2 C–H Activation of the Carbazole C1 Position 63
2.3 Conclusion 66
2.4 Experimental Procedures 67
2.4.1 General Procedure for the Synthesis of *N*-substituted Indole and Carbazoles 67
2.4.2 General Procedure for the Synthesis of 1-Phenyl-9*H*-carbazole. 70
2.4.3 General Procedure for the Acetoxylation of Carbazole Derivatives 70
Chapter 3 Towards a Phosphine Helical Ligand 72
3.1 Introduction 72
3.1.1 Select Recent Approaches Towards the Synthesis of Racemic [*n*]Helicenes 72
3.1.2 Research Goals 74
3.2 Results and Discussion 76
3.2.1 Approach via Olefin Metathesis 76
3.2.2 Approach via Radical Photocyclization 79
3.3 Conclusion 81
3.4 Experimental Procedures 82
3.4.1 General Procedure for the Synthesis of 1-Bromo-2-(dibromomethyl) naphthalene 82

3.4.2 General Procedure for the Synthesis of 1-Bromo-2-naphthaldehyde 82

3.4.3 General Procedure for the Synthesis of 8-Methoxynaphthalen-1-ol 83

3.4.4 General Procedure for the Synthesis of 1-Hydroxy-8-methoxy-2-naphthaldehyde 84

3.4.5 General Procedure for the Synthesis of 7-Bromo-3,4-dihydronaphthalen-1(2*H*)-one 85

3.4.6 General Procedure for the Synthesis of 7-Bromo-1-methoxynaphthalene 86

3.4.7 General Procedure for the Synthesis of 1-Methoxy-7-(2-(naphthalen-2-yl)vinyl)naphthalene 86

Appendix A. NMR Spectra 88

List of Abbreviations

^{13}C	carbon 13 NMR
^{1}H	proton NMR
^{31}P	phosphorous 31 NMR
BINAP	2,2'-bis(diphenylphosphino)-1,1'-binaphthyl
Bu	butyl
C–H bond	carbon–hydrogen bond
CsOPiv	cesium pivalate
d.r.	diastereomeric ratio
dba	dibenzylideneacetone
DCE	1,2-dichloroethane
DMA	dimethylacetamide
DMAP	4-dimethylaminopyridine
DMF	dimethylformamide
dppp	1,3-bis(diphenylphosphino)propane
ee	enantiomeric excess
EI	electron ionization
ESI	electrospray ionization
Et	ethyl

equiv	equivalent
GC-FID	gas chromatography-flame ionization detector
GC-MS	gas chromatography-mass spectrometry
h	hours
HBPin	pinacolborane
HMPA	hexamethylphosphoramide
HOTf	triflic acid
HPLC	high pressure liquid chromatography
HRMS	high resolution mass spectrometry
Hz	hertz
IMes	*N,N*′-bis(2,4,6-trimethylphenyl)imidazolin-2-ylidene)
IR	infrared spectroscopy
LA	Lewis acid
LiHMDS	lithium hexamethyldisilazide
min	minutes
Me	methyl
MeI	iodomethane
mg	milligrams
mL	millilitres
mmol	millimoles

MS	mass spectrometry
NBS	*N*-bromosuccinimide
n-BuLi	*n*-butyllithium
NCS	*N*-chlorosuccinimide
NMR	nuclear magnetic resonance
PhH	benzene
PhMe	toluene
PivOH	pivalic acid
ppm	parts per million
p-TSA (TsOH)	*p*-toluenesulfonic acid
Py	pyridine
rt	room temperature
Tf_2O	triflic anhydride
TFA	trifluoroacetic acid
THF	tetrahydrofuran
TLC	thin layer chromatography
TMS	trimethylsilane
µL	microlitre
µw	microwave

List of Tables

Table 1. Palladium-catalyzed oxidation of *trans*-stilbene with hypervalent iodine. 7

Table 2. Dioxygenation of 1-(*p*-substituted)phenyl-1-cyclohexene substrates. 17

Table 3. Relative rate of dioxygenation of 1-(*p*-substituted)phenyl-1-cyclohexene substrates.... 18

Table 4. Dihalogenation and(or) haloacetoxylation of styrene. 21

Table 5. Dioxygenation of styrene in the presence of BF_3•OEt_2. 22

Table 6. Triflic acid catalyzed styrene dioxygenation. 24

Table 7. ^{31}P NMR shifts for $[Pd(dppp)(H_2O)_2](OTf)_2$ with various concentrations of $PhI(OAc)_2$ oxidant in acetic acid, where peaks were referenced to phosphoric acid. 26

Table 8. The intramolecular palladium-catalyzed dioxygenation of various substrates including aryl substituted (*E*)-5-phenylpent-4-en-1-ol derivatives. 28

Table 9. Synthesis of *N,N*,2-trimethyl-1*H*-indole-1-carboxamide. 60

Table 10. Examining direct arylation of *N,N*,2-trimethyl-1*H*-indole-1-carboxamide by varying the identity of the base under palladium catalysis. 61

Table 11. Attempts at arylating C7 of *N,N*,2-trimethyl-1*H*-indole-1-carboxamide with published methodologies. 62

Table 12. Attempts at brominating C7 of *N,N*,2-trimethyl-1*H*-indole-1-carboxamide with published methodologies. 63

List of Schemes

Scheme 1. Pd $^{II/IV}$ catalytic cycle proposed by Sanford in chelate-assisted C–H bond oxygenation. 5

Scheme 2. General reaction design for palladium-catalyzed olefin dioxygenation. 7

Scheme 3. Intramolecular palladium-catalyzed oxidative ring-forming examples. 9

Scheme 4. Proposed mechanism for palladium-catalyzed olefin dioxygenation by Chen. 10

Scheme 5. Palladium-catalyzed olefin dioxygenation in the presence of $H_2{}^{18}O$. 15

Scheme 6. Quenching of the acetoxonium ion intermediate by two routes. 15

Scheme 7. Proposed palladium-catalyzed olefin dioxygenation catalytic cycle. 19

Scheme 8. Proposed mechanism for Lewis acid or triflic acid catalyzed olefin. dioxygenation. 24

Scheme 9. [Pd((*R*)-BINAP(μ-OH)$_2$]$_2$(OTf)$_2$ catalyzed cyclization of (*E*)-5-phenylpent-4-en-1-ol to afford two diastereomeric tetrahydrofuran products. 26

Scheme 10. General scheme for chelate-assisted C–H bond functionalization. 51

Scheme 11. Directed metal insertion into the C1 C–H bond of functionalized carbazoles. 64

Scheme 12. Exploring the bromination, arylation and acetoxylation of *N,N*-dimethyl-9*H*-carbazole-9-carboxamide through C–H bond activation strategies. 65

Scheme 13. Proposal for [5]helicene ligand. 75

Scheme 14. Approach towards a helical phosphine ligand with a key olefin metathesis reaction. 76

Scheme 15. Internal H-bond presumed to occur in 1-hydroxy-8-methoxy-2-naphthaldehyde. ... 78

Scheme 16. Approach towards a helical phosphine ligand with a key photocyclization reaction. 79

List of Figures

Figure 1. A. Initial rate reaction kinetics with respect to the olefin substrate concentration. B. Initial rate reaction kinetics with respect to the [Pd(dppp)(H_2O)$_2$](OTf)$_2$ catalyst concentration. 13

Figure 2. A. Initial rate reaction kinetics with respect to the PhI(OAc)$_2$ oxidant concentration. B. Initial rate reaction kinetics with respect to the water concentration. 14

Figure 3. Hammett plot derived from the dioxygenation of 1-(*p*-substituted)phenyl-1-cyclohexene substrates. 18

Chapter 1
Palladium-Catalyzed Olefin Dioxygenation

1.1 Introduction

1.1.1 Olefin Dioxygenation via Osmium Catalysis

In the 1980's the synthesis of dioxygenated substrates was revolutionized with the development of the Sharpless asymmetric dihydroxylation. With this approach, it was possible to take various substituted olefins and upon the treatment with catalytic osmium tetroxide, potassium ferricyanide and a dihydroquinine acetate ligand, both enantiomers of the *syn* dioxygenated products could selectively be accessed (eq 1).[1]

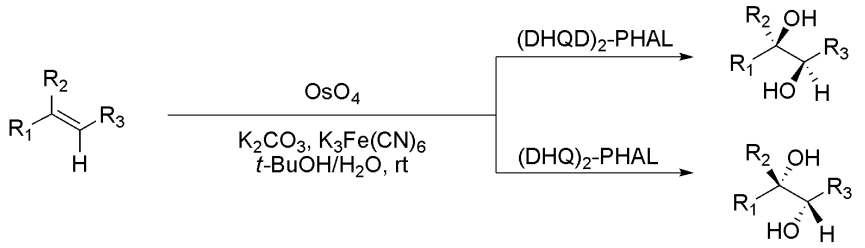

(1)

Advantages for this methodology include a wide substrate scope, high functional group tolerance, and high levels of asymmetric induction. However, in practice, both the toxicity and the high cost of osmium are limitations to this methodology. Since Sharpless' seminal publication, many studies have been undertaken by research groups to continue advancing osmium-catalyzed olefin dioxygenation.[2] On the other hand, work into the development of new catalytic olefin dioxygenation methods has been sparse.

1.1.2 Vicinal Olefin Oxidations via Palladium Catalysis

Palladium-catalyzed vicinal oxidation is an attractive synthetic tool that can be used to transform simple and readily available alkenes into valuable products. In one step, functionalized molecules

---

[1] (a) Jacobsen, E. N.; Marko, I.; Mungall, W. S.; Schroeder, G.; Sharpless, K. B. *J. Am. Chem. Soc.* **1988**, *110*, 1968. (b) Kolb, H. C.; Van Nieuwenhze, M. S.; Sharpless, K. B. *Chem. Rev.* **1994**, *94*, 2483.

[2] For some recent examples see: (a) Jun, B.-H.; Kim, J.-H.; Park, J.; Kang, H.; Lee, S.-H.; Lee, Y.-S. *Synlett* **2008**, 2313. (b) Tang, W.-J.; Yang, N.-F.; Yi, B.; Deng, G.-J.; Huang, Y.-Y.; Fan, Q.-H. *Chem. Commun*. **2004**, *12*, 1378. (c) Huang, Y.; Meng, W.-D.; Qing, F.-L. *Tetrahedron. Lett*. **2004**, *45*, 1965.

can be generated by methods such as diamination, aminooxygenation, and dimethoxylation of olefins.

In one of the first examples published on diamination of alkenes, Muñiz showed the intramolecular reaction of a 1,3-diamine with a pendant olefin to yield a [6,5] fused bicyclic heterocycle (eq 2).[3] This reaction was carried out with a palladium(II) catalyst and in the presence of a strong hypervalent iodide oxidant ($PhI(OAc)_2$).

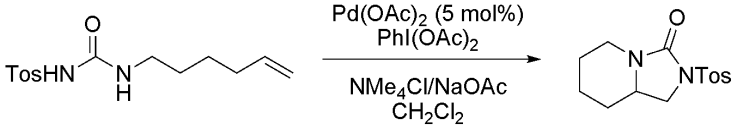

(2)

More recently, the Shi group has published an asymmetric palladium(0)-catalyzed diamination of conjugated dienes and trienes using di-*tert*-butyldiaziridinone as the nitrogen source in their reactions.[4] This transformation is highly regioselective and can produce functionalized substrates in excellent enantioselectivity. Products such as the one shown in eq 3 are potentially valuable intermediates for the synthesis of various optically active diamines and 2,3-diamino acids.

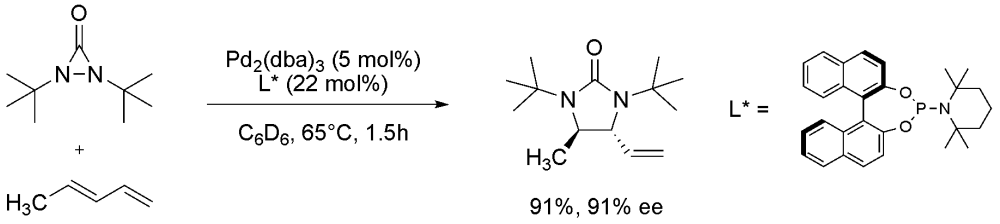

(3)

In addition to diamination, palladium catalysts have been valuable in olefin aminooxygenation. In 2005, Sorensen's group developed an intramolecular aminooxygenation which can furnish five to seven membered aliphatic nitrogen heterocycles from a range of nitrogen nucleophiles and substituted alkenes.[5] This mild, palladium(II)-catalyzed transformation can proceed in high regio- and stereocontrol, making it a useful method in organic synthesis. In eq 4, the cyclization

---

[3] Streuff, J.; Hvelmann, C. H.; Nieger, M.; Muñiz, K. *J. Am. Chem. Soc*. **2005**, *127*, 14586.

[4] Du, H.; Yuan, W.; Zhao, B.; Shi, Y. *J. Am. Chem. Soc.* **2007**, *129*, 11688.

[5] Alexanian, E. J.; Lee, C.; Sorensen, E. J. *J. Am. Chem. Soc*. **2005**, *127*, 7690.

of an amide substrate to the corresponding five-membered lactam is shown. The oxygen heteroatom added across the double bond is in form of an acetate group.

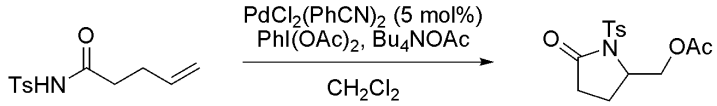

(4)

Similar to Sorensen's work, Stahl showed that intermolecular aminooxygenation was also possible with terminal alkenes (eq 5).[6] Phthalimide was used as the nitrogen nucleophile in all of the reported cases, with particularly good reactivity with allyl ethers due to a presumed chelating effect with the oxygen heteroatom. It is important to note that in both the aminooxygenations developed by Sorensen and Stahl a $Pd^{II/IV}$ catalytic cycle is the proposed reaction mechanism.

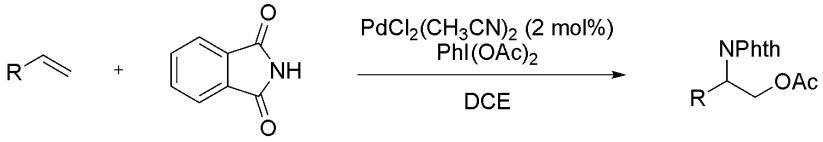

(5)

Another vicinal oxidation process that has garnered some recent interest is the dialkoxylation of olefins. In a few publications, Sigman has shown that the dialkoxylation of styrenes could be carried out in not only in good yield and moderate diastereoselectivity (eq 6),[7] but also with good enantioselectivity.[8] It was found that this methodology was profoundly influenced by an *ortho*-phenol moiety in the reacting substrates, which is hypothesized to prevent *β*-hydride elimination of the catalyst after the initial oxypalladation step.

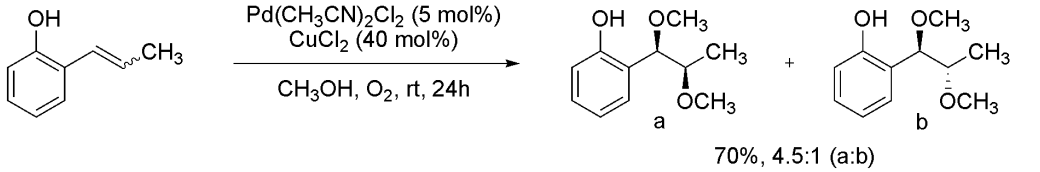

(6)

---

[6] Liu, G.; Stahl, S. S. *J. Am. Chem. Soc*. **2006**, *128*, 7179.

[7] Schultz, M. J.; Sigman, M. S. *J. Am. Chem. Soc*. **2006**, *128*, 1460.

[8] Zhang, Y.; Sigman, M. S. *J. Am. Chem. Soc.* **2007**, *129*, 3076.

The functionalization of alkenes has not been limited to only the addition of heteroatoms across double bonds, rather other transformations that simultaneously form a carbon–heteroatom and carbon–carbon bond are also possible. With respect to carboetherification, the Wolfe group has made significant progress in expanding the scope of the palladium-catalyzed reaction of aryl bromides with *γ*-hydroxy alkenes (eq 7).[9] In this system, it is proposed that an ArPdX intermediate adds to the double bond of the olefin substrate thereby installing the new carbon–aryl bond. The subsequent formation of the carbon–oxygen bond occurs when the *γ*-hydroxy group cyclizes to reductively eliminate the palladium catalyst, thus forming the final tetrahydrofuran product.

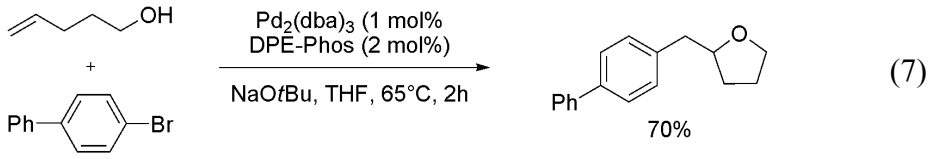

(7)

By slightly modifying the reaction conditions, Wolfe was able to carry out the carboamination of alkenes as well. Via palladium catalysis, the tandem arylation of 2-allylanilines to produce *N*-aryl-2-benzylindoline derivatives was realized (eq 8).[10] This transformation occurs by the formation of two C–N bonds and one C–C bond simultaneously.

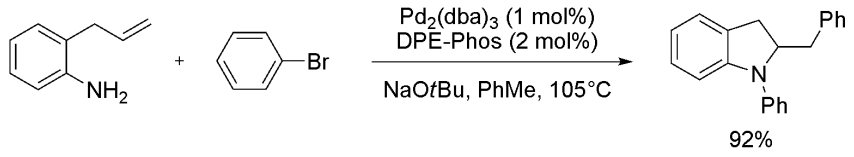

(8)

1.1.3 $Pd^{II/IV}$ Catalyst Cycles

Relatively speaking, $Pd^{II/IV}$ chemistry is a novel field of catalysis. By far, the most common form of catalysis for palladium is through a 0/II catalytic cycle, and this is represented by many of the popular cross coupling reactions such as the Suzuki and Sonogashira. The use or existence of

---

[9] Wolfe, J. P.; Rossi, M. A. *J. Am. Chem. Soc*. **2004**, *126*, 1620.

[10] Lira, R.; Wolfe, J. P. *J. Am. Chem. Soc*. **2004**, *126*, 13906.

Pd^{IV} was not fully realized until Crabtree had reported the acetoxylation of benzene with catalytic $Pd(OAc)_2$ and $PhI(OAc)_2$ in 1996 (eq 9).[11]

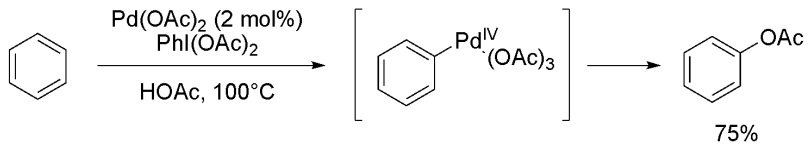

(9)

Though numerous $Pd^{II/IV}$ catalyzed reactions have been published to date, our understanding of this mode of catalysis is still poor. In recent years, it has been the work of Sanford that has acquired this mechanistic design more attention. In her first publications in this field, she presented a new chelate-assisted carbon–hydrogen (C–H) bond oxygenation with pyridine, pyrazole, azobenzene and imine directing groups (eq 10).[12] The mechanism proposed was a very general $Pd^{II/IV}$ catalytic cycle (Scheme 1).

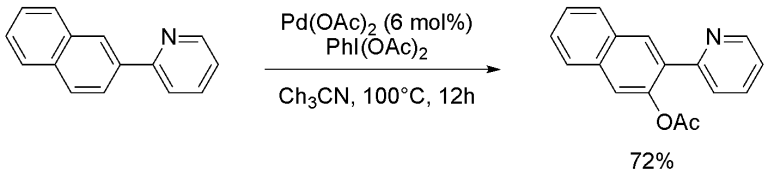

(10)

Scheme 1. $Pd^{II/IV}$ catalytic cycle proposed by Sanford in chelate-assisted C–H bond oxygenation.

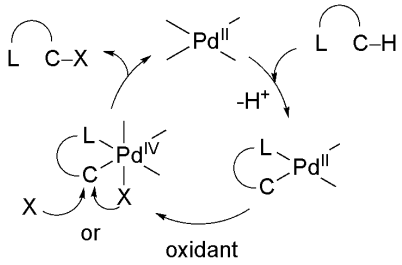

In addition to C–H bond activations, $Pd^{II/IV}$ mechanisms have also extensively been cited in the vicinal oxidation of olefins. This will become important for mechanistic considerations in the palladium-catalyzed dioxygenation of alkenes.

---

[11] Yoneyama, T.; Crabtree, R. H. *J. Mol. Cat. A* **1996**, *108*, 35.

[12] Dick, A. R.; Hull, K. L.; Sanford, M. S. *J. Am. Chem. Soc.* **2004**, *126*, 2300.

1.1.4 Enantioselective $Pd^{II/IV}$ Catalyst Cycles

To the best of our knowledge, there is only one account of an asymmetric $Pd^{II/IV}$ catalytic cycle to date. Overall, little is known with regards to the appropriate ligand choice for palladium(IV) intermediates, even more so when these ligands are chiral. In Sasai's report, a $Pd(TFA)_2$ catalyst was used in combination with a spiro bis(isoxazoline) ligand (SPRIX) and the hypervalent iodine oxidant iodobenzene diacetate to synthesize bicycle[3.1.0]hexanes through an oxidative cyclization of enyne substrates (eq 11).[13] The high affinity of SPRIX ligands for palladium(II) centres, and their notable stability under oxidative conditions made them quite valuable in these reactions. Most impressively, in this system two chiral quaternary carbon centres were set in up to 95% ee.

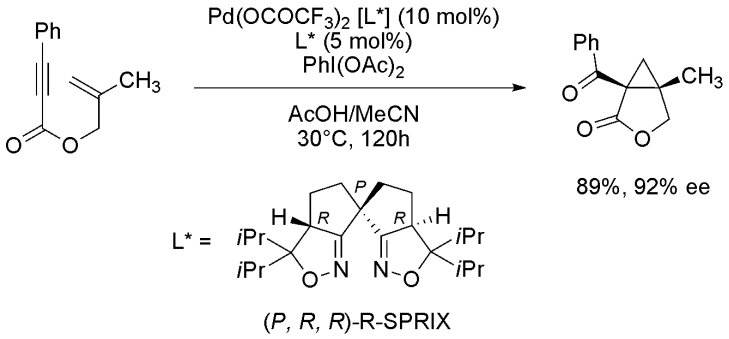

(11)

1.1.5 Palladium-Catalyzed Olefin Dioxygenation

Inspired by the recent reports on palladium-catalyzed vicinal oxidations of olefins, the Dong and Song groups became interested in designing a strategy for the dioxygenation of olefins. Due to the low cost and toxicity of palladium salts in comparison to osmium catalysts, it was proposed that this strategy could become a compliment to the Sharpless dihydroxylation. The reaction design was modelled on a $Pd^{II/IV}$ catalytic cycle where the first step of the transformation would be analogous to the Wacker Process (Scheme 2).[14] Mechanistically, it was envisioned that an alkene could undergo oxypalladation to form an alkyl Pd^{II} intermediate, which then instead of continuing in a Wacker type reaction would be intercepted by oxidation to generate a Pd^{IV}

---

[13] Tsujihara, T.; Takenaka, K.; Onitsuka, K.; Hatanaka, M.; Sasai, H. *J. Am. Chem. Soc.* **2009**, *131*, 3452.

[14] Li, Y.; Song, D.; Dong, V. M. *J. Am. Chem. Soc.* **2008**, *130*, 2962.

species. Subsequently, the reductive elimination of the very electron poor Pd^{IV} intermediate would be facile and in the presence of an oxygen nucleophile a dioxygenated product would be formed.

Scheme 2. General reaction design for palladium-catalyzed olefin dioxygenation.

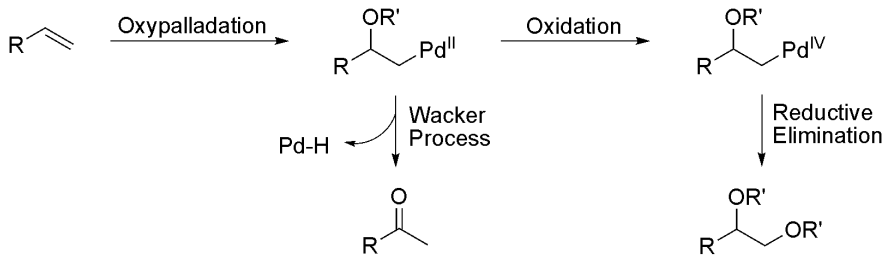

When identifying a catalyst that was capable of catalyzing the vicinal dioxygenation of *trans*-stilbene, with iodobenzene diacetate as the terminal oxidant and in acetic acid, it was found that the common catalysts in palladium-catalyzed aminooxygenations were not effective in this circumstance. With further investigation, it was determined that the palladium catalyst required a phosphine based ligand as well as a non-coordinating counterion for increased activity (Table 1). Eventually, the cationic complex $[Pd(dppp)(H_2O)_2](OTf)_2$ was found to catalyze the dioxygenation of *trans*-stilbene in the shortest reaction time and best yield of the hydroxyacetate product.

Table 1. Palladium-catalyzed oxidation of *trans*-stilbene with hypervalent iodine.

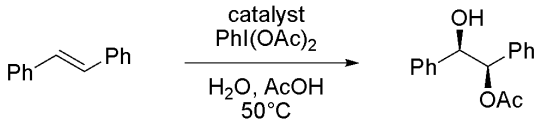

Entry	Catalyst	Loading	Time	Yield[a]
1	$Pd(OAc)_2$	5%	16	0%
2	$PdCl_2(CH_3CN)_2$	5%	16h	0%
3	$Pd(bpy)(OAc)_2$	5%	16h	0%
4	$Pd(BINAP)(OAc)_2$	5%	16h	24%
5	$Pd(BINAP)(TFA)_2$	5%	16h	46%
6	$[Pd(dppp)(H_2O)_2](OTf)_2$	2%	2h	72%

[a] ^1H NMR yield using internal standard.

The hydroxyacetate products were converted to their corresponding diacetate derivatives by treating the crude reaction mixtures with acetic anhydride at room temperature. In general, this methodology was found to be very successful in that many olefins, including terminal, di- and tri-substituted substrates could be dioxygenated in very good yield.

1.1.5.1 Intermolecular Palladium-Catalyzed Olefin Dioxygenation

In examining the scope of this transformation, different terminal olefins were subjected to vicinal oxidation under the standard conditions that were developed by the Dong and Song groups. Electron deficient styrene derivatives were found to be highly tolerated in this system (eq 12), without the need for directing groups as in other publications[7,8]. Simple aliphatic alkenes, such as 1-decene and allyl benzene were also diacetoxylated in very good yield.

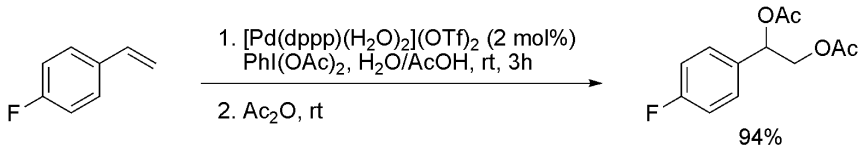

(12)

Dioxygenation of 1,2- and 1,1-disubstitued olefins was also carried out to furnish functionalized products with vicinal stereocentres and with good diastereocontrol. Due to ring strain, indene and 1,2-dihydronaphthalene were particularly reactive substrates. In eq 13, the vicinal oxidation of a cinnamyl ether is displayed, where the formation of the *syn*-diacetate is exclusive.

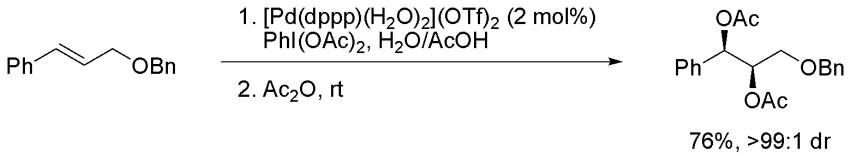

(13)

Lastly, trisubstituted olefins can also be dioxygenated via palladium catalysis to afford the tertiary alcohol products in good yield and high regioselectivity. Since the tertiary alcohols were the sole products in these reactions, there was no need to treat the reaction mixtures with acetic anhydride. The palladium-catalyzed dioxygenation of 1-chloro-4-(prop-1-en-2-yl)benzene is shown in eq 14.

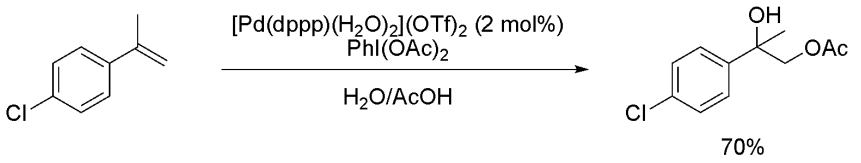

(14)

1.1.5.2 Intramolecular Palladium-Catalyzed Olefin Dioxygenation

In addition to the numerous intermolecular examples, intramolecular palladium-catalyzed olefin dioxygenation of substrates with pendant oxygen nucleophiles leads to the formation of tetrahydrofuran (THF) and lactone rings. As reported, this transformation was not only limited to primary alcohols, but could also be extended to secondary and tertiary alcohols, or even carboxylic acids (Scheme 3).[14]

Scheme 3. Intramolecular palladium-catalyzed oxidative ring-forming examples.

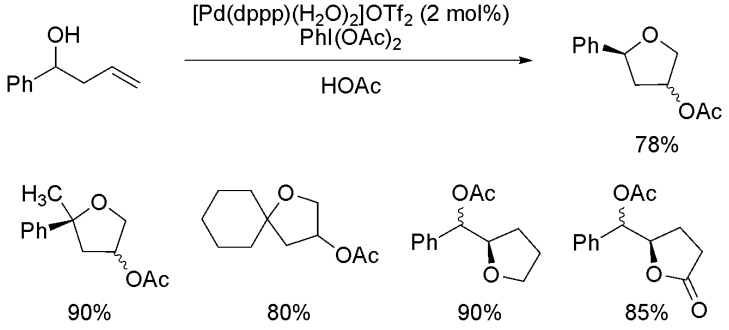

The synthesis of tetrahydrofurans is an attractive goal in organic chemistry due to the prevalence of this type of scaffold in natural products.[15] Thus, there is a need to develop and expand upon ways of generating tetrahydrofuran architectures. Transition metal catalysis specifically has not only enabled the synthesis of novel THF rings, but has also allowed for the enantioselective production of THF structures.[16]

---

[15] For reviews of natural products: (a) Zeng, L.; Ye, Q.; Oberlies, N. H.; Shi, G.; Gu, Z. M.; He, K.; McLaughlin, J. L. *Nat. Prod. Rep.* **1996**, *13*, 275. (b) Dutton, C. J.; Banks, B. J.; Cooper, C. B. *Nat. Prod. Rep.* **1995**, *12*, 165.

[16] For reviews on THF synthesis: (a) Boivin, T. L. B. *Tetrahedron* **1987**, *43*, 3309. (b) Wolfe, J. P.; Hay, M. B. *Tetrahedron* **2007**, *63*, 261.

1.1.5.3 Recent Advances in Palladium-Catalyzed Olefin Dioxygenation

Earlier this year, a new type of palladium-catalyzed olefin dioxygenation was reported by the Chen group.[17] They found that the diacetoxylation of alkenes could be achieved with a $Pd(OAc)_2$ catalyst and with molecular oxygen as the only oxidant in acetic acid (eq 15). The transformation could be applied to numerous mono- and di-substituted alkenes with differing electronic properties. One advantage of this approach is that the use of stoichiometric hypervalent iodide oxidant is circumvented, as is common in other vicinal oxidation methodologies.

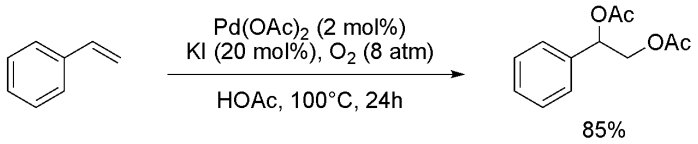

(15)

However, one topic that was not addressed in this report was the role of the potassium iodide additive without which the reaction could not proceed. With little evidence, the authors speculate that the mechanism of this transformation was a $Pd^{II/IV}$ catalytic cycle (Scheme 4). They propose that the Pd^{II} catalyst undergoes *cis*-acetoxypalladation with the olefin substrate, followed by oxidation of the catalyst by O_2 to a Pd^{IV} intermediate and lastly reductive elimination of the palladium results in a new carbon-oxygen bond formation.

Scheme 4. Proposed mechanism for palladium-catalyzed olefin dioxygenation by Chen.

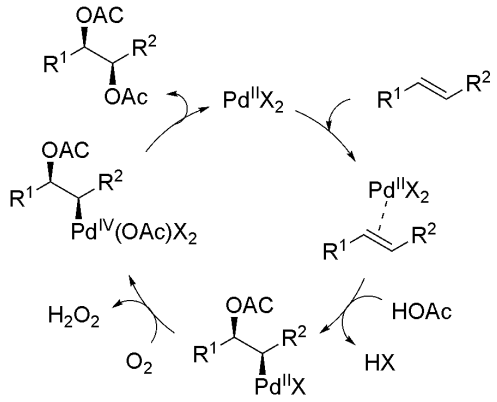

[17] Wang, A.; Jiang, H.; Chen, H. *J. Am. Chem. Soc.*, **2009**, *131*, 3846.

1.1.6 Research Goals

With the discovery of palladium-catalyzed olefin dioxygenation,[14] and especially its broad substrate scope, the Dong research group became interested in examining the mechanistic underpinnings of this reaction. By investigating the reaction kinetics and carrying out a Hammett study of the transformation we hoped to understand the mechanism of reaction as well as identify the rate determining step. For the kinetics it was decided that initial rate kinetics would be the most succinct in studying this reaction. As for the Hammett study, a variety of aryl substituted 1-phenyl-1-cyclohexene derivatives were required in order to probe the electronic effects on the rate of reaction. These substrates were to be synthesized following a two step route (eq 16) from cyclohexanone.

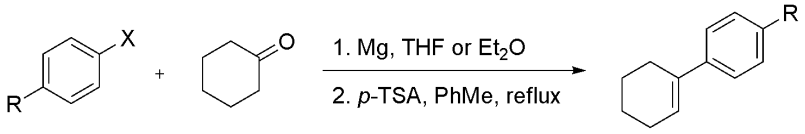

(16)

In addition to studying the mechanism of reaction, we hoped to extend the palladium-catalyzed olefin dioxygenation to include enantioselective variants (eq 17). Thus, a variety of chiral cationic palladium(II) catalysts were explored in intramolecular olefin dioxygenation reactions of alkene substrates with pendant alcohols. Again, these substrates were to be synthesized from commercially available starting materials. With this methodology it was envisioned that enantiopure tetrahydrofuran products, which are represented in many important natural products and pharmaceutical agents,[18] could be synthesized.

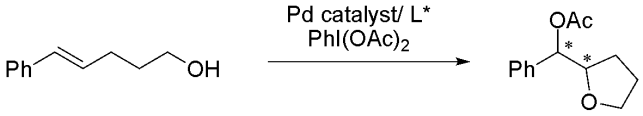

(17)

[18] For some examples see: (a) Ghosh, A. K.; Sridhar, P. R; Kumaragurubaran, N.; Koh, Y.; Weber, I. T.; Mitsuya, H. *Chem. Med. Chem*. **2006**, *1*, 939. (b) Faul, M. M.; Huff, B. E. *Chem. Rev*. **2000**, 100, 2407.

1.2 Results and Discussion

1.2.1 Mechanism of Palladium-Catalyzed Olefin Dioxygenation

1.2.1.1 Kinetic Studies

After the discovery and development of palladium-catalyzed olefin dioxygenation, steps were taken to investigate the mechanistic underpinnings of this powerful reaction. One of the most useful ways to identify the mechanism of a chemical transformation is by studying the reaction kinetics of the different components in the reaction mixture and ultimately deriving a rate law. In order to carry out the olefin dioxygenation kinetics experiments accurately, the substrate of choice was 1-phenyl-1-cyclohexene. In the presence of a catalytic amount of a cationic palladium catalyst, iodobenzene diacetate oxidant, and in an acetic acid solvent, the hydroxyacetate product of 1-phenyl-1-cylcohexene (eq 18) could be furnished in high yield and excellent diastereoselectivity, thereby making this reaction easy to monitor with analytical tools.

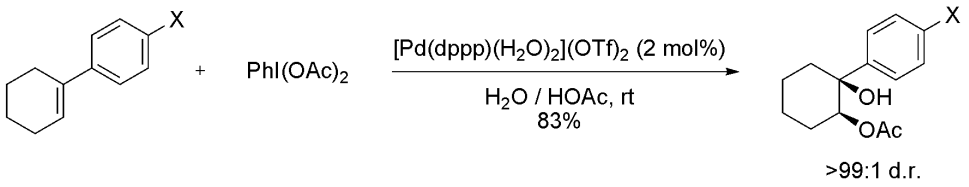

(18)

Dr. Yang Li initiated the mechanistic studies with 1-phenyl-1-cyclohexene by examining the effects of substrate (or starting material) and catalyst concentrations on the initial rate of reaction while all other variables were kept constant (as described in eq 18). For all kinetic experiments, reactions were monitored by GC-FID analysis at specific time intervals. In Figure 1 (A) the relationship between the concentration of substrate and the initial rate of reaction is shown to be linear. This indicates a first order dependence on the olefin substrate in the reaction.

Figure 1. A. Initial rate reaction kinetics with respect to the olefin substrate concentration. **B**. Initial rate reaction kinetics with respect to the $[Pd(dppp)(H_2O)_2](OTf)_2$ catalyst concentration.

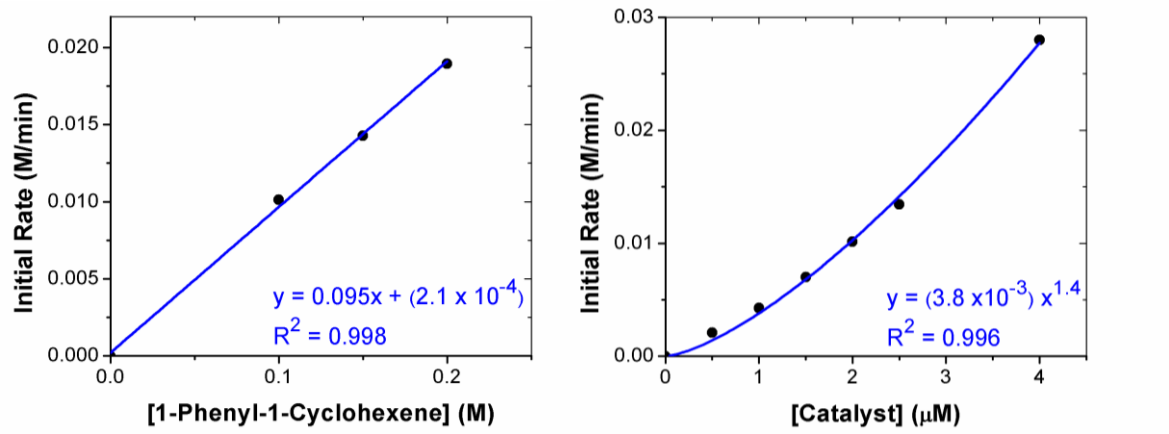

On the contrary, the initial rate of reaction has a pseudo-first order dependence on the concentration of the $[Pd(dppp)(H_2O)_2](OTf)_2$ catalyst (Figure 1B). As indicated by the equation of the line $y = (3.8x10^{-3})x^{1.4}$, the order of the palladium catalyst is 1.4. A reaction order of 1.4 is in essence impossible; however, it can be explained if the reaction mechanism is assumed to have a major and a minor pathway that are operating. The combination of a major reaction pathway which involves a first order dependence on the catalyst with a minor pathway which has a second order dependence on the catalyst could effectively yield an observable 1.4 order in catalyst and would explain for the curvature in the line of best fit.

Subsequently, the effects of oxidant concentration on the initial rate of reaction were studied. Surprisingly, we observed classical saturation kinetics with respect to the oxidant concentration (Figure 2A). In other words, under low concentrations of oxidant the system behaves like it is first order in oxidant. However, at high concentrations of oxidant the increase of the initial rate of reaction will begin to plateau and have less of an effect on the overall rate.

Figure 2. A. Initial rate reaction kinetics with respect to the $PhI(OAc)_2$ oxidant concentration. **B**. Initial rate reaction kinetics with respect to the water concentration.

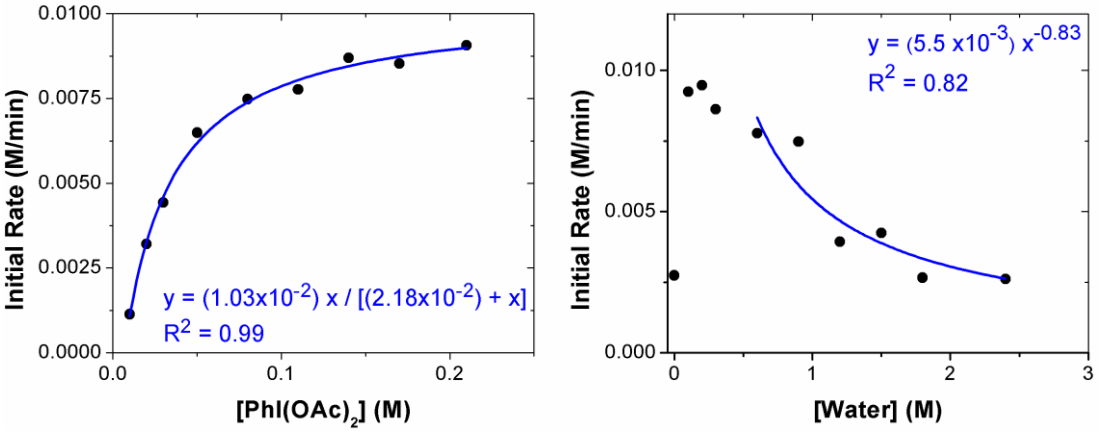

Lastly, it was found that the water content of the reaction medium also has a great effect on reactivity. According the equation of the line in Figure 2B, the palladium-catalyzed dioxygenation reaction is approximately *inverse* first order in water. At high concentrations of water the reaction will proceed very slowly. Moreover, this is also true when the concentration of water is too low. In other words, there is an ideal concentration of water for the dioxygenation reaction to proceed optimally. Note that in deriving the inverse first order dependence on water, concentrations below 2.4 M were not used in the plot. At low concentrations of water, the kinetics become less accurate due to the extremely hygroscopic nature of acetic acid, thus the *actual* water content is less predictable.

Although unusual, the effects of water on the rate of palladium-catalyzed olefin dioxygenation can be rationalized with the generation of an acetoxonium intermediate prior to the formation of the final hydroxyacetate product. By using $H_2{}^{18}O$ under the standard dioxygenation conditions with stilbene, it was possible to determine that the labelled oxygen would be incorporated into the acetate carbonyl oxygen of the hydroxyacetate product (Dr. Yang Li, Scheme 5). This was confirmed by the use of infrared spectroscopy, where the stretching frequencies of the unlabelled

carbonyl double bond and the ^{18}O labelled carbonyl double bond had distinct differences. Similar results were obtained when 1-phenyl-1-cyclohexene was used in the labelling study, instead of stilbene, corroborating that this was not simply substrate dependent, but rather a general trend.

Scheme 5. Palladium-catalyzed olefin dioxygenation in the presence of $H_2{}^{18}O$.

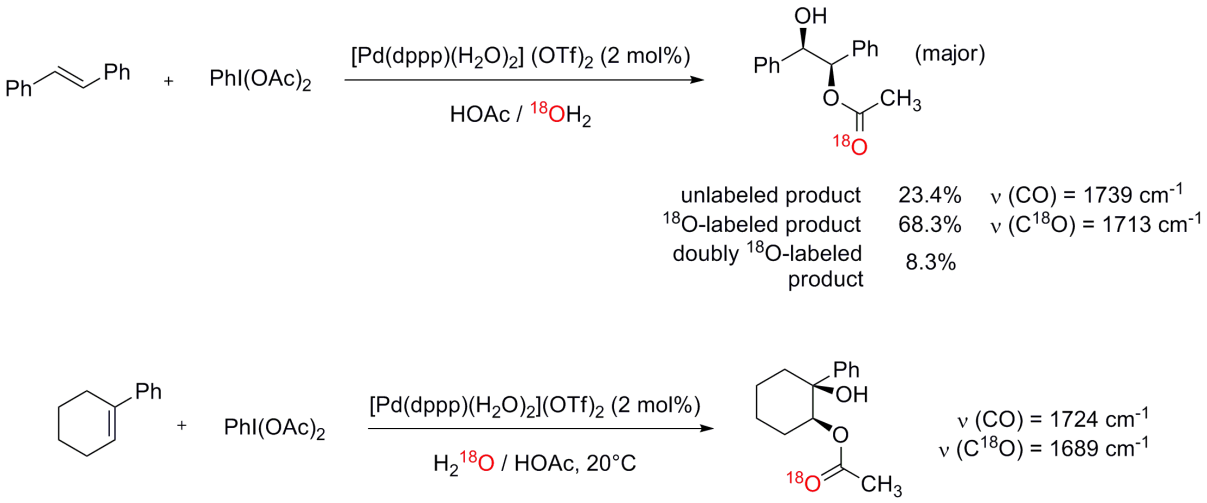

As shown in Scheme 6, hydrolysis of the proposed acetoxonium ion intermediate with water will furnish the desired hydroxyacetate product. If the water is labelled with ^{18}O, then the final product will have ^{18}O at the carbonyl of the acetate group. However, if the acetoxonium ion is

Scheme 6. Quenching of the acetoxonium ion intermediate by two routes.

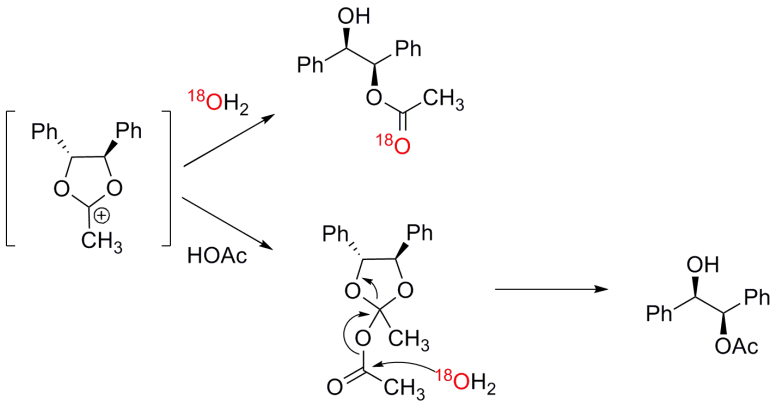

quenched with acetic acid (the reaction solvent) then a subsequent attack of water onto the new acetate group would cause a ring-opening event which would yield an unlabelled hydroxyacetate product, even in the presence of $H_2{}^{18}O$. It is important to note that both of these products were indeed observed experimentally.

Thus, at low concentrations of water (0 to 0.4 M) the rate limiting step becomes the hydrolysis of the acetoxonium ion, which affects the inverse first order nature of the water dependence (i.e. less accurate correlation is observed if these values are included in the line of best fit calculated in Figure 2B). Conversely, at slightly higher concentrations of water (0.6 to ~2 M) the hydrolysis of the acetoxonium ion is not impeded and water dependence is effectively in inverse first order.

To complete the kinetic studies on the palladium-catalyzed dioxygenation of 1-phenyl-1-cyclohexene, the results were compiled into an empirical rate law (eq 19). This rate law holds true at concentrations of water beyond 0.6M. The palladium catalyst and the substrate are in first order dependence, while the oxidant is described by saturation kinetics. Recall, this rate law is in reality simplified since the actual catalyst order deviates from true first order dependence.

$$\frac{d[P]}{dt} = \frac{k_{obs}[cat.][substrate][PhI(OAc)_2]}{[H_2O] + [PhI(OAc)_2]} \qquad (19)$$

1.2.1.2 Hammett Study

In addition to exploring the reaction kinetics of the palladium-catalyzed dioxygenation, it was important to examine electronic effects on the system. This study was carried out by varying the substituent at the *para* position of the aryl ring and then subsequently examining the effects on the initial rate of dioxygenation. These *p*-substituted derivatives were generated in two steps (eq 20): addition of an aryl-Grignard reagent to cyclohexanone to afford the tertiary alcohol, followed by a dehydration of the alcohol to the final olefin product under acidic conditions.

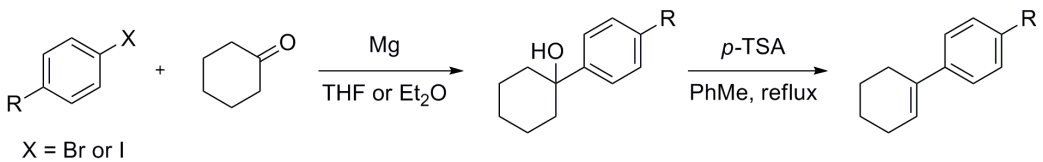

(20)

The 1-(*p*-substituted)phenyl-1-cyclohexene derivatives were dioxygenated to furnish the corresponding hydroxyacetate products under standard palladium-catalyzed conditions (Table 2). From Table 2 it can be seen that electron donating groups increase the initial rate of reaction while electron withdrawing groups can drastically decrease the rate. Most substrates were transformed to the desired product in good yield with the exception of 1-cyclohexenyl-4-methoxybenzene which was observed to produce significant byproducts including 1-(4-methoxyphenyl)-7-oxabicyclo[4.1.0]heptane (an epoxide). Although 4-cyclohexenyl-*N,N*-dimethylaniline is very electron rich, when dissolved in an acetic acid solvent, the dimethylamine moiety becomes protonated which in turn makes the substrate very electron poor and thus as shown in Table 2 no reaction was observed for this substrate.

Table 2. Dioxygenation of 1-(*p*-substituted)phenyl-1-cyclohexene substrates.

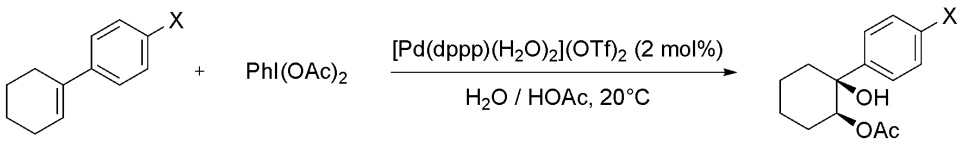

Entry	X	Rxn Time	Yield
1	OMe	10 m	28%
2	$N(Me)_2$	-	-
3	*t*-Bu	10 m	66%
4	Me	10 m	48%
5	Cl	2 h	79%
6	F	2 h	58%
7	CF_3	16 h	36%

Due to the significant changes in rate, the optimal method for obtaining relative rates (to the unsubstituted substrate) of reaction was through competitive kinetic experiments between pairs of substrates. In Table 3 the relative initial rates of reaction of the five substituted substrates can be seen.

Table 3. Relative rate of dioxygenation of 1-(*p*-substituted)phenyl-1-cyclohexene substrates.

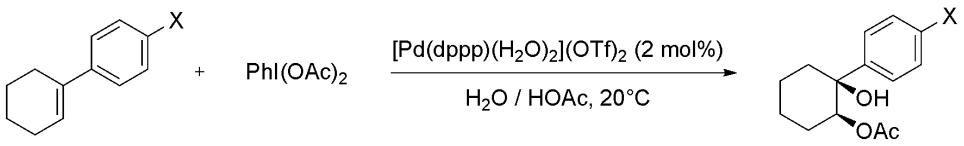

Entry	X	k_{rel}
1	Me	8.25
2	*t*-Bu	11.83
3	H	1.00
4	F	0.94
5	Cl	0.25
6	CF_3	0.013

By taking the log of the initial rate of reaction for each substituted substrate and plotting it versus the appropriate Hammett σ_p parameter, the Hammett Plot was prepared (Figure 3). The relative rates were found to correlate very well ($R^2 = 0.98$) to the σ_p parameter. The Hammett plot yielded a slope or ρ value of -3.9, showing that there is a significant electronic effect on the reaction. A negative slope is consistent with the development of a positive charge in the transition state prior to, or in the rate determining step of the transformation.

Figure 3. Hammett plot derived from the dioxygenation of 1-(*p*-substituted)phenyl-1-cyclohexene substrates.

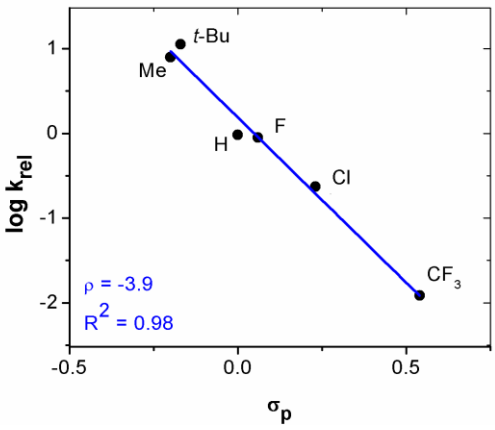

1.2.1.3 Proposed Catalytic Cycle: A $Pd^{II/IV}$ Mechanism

Based on the reaction kinetics, ^{18}O labelling experiments and Hammett study, the proposed mechanism (consistent with the experimental data) for the newly developed palladium-catalyzed olefin dioxygenation system is one which involves a $Pd^{II/IV}$ catalytic cycle (Scheme 7). In this catalytic cycle the catalyst resting state is a cationic Pd(dppp) bis-aqua species which upon the

Scheme 7. Proposed palladium-catalyzed olefin dioxygenation catalytic cycle.

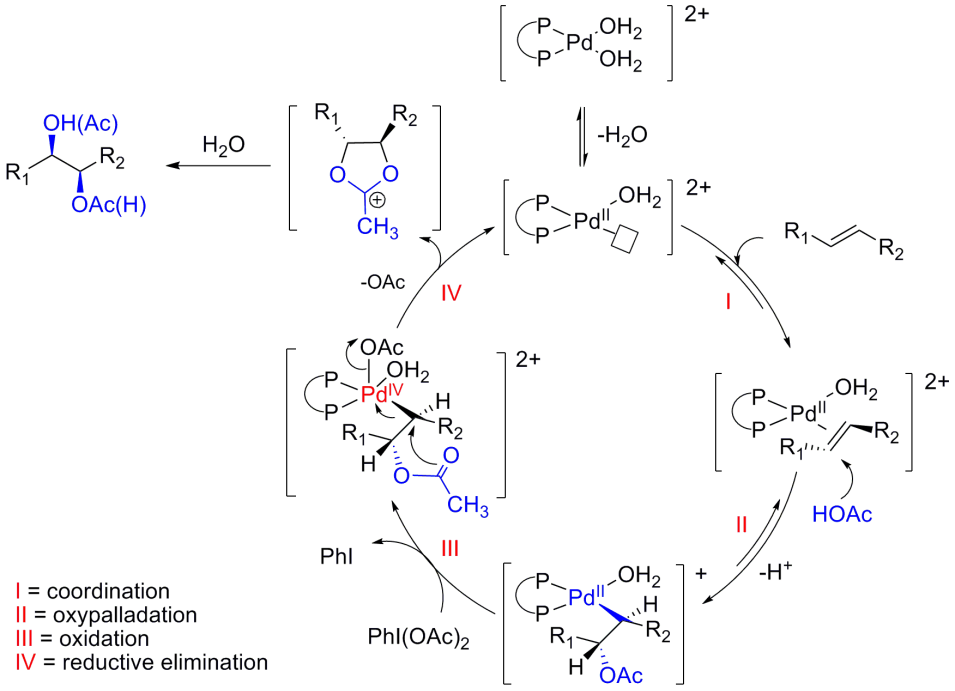

dissociation of one water molecule will form the active palladium catalyst. The active catalyst has a free ligand site by which it can coordinate to the olefin substrate π system. After coordination, *trans*-acetoxypalladation of the olefin by an outer sphere attack with acetic acid generates a new alkyl Pd^{II} species. A subsequent oxidation of the alkyl Pd^{II} species with the strong oxidant $PhI(OAc)_2$ circumvents *β*-hydride elimination and produces a Pd^{IV} intermediate and iodobenzene as the byproduct. This Pd^{IV} intermediate will then undergo an intramolecular cyclization to generate an acetoxonium ion, while also reductively eliminating the palladium catalyst (in an S_N2-type fashion) so that it can then re-enter the catalytic cycle. The acetoxonium ion is then quenched with water in order to yield the final hydroxyacetate product.

In this mechanistic proposal the major pathway is first order in palladium catalyst, which would be consistent with the reaction kinetics results which indicated that major (first order in catalyst) and minor (second order in catalyst) pathways could be operational (Figure 1B). The dependence on the olefin substrate is also first order, which is consistent with the kinetics results (Figure 1A). Although the dependence on oxidant is experimentally shown to follow saturation kinetics (Figure 2A), at low concentrations of oxidant a linear relationship between oxidant concentration and initial rate of reaction is observed, indicating that a first order dependence is effective. In this mechanistic proposal we assume the oxidant concentration is below the saturation point (i.e. low) and thereby has a first order dependence. Lastly, the inverse first order in water concentration can also be accounted for in this proposed mechanism. As mentioned, the active catalyst must have an empty coordination site for the incoming olefin substrate which means that one molecule of water must be lost from the Pd(dppp) bis-aqua catalyst. The loss of one water molecule would effectively make the dependence on water to be inverse first order. This also explains for the fact that at very low or very high concentrations of water the dioxygenation reaction is impeded. At low concentrations of water the rate determining step of the transformation becomes the hydrolysis of the acetoxonium ion intermediate. While at high concentrations of water, Le Châtalier's Principle ensures that the equilibrium between the Pd(dppp) bis-aqua and mono-aqua catalysts lies heavily on the side of the bis-aqua complex, preventing much of the palladium catalyst from entering the catalytic cycle.

With results from the Hammett study, we were able to learn that there was a build up of positive charge prior to, or in the rate determining step of the palladium-catalyzed dioxygenation reaction. With this in mind, it is proposed that the oxidation of Pd^{II} to Pd^{IV} is the rate limiting step. In order to generate the Pd^{IV} intermediate, the Pd^{II} precursor must lose electrons which would be consistent with a positive charge buildup. Also, since more electron rich olefin substrates yield greater reactivity (Table 3), then the oxypalladation step of the catalytic cycle can be ruled out as the rate limiting step. One can imagine that the rate of oxypalladation could only become faster if there was *decreased* olefinic electron density to cause less electron repulsion between the olefin π system and the incoming acetic acid nucleophile. In essence, oxypalladation would only become more facile if the olefin substrate were electron poor; however, this was not observed experimentally. Conversely, the oxidation of Pd^{II} to Pd^{IV} would be aided with more electron rich

substrates considering that it would be easier to remove electrons (oxidize) from an electron rich rather than electron poor substrate.

1.2.1.4 Olefin Dioxygenation via Other Modes of Catalysis

Inspired by recent literature that reports $Pd(OAc)_2$ catalyzed olefin dioxygenation with a potassium iodide additive,[17] some readily available halide salts were tested for dioxygenation reactivity with styrene without any palladium catalyst. The purpose of these experiments was to gain more insight into the mechanistic role of the inorganic salt in the reported reaction. In acetic acid with a strong oxidant such as $PhI(OAc)_2$ and with stoichiometric amounts of various halide salts or Lewis acid (BBr_3) it was found that the dihalogenated or haloacetoxylated styrene derivatives (I and II, respectively in Table 4) were produced. Overall, the distribution and selectivity of products seemed to depend on the source and identity of halide ion.

Table 4. Dihalogenation and(or) haloacetoxylation of styrene.

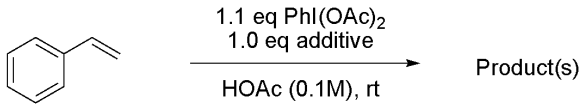

Entry	Additive (1.0 eq)	Product(s)	Yield[a]
1	BBr_3	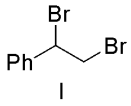 I 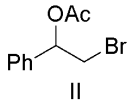 II	21% I, 26% II
2	LiBr		8% I, 15% II
3	KBr		9% I, 34% II
4	KI	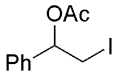	64%[b]

[a] Conversion as determined by GC-FID analysis with dodecane internal standard
[b] Isolated yield

The haloacetoxylation of styrene is not a novel concept in that other research groups have observed similar reactivity that can only be described as modifications of the Prévost reaction.[19]

[19] For a recent example see: Emmanuvel, L.; Shaikh, T. M. A.; Sudalai, A. *Org. Lett.* **2005**, *7*, 5071.

With this train of thought, it was expected that a Lewis acid such as BF_3•OEt_2 might produce similar haloacetoxylation products with an olefin substrate, an oxidant and in acetic acid conditions. Instead, it was observed that BF_3•OEt_2 can catalyze the formation of the diacetate and two hydroxyacetate regioisomers of styrene in good yield (Table 5).

Table 5. Dioxygenation of styrene in the presence of BF_3•OEt_2.

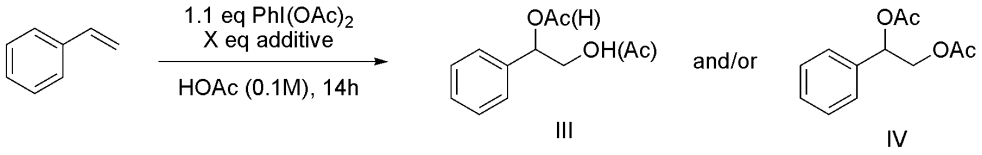

Entry	HOAc Type	Additive	Temp. (°C)	Yield III[a,b]	Yield IV[a]
1	Stock	-	rt	-	-
2	Stock	-	120	-	40%
3	Stock	0.2 eq BF_3•OEt_2	rt	7%, 22%	2%
4	Stock	1.0 eq BF_3•OEt_2	rt	7%, 24%	7%
5	Stock	1.0 eq BF_3•OEt_2	50	-	58%
6	Stock	-	50	4%, 11%	4%
7	Dry	1.0 eq BF_3•OEt_2	rt	-	85%
8	Dry	-	rt	-	-
9	Dry	0.2 eq BF_3•OEt_2	rt	-	74%

[a] Conversion as determined by GC-FID analysis with dodecane internal standard
[b] Conversions to both regioisomeric products of III are listed

Control reactions in both stock and dry acetic acid solvents showed that without BF_3•OEt_2 there was no conversion to either the diacetate or hydroxyacetate products (entries 1 and 8). However, with heating to 120°C the 1-phenylethane-1,2-diyl diacetate product could be furnished (entry 2). At room temperature, the addition of catalytic and stoichiometric amounts of BF_3•OEt_2 could generate low quantities of the desired dioxygenated products (entries 3 and 4). With additional heating to 50°C, the product conversion did increase, but so did the background reaction without any Lewis acid additive (entries 5 and 6). The best results were obtained when anhydrous acetic acid solvent was used, in that high conversions and selectively for the 1-phenylethane-1,2-diyl

diacetate product were obtained (entry 7). Furthermore, when the loading of BF_3•OEt_2 was reduced to 20 mol% the product conversion was still very good (entry 9).

With these new results in hand, it was postulated that a chiral boron Lewis acid may be able to catalyze olefin dioxygenation enantioselectively. Thus, a stoichiometric amount of the Soderquist catalyst was tested for olefin dioxygenation reactivity (eq 21). Unfortunately no reaction was observed when BF_3•OEt_2 was substituted for the Soderquist reagent. The two Lewis acids are so different chemically (for example, the ligands around either boron centre are not similar sterically or electronically) that their reactivity should have not been expected to be alike.

(21)

In addition to the use of BF_3•OEt_2 in olefin dioxygenation, it was found that triflic acid can also catalyze the same transformation. With styrene, a 5 mol% loading of triflic acid could predominantly yield the diacetate product with low to trace amounts of the hydroxyacetate products (Table 6, entry 2). It also showed that higher conversions could be obtained when strictly anhydrous conditions were used (entry 3). It was noted that with no oxidant in the reaction mixture, triflic acid itself was not able to catalyze the reaction since only a very trace amount of dioxygenated product was observed (entry 4).

Table 6. Triflic acid catalyzed styrene dioxygenation.

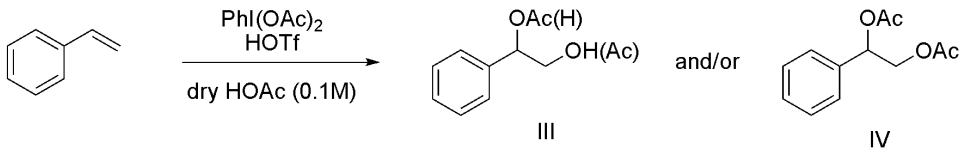

Entry	$PhI(OAc)_2$ (Equiv.)	H_2O (Equiv.)	HOTf (Equiv.)	Yield III[a,b]	Yield IV[a]
1	1.1	3.0	1.0	-	52%
2	1.1	3.0	0.05	0.6%, 7%	44%
3	1.1	-	1.0	-	80%
4	-	3.0	1.0	-	0.6%

[a] Conversion as determined by GC-FID analysis with dodecane internal standard
[b] Conversions to both regioisomeric products of III are listed

1.2.1.5 Alternate Mechanistic Proposal for Olefin Dioxygenation

The BF_3•OEt_2 and triflic acid catalyzed olefin dioxygenation transformations are mechanistically very different from the proposal in section 1.2.1.3. Due to the lack of mechanistic experiments for either the BF_3•OEt_2 or triflic acid modes of catalysis, any mechanistic proposal at this time is a hypothesis. Nonetheless, one route by which the hydroxyacetate and diacetate products could be generated is shown in Scheme 8. Through a reversible process it is possible that the Lewis

Scheme 8. Proposed mechanism for Lewis acid or triflic acid catalyzed olefin.

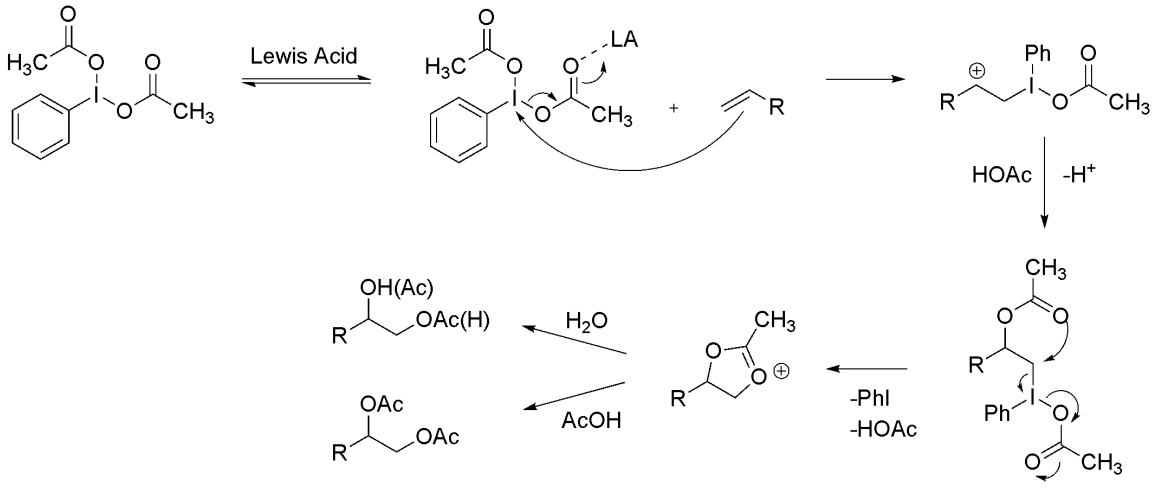

acid (BF_3•OEt_2) is coordinating to the acetate carbonyl of $PhI(OAc)_2$ thereby making the oxidant even more electrophilic and increasing the propensity towards an attack from the alkene π system. Upon the alkene attack, a carbocation intermediate would be formed where the positive charge could lie on a carbon atom or even the iodine in an iodonium type structure. Quenching of the positive charge with acetic acid would afford a new I^{III} species which could easily undergo an intramolecular cyclization to reductively eliminate iodobenzene (an I^{I} species) and to form an acetoxonium ion product. Depending on whether the acetoxonium is opened with acetic acid or water, either the diacetate or hydroxyacetate products will be furnished, respectively. With a triflic acid catalyst, it can be imagined that a similar mechanism would operate; however, in this case the oxidant would be activated by protonation of the acetate carbonyl of $PhI(OAc)_2$.

In the case of palladium-catalyzed olefin dioxygenation a $Pd^{II/IV}$ mechanism was proposed, although if we consider this novel cationic mechanism, maybe there is a way that palladium-catalyzed dioxygenation can also be explained through a cationic mechanism. In literature, palladium metals have been previously used as Lewis acids,[20] and if in this case we consider the $[Pd(dppp)(H_2O)_2](OTf)_2$ catalyst as a Lewis acid then the proposed cationic mechanism could make sense in this scenario. The best link between palladium-catalyzed dioxygenation and the cationic mechanism is the ρ value of the Hammett plot in Figure 3. The ρ value (-3.9) is unusually high for a traditional transition metal catalyzed process[21] such as the $Pd^{II/IV}$ proposal; however, it is more consistent with a cationic process.[22] Also with ^{31}P NMR, we know that there is an equilibrium interaction between the palladium catalyst and the $PhI(OAc)_2$ oxidant as indicated by the coalescing phosphorous peak for the dppp ligand (Table 7). It is possible that this interaction could be another indication that a cationic mechanism is plausible for the palladium-catalyzed dioxygenation of alkenes. Overall, further investigation into the relevance of the cationic mechanism with respect to palladium-catalyzed olefin dioxygenation is warranted.

---

[20] (a) Strukul, G. *Topics in Catalysis* **2002**, *19*, 33. (b) Fujii, A.; Hagiwara, E.; Sodeoka, M. *J. Am. Chem. Soc.* **1999**, *121*, 5450. (c) Hamashima, Y.; Hotta, D.; Sodeoka, M. *J. Am. Chem. Soc.* **2002**, *124*, 11240.

[21] For some examples see: (a) Jiang, N.; Ma, Z.; Qu, Z.; Xing, X.; Xie, L.; Wang, J. *J. Org. Chem*. **2003**, *68*, 893. (b) Larsen, J.; Jorgensen, K. A. *J. Chem. Soc. Perkin Trans. 2* **1992**, 1213.

[22] For some examples see: (a) Creary, X.; O'Donnell, B. D.; Vervaeke, M. *J. Org. Chem*. **2007**, *72*, 3360. (b) Creary, X.; Willis, E. D.; Gagnon, M. *J. Am. Chem. Soc.* **2005**, *127*, 18114.

Table 7. ^{31}P NMR shifts for $[Pd(dppp)(H_2O)_2](OTf)_2$ with various concentrations of $PhI(OAc)_2$ oxidant in acetic acid, where peaks were referenced to phosphoric acid.

Entry	$[Pd(dppp)(H_2O)_2](OTf)_2$ (Equiv.)	$PhI(OAc)_2$ (Equiv.)	^{31}P shift (ppm)
1	1.0	-	15.527
2	1.0	1.1	15.815
3	1.0	0.5	15.623

1.2.2 Enantioselective Palladium-Catalyzed Olefin Dioxygenation

In addition to a vast array of intermolecular dioxygenation reactions, palladium-catalyzed olefin dioxygenation proved very effective in intramolecular examples as well. This was an important application in that substituted tetrahydrofuran rings could be synthesized from readily available building blocks. To investigate the asymmetric synthesis of tetrahydrofurans a variety of cationic chiral palladium catalysts were screened for enantioinduction (Dr. Yang Li). Of the catalysts tried, a dimeric palladium catalyst with an (*R*)-BINAP backbone was found to be the most successful. With this catalyst (*E*)-5-phenylpent-4-en-1-ol was cyclized to the corresponding tetrahydrofuran diastereomers in 75% yield and in modest diastereoselectivity, but most importantly in 22% and 36% enantiomeric excess (Scheme 9).

Scheme 9. $[Pd((R)\text{-BINAP}(\mu\text{-}OH)_2]_2(OTf)_2$ catalyzed cyclization of (*E*)-5-phenylpent-4-en-1-ol to afford two diastereomeric tetrahydrofuran products.

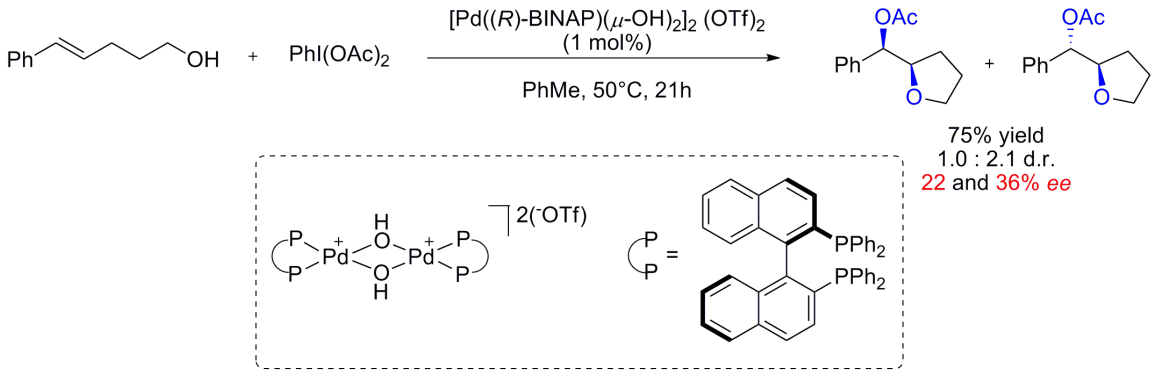

With these exciting results, our goal was to synthesize other derivatives of (*E*)-5-phenylpent-4-en-1-ol to determine whether sterics or electronics could bias the system and achieve greater enantioselectivities with the same catalyst. To do so, a two step procedure was followed: Sonogashira coupling of substituted iodobenzenes with 4-pentyne-1-ol to afford the alkyne product (eq 22) and followed by a $LiAlH_4$ reduction in tetrahydrofuran to afford the (*E*)-alkene selectively (eq 23).

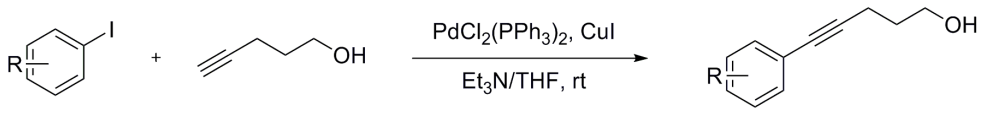

(22)

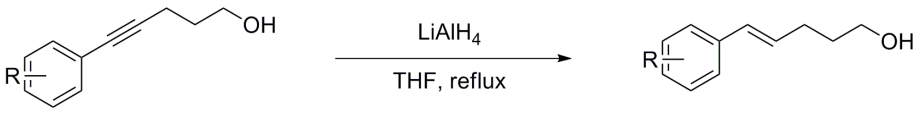

(23)

With the new substrates in hand, the intramolecular palladium-catalyzed dioxygenation was carried out in toluene, at 50°C for 21 hours. The corresponding tetrahydrofuran products were formed in poor yield, and none were shown to have higher enantioselectivities than the benchmark 36% ee for (*E*)-5-phenylpent-4-en-1-ol (Table 8). By using electron rich substrates (such as in entries 2 and 3) the enantioselectivity seemed to decrease quite drastically. In comparison to the electron rich substrates, sterically bulky substrates such as the naphthyl-substituted derivative (entry 4) only had a mild improvement in ee. To test the intramolecular dioxygenation of electron poor substrates the synthesis of (*E*)-5-(4-fluorophenyl)pent-4-en-1-ol was attempted with the route described above. However, the $LiAlH_4$ reduction of the alkyne was observed to reduce the C–F bond to a C–H bond in small quantities. Due to the inseparability of these two olefin products by column chromatography, the isolation of this substrate was not achieved. Other substrates (entries 5, 6 and 7) that could undergo intramolecular palladium-catalyzed dioxygenation in acetic acid were subjected to non-chiral cyclization conditions in toluene. It was found that these reactions did not proceed in toluene and thus the asymmetric versions of these reactions were not examined.

Table 8. The intramolecular palladium-catalyzed dioxygenation of various substrates including aryl substituted (*E*)-5-phenylpent-4-en-1-ol derivatives.

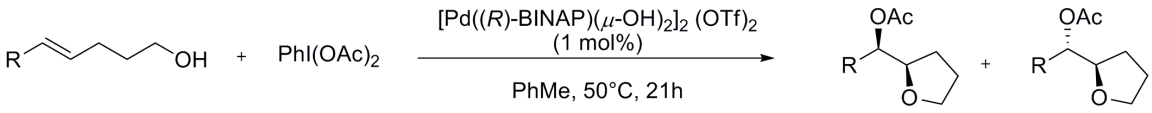

Entry	Substrate	Product	Yield[a]	% ee[b]
1	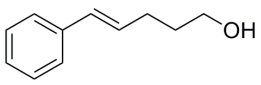	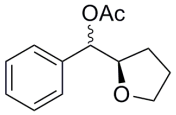	75%	22%, 36%
2	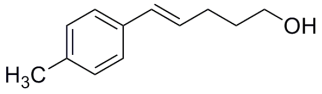	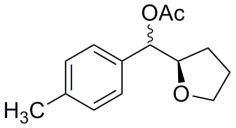	9%	9%, 9%
3	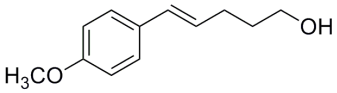	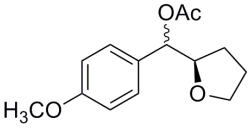	30%	16%, 5%
4	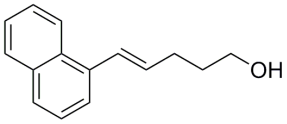	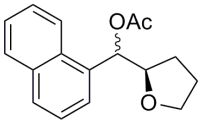	37%	19%[c]
5[d]	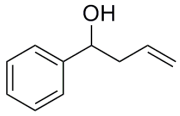	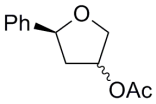	NR	-
6[d]	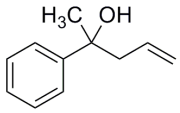	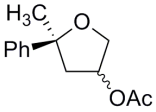	NR	-
7[d]	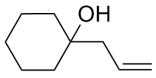	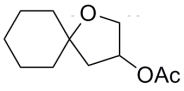	NR	-

[a] Combined Isolated yield of both diastereomers. [b] Enantiomeric excess determined with chiral HPLC analysis. [c] The other enantiomer pair could not be separated by chiral HPLC analysis. [d] No reaction was shown with $[Pd(dppp)(H_2O)_2](OTf)_2$ thus the chiral Pd catalyst was never used.

1.3 Conclusion

Palladium-catalyzed olefin dioxygenation is a powerful tool in the synthesis of highly functionalized compounds, which has been shown to be compatible with a broad scope of substrates including mono-, di-, and tri-substituted alkenes. Kinetic studies measuring the initial rate of reaction of this transformation indicate that the reacting substrate concentration is in first order dependence, water concentration is in an inverse first order, and the catalyst concentration is in a nearly first order (which implies a combination of first and second order dependence). Lastly, oxidant concentration was found to follow saturation kinetics; however at low concentrations of oxidant a first order dependence can be observed. A Hammett plot revealed that electron rich olefin substrates react faster under these dioxygenation conditions in comparison to other electron poor olefins. Mechanistically, our working hypothesis is that a $Pd^{II/IV}$ catalytic cycle is in operation, where the oxidation of the alkyl Pd^{II} intermediate to a Pd^{IV} species is the rate determining step of the transformation. Interestingly, it was also discovered that substoichiometric quantities of $BF_3 \bullet OEt_2$ and triflic acid can catalyze the dioxygenation of styrene. In this case, it is hypothesized that the dioxygenation occurs through a cationic mechanism.

In addition to the mechanistic insight gained, our studies on asymmetric palladium-catalyzed olefin dioxygenation have shown that moderate levels of enantioselectivity can be achieved (up to 36% ee) with a chiral palladium catalyst, towards the synthesis of tetrahydrofuran products.

1.4 Experimental Procedures

1.4.1 General Experimental

All reactions were carried out in flasks or sealed vials (1DR, 1 mL) fitted with rubber septa or Teflon screw caps and containing magnetic stir bars, unless otherwise noted. Reactions involving reagents that were sensitive to air or moisture were carried out in flame dried flasks or vials that were purged with argon gas for a minimum of five minutes. Reagents were then added by syringe under an argon atmosphere.

Crude reaction mixtures were concentrated by rotary evaporation under vacuum. Subsequent product purification was completed by column chromatography using EMD Silica Gel 60 (particle size 0.040-0.063 mm, 230-400 mesh ASTM) or by preparative thin layer chromatography (EMD Silica Gel 60 F_{254} pre-coated plates, 2mm). Thin layer chromatography was carried out on glass plates pre-coated with silica gel (EMD Silica Gel 60 F_{254}) and detection was accomplished with ultraviolet light or by staining with potassium permanganate, phosphomolybdic acid (PMA), or cerium molybdate (Hanessian's stain) followed by heating.

1.4.2 Materials

$Pd(OAc)_2$ and $PdCl_2$ were purchased from Strem Chemicals Inc. and used directly. $[Pd(dppp)(H_2O)_2](OTf)_2$ was prepared from $(dppp)Pd(OTf)_2$,[23] while $[Pd(R)\text{-}BINAP(\mu\text{-}OH)_2]_2(OTf)$ was prepared from $Cl_2Pd(R)$-BINAP[20b] following literature procedures (by Dr. Yang Li). Tetrahydrofuran, diethyl ether, toluene, and dichloromethane were used directly from a Pure Solv. solvent purification system (Innovative Technology, Inc.). Acetic acid (500 mL) was refluxed over potassium permanganate (2.0 g) and acetic anhydride (30 mL) for 24 hours and then distilled into a schlenk bomb under argon atmosphere. The concentration of *n*-BuLi was determined by titration completed in THF at room temperature with diphenylacetic acid. Other commercial materials were used without further purification, unless specified. *n*-Hexanes and ethyl acetate used for chromatographic purification were purchased from Sigma-Aldrich and Caledon Laboratories Ltd., respectively.

---

[23] Stang, P. J.; Cao, D. H.; Poulter, G. T.; Arif, A. M. *Organometallics* **1995**, *14*, 1110.

1.4.3 Instrumentation

All NMR spectra were recorded on a Bruker Avance400 (400/100 MHz), Varian 400 (400/100 MHz) or Varian 300 (300/75 MHz) in ambient conditions with shifts reported in parts per million (ppm) where the solvent or trimethylsilane was the internal standard ($CDCl_3$ at 7.26 ppm or TMS at 0.0 ppm for ^{1}H NMR, $CDCl_3$ at 77.00 ppm for ^{13}C NMR, and H_3PO_4 at 0.0 ppm for ^{31}P NMR). NMR data is reported as: chemical shift, multiplicity (ap = apparent, br = broad, s = singlet, d = doublet, t = triplet, q = quartet, qn = quintet, sx = sextet, sp = septuplet, m = multiplet), integration and coupling constant(s) in Hz. Infrared spectra were collected on a Perkin-Elmer 1000 FT-IR spectrometer. Mass spectra (MS) were recorded on a Sciex Qstar Mass Spectrometer. High-resolution mass spectra (HRMS) were recorded on a micromass 70S-250 spectrometer (EI) or an ABI/Sciex Qstar mass spectrometer (ESI). Melting point was measured with a Gallenkamp melting point apparatus. GC-MS analysis was performed on an Agilent Technologies 7890A (GC) and 5975C inert XL EI/CI MSD system with an HP-5 column (0.320 mm, 0.25 μm film). GC-FID analysis was performed on an Agilent Technologies (7890A) system. HPLC analysis was performed on a HP1100 Series modular system from Agilent with ChemStation LC3D software v.10.02. The chiral columns used were from Dicel Chemical Industries Ltd. (chiralpak AD-H, chiralcel OD-H, or chiralcel OJ).

1.4.4 Experimental Procedures and Characterizations

1.4.4.1 General Procedure for the Synthesis of 1-Phenyl-1-cyclohexanol Derivatives

In a flame dried flask that was purged with argon gas, a stir bar, anhydrous Et_2O or THF and magnesium shavings (1.0 equiv) were added. The aryl halide reagent (1.0 equiv) was dissolved in 10 mL of solvent and then slowly added to the stirring magnesium mixture. When cloudiness or colour change (to yellow or brown) was observed, the Grignard reagent had formed. If no Grignard formation occurred within the addition of the first 10% of the aryl halide solution, then gentle heating, refluxing, and/or addition of I_2 crystals was necessary to initiate the Grignard. After all the magnesium turnings had disappeared, a solution of cyclohexanone (1.3 equiv in 5 mL of solvent) was added dropwise at 0°C. The solution was subsequently stirred at room temperature for 3 hours (under an argon atmosphere) and then washed with water and a 10% HCl solution. The aqueous layers were extracted with EtOAc (3x) and the combined organic phases

were dried with $MgSO_4$ and filtered. Concentration of the organic phases yielded the crude products which were then purified by silica gel chromatography.

1-(4-methoxyphenyl)cyclohexanol

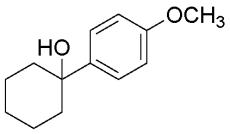

The reaction was completed with 2.0 g of 4-iodoanisole (8.6 mmol), 208 mg of Mg, and 1.2 mL of cyclohexanone in anhydrous Et_2O to afford 1.3 g (74%) of a yellow oil after silica gel chromatography (10-20% EtOAc-hexanes). IR (neat): 3420, 2929, 2858, 1694, 1609, 1511, 1447, 1299, 1246, 1212, 1178, 1148, 1130, 1112, 1037, 966, 823 cm^{-1}. ^1H NMR (300 MHz, $CDCl_3$) δ 7.42 (d, *J* = 8.9 Hz, 2H), 6.88 (d, *J* = 8.9 Hz, 2H), 3.80 (s, 3H), 1.84-1.69 (m, 7H), 1.65-1.54 (m, 4H). ^{13}C NMR (75 MHz, $CDCl_3$) δ 158.3, 141.6, 125.8, 113.5, 72.7, 55.2, 38.9, 25.5, 22.3. HRMS (EI) *m*/*e* calcd. for $C_{13}H_{18}O_2$ $[M-H]^+$: 206.1307; found: 206.1308.

1-(4-methylphenyl)cyclohexanol

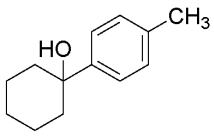

The reaction was completed with 2.0 g of 4-iodotoluene (9.2 mmol), 223 mg of Mg, and 1.2 mL of cyclohexanone in anhydrous Et_2O to afford 0.95 g (54%) of a white solid after silica gel chromatography (5-10% EtOAc-hexanes). m.p. 48-49°C. IR (neat): 3398, 2925, 2858, 1513, 1447, 1375, 1350, 1257, 1132, 1035, 1014, 966, 905, 849, 811 cm^{-1}. ^1H NMR (400 MHz, $CDCl_3$) δ 7.37 (d, *J* = 8.3 Hz, 2H), 7.13 (d, *J* = 8.0 Hz, 2H), 2.32 (s, 3H), 1.85-1.67 (m, 8H), 1.63-1.55 (m, 2H). ^{13}C NMR (100 MHz, $CDCl_3$) δ 146.5, 136.2, 128.9, 124.5, 73.0, 38.9, 25.5, 22.2, 20.9. HRMS (EI) *m*/*e* calcd. for $C_{13}H_{18}O$ $[M-H]^+$: 190.1358; found: 190.1357.

1-(4-fluorophenyl)cyclohexanol

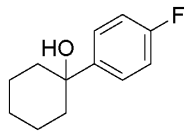

The reaction was completed with 2.0 g of 1-bromo-4-fluorobenzene (11.4 mmol), 277 mg of Mg, and 1.45 mL of cyclohexanone in anhydrous THF to afford 1.34 g (61%) of a white solid after silica gel chromatography (10% EtOAc-hexanes). m.p. 68-70°C. IR (neat): 3307, 2926, 2856, 1600, 1509, 1447, 1384, 1353, 1258, 1231, 1208, 1161, 1136, 1034, 1012, 976, 904, 830, 812, 700 cm^{-1}. ^{1}H NMR (300 MHz, $CDCl_3$) δ 7.47 (dd, J = 5.5 Hz, J = 8.6 Hz, 2H), 7.01 (t, J = 8.7 Hz, 2H), 1.88-1.56 (m, 11H). ^{13}C NMR (75 MHz, $CDCl_3$) δ 161.6 (d, J = 244 Hz), 145.2 (d, J = 3 Hz), 126.3 (d, J = 8 Hz), 114.8 (d, J = 21 Hz), 72.8, 39.0, 25.4, 22.2. HRMS (EI) *m*/*e* calcd. for $C_{12}H_{15}FO$ $[M-H]^+$: 194.1107; found: 194.1111.

1-(4-chlorophenyl)cyclohexanol

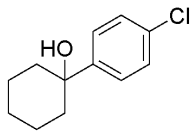

The reaction was completed with 2.0 g of 1-bromo-4-chlorobenzene (10.4 mmol), 253 mg of Mg, and 1.40 mL of cyclohexanone in anhydrous THF to afford 0.64 g (29%) of a white solid after silica gel chromatography (10% EtOAc-hexanes). m.p. 77-78.5°C. IR (neat): 3339, 2924, 2857, 1495, 1446, 1381, 1133, 1094, 1034, 1010, 974, 966, 903, 821cm^{-1}. ^{1}H NMR (400 MHz, $CDCl_3$) δ 7.43 (m, 2H), 7.30 (m, 2H), 1.84-1.56 (m, 11H). ^{13}C NMR (100 MHz, $CDCl_3$) δ 147.9, 132.4, 128.2, 126.1, 72.9, 38.8, 25.4, 22.1. HRMS (EI) *m*/*e* calcd. for $C_{12}H_{18}ClO$ $[M-H]^+$: 210.0811; found: 210.0813.

1-(4-(trifluoromethyl)phenyl)cyclohexanol

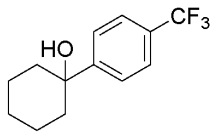

The reaction was completed with 2.5 g of 4-bromobenzotrifluoride (11.1 mmol), 270 mg of Mg, and 1.49 mL of cyclohexanone in anhydrous THF to afford 1.60 g (59%) of a pale yellow-white solid after silica gel chromatography (10% EtOAc-hexanes). m.p. 61-62°C. IR (neat): 3331, 2935, 2862, 1618, 1450, 1405, 1323, 1159, 1107, 1069, 1034, 1010, 978, 830, 710 cm^{-1}. ^{1}H NMR (400 MHz, $CDCl_3$) δ 7.47 (dd, J = 8.7 Hz, J = 8.7 Hz, 4H), 1.88-1.62 (m, 11H). ^{13}C NMR (100 MHz, $CDCl_3$) δ 153.4, 125.20, 125.16, 125.13, 125.0, 73.2, 38.8, 25.3, 22.0. HRMS (EI) *m*/*e* calcd. for $C_{13}H_{15}F_3O$ $[M-H]^+$: 244.1075; found: 244.1069.

4-cyclohexenyl-*N,N*-dimethylaniline

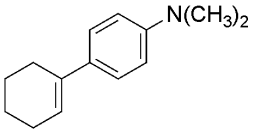

Unexpectedly, the tertiary alcohol product was dehydrated and the alkene product was made in one step rather than two. The reaction was completed with 2.5 g of 4-bromo-*N,N*-dimethylaniline (12.5 mmol), 304 mg of Mg, and 1.68 mL of cyclohexanone in anhydrous THF to afford 1.21 g (44%) of a white solid after silica gel chromatography (5-10% Et_2O-hexanes). ^{1}H NMR spectrum was in accordance with literature sources.[24]

1.4.4.2 General Procedure for the Synthesis of 1-Phenyl-1-cyclohexene Derivatives

The appropriate cyclohexanol derivative (1.0 equiv) and *p*-toluenesulfonic acid (0.05 equiv) were dissolved in toluene (0.1M) in a flask equipped with a magnetic stir bar, Dean-Stark apparatus and condenser. The solution was refluxed (130°C) for 2 hours and then cooled to room

[24] Oosterbaan, W. D.; van Gerven, P. C. M.; van Walree, C. A.; Koeberg, M.; Piet, J. J.; Havenith, R. W. A.; Zwikker, J. W.; Jenneskens, L. W.; Gleiter, R. *Eur. J. Org. Chem.* **2003**, 3117.

temperature. The mixture was washed with H_2O (3x) upon which the organic layer was dried with $MgSO_4$, filtered and concentrated. Lastly, the products were purified by silica gel chromatography.

1-methoxy-4-cyclohexenylbenzene

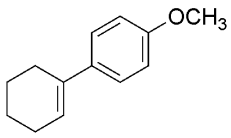

The reaction was completed with 500 mg of 1-(4-methoxyphenyl)cyclohexanol (2.42 mmol), and 23 mg of *p*-toluenesulfonic acid in refluxing toluene, to afford 243 mg (53%) of a pale yellowish-white solid after silica gel chromatography (0-5% Et_2O-hexanes). ^1H NMR spectrum was in accordance with literature sources.[25]

1-methyl-4-cyclohexenylbenzene

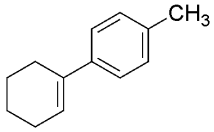

The reaction was completed with 700 mg of 1-(4-methylphenyl)cyclohexanol (3.68 mmol), and 34 mg of *p*-toluenesulfonic acid in refluxing toluene, to afford 525 mg (83%) of a white solid after silica gel chromatography (2-5% EtOAc-hexanes). ^1H NMR spectrum was in accordance with literature sources.[26]

---

[25] Yuan, D.-Y.; Tu, Y.-Q.; Fan, C.-A. *J. Org. Chem.* **2008**, *73*, 7797.

[26] Gauthier, D.; Beckendorf, S.; Gosig, T. M.; Lindhardt, A. T.; Skrydstrup, T. *J. Org. Chem.* **2009**, *74*, 3536.

1-fluoro-4-cyclohexenylbenzene

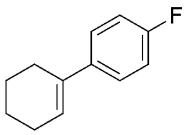

The reaction was completed with 1.0 g of 1-(4-fluorophenyl)cyclohexanol (5.15 mmol), and 50 mg of *p*-toluenesulfonic acid in refluxing toluene, to afford 733 mg (81%) of a clear and colourless solid after silica gel chromatography (2-5% EtOAc-hexanes). m.p. 31°C. IR (neat): 2928, 2860, 2838, 1640, 1596, 1504, 1436, 1225, 1161, 1137, 1100, 1011, 917, 851, 814, 798, 736 cm^{-1}. ^{1}H NMR (400 MHz, $CDCl_3$) δ 7.34-7.28 (m, 2H), 7.00-6.3 (m, 2H), 6.06-6.02 (m, 1H), 2.39-2.32 (m, 2H), 2.22-2.14 (m, 2H), 1.80-1.72 (m, 2H), 1.68-1.60 (m, 2H). ^{13}C NMR (100 MHz, $CDCl_3$) δ 161.8 (d, J = 243 Hz), 138.8 (d, J = 4 Hz), 135.7, 126.4 (d, J = 7 Hz), 124.6, 114.8 (d, J = 20 Hz), 27.5, 25.8, 23.0, 22.1. HRMS (EI) *m*/*e* calcd. for $C_{12}H_{13}F$ $[M-H]^+$: 176.1001; found: 176.1002.

1-chloro-4-cyclohexenylbenzene

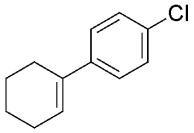

The reaction was completed with 500 mg of 1-(4-chlorophenyl)cyclohexanol (2.37 mmol), and 23 mg of *p*-toluenesulfonic acid in refluxing toluene, to afford 442 mg (97%) of a white solid after silica gel chromatography (2-5% EtOAc-hexanes). ^{1}H NMR spectrum was in accordance with literature sources.[27]

[27] Olsson, V. J.; Szabo, K. J. *Angew. Chem. Int. Ed.* **2007**, *46*, 6891.

1-trifluoromethyl-4-cyclohexenylbenzene

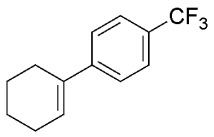

The reaction was completed with 1.0 g of 1-(4-(trifluoromethyl)phenyl)cyclohexanol (4.10 mmol), and 39 mg of *p*-toluenesulfonic acid in refluxing toluene, to afford 764 mg (80%) of a clear and colourless solid after silica gel chromatography (2% EtOAc-hexanes). m.p. 32°C. IR (neat): 2938, 2839, 1613, 1412, 1320, 1164, 1112, 1069, 1012, 921, 862, 823, 800, 731, 672 cm^{-1}. ^{1}H NMR (400 MHz, $CDCl_3$) δ 7.53 (d, *J* = 8.0 Hz, 2H), 7.44 (d, *J* = 8.0 Hz, 2H), 6.22-6.16 (m, 1H), 2.42-2.34 (m, 2H), 2.25-2.17 (m, 2H), 1.82-1.73 (m, 2H), 1.70-1.61 (m, 2H). ^{13}C NMR (100 MHz, $CDCl_3$) δ 146.2, 135.7, 129.0, 128.6, 128.5, 128.3, 128.0, 127.0, 125.8, 125.1, 125.1, 125.08, 123.1, 27.3, 25.9, 22.9, 22.0. HRMS (EI) *m*/*e* calcd. for $C_{13}H_{13}F_3$ $[M-H]^+$: 226.0969; found: 226.0966.

1-*tert*-butyl-4-cyclohexenylbenzene

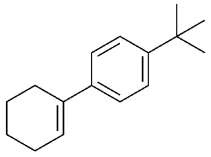

Clear oil prepared by Dr. Yang Li. IR (neat): 2961, 2928, 2859, 2834, 1508, 1475, 1462, 1362, 1269, 1112, 919, 820, 800, 738, 701 cm^{-1}. ^{1}H NMR (400 MHz, $CDCl_3$) δ 7.31 (s, 4H), 6.11-6.06 (m, 1H), 2.43-2.35 (m, 2H), 2.22-2.40 (m, 2H), 1.80-1.72 (m, 2H), 1.68-1.59 (m, 2H), 1.31 (s, 9H). ^{13}C NMR (100 MHz, $CDCl_3$) δ 149.4, 139.8, 136.3, 125.0, 124.6, 124.0, 34.4, 31.3, 27.4, 25.9, 23.1, 22.2. HRMS (EI) *m*/*e* calcd. for $C_{16}H_{22}$ $[M-H]^+$: 214.1722; found: 214.1723.

1.4.4.3 General Procedure for the Synthesis of 1-Phenyl-1-cylohexyl hydroxyacetate Derivatives

The appropriate cyclohexenylbenzene derivative (1.0 equiv) and $PhI(OAc)_2$ (1.1 equiv) were added to a flask containing a stir bar, acetic acid (0.1M) and H_2O (3.0 equiv). After stirring, the $[Pd(dppp)(H_2O)_2](OTf)_2$ catalyst (0.02 equiv) was added and the reaction mixture was stirred at

room temperature. Upon completion, the crude mixture was concentrated on a rotary evaporator and purified by silica gel chromatography (10-20% EtOAc-hexanes).

(1*S*,2*S*)-2-(4-methoxyphenyl)-2-hydroxycyclohexyl acetate

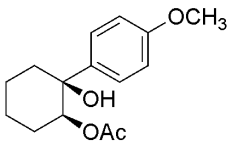

The dioxygenation was carried out with 94 mg of 1-methoxy-4-cyclohexenylbenzene (0.5 mmol), 177 mg of $PhI(OAc)_2$, 27 μL of H_2O, and 8.5 mg of $[Pd(dppp)(H_2O)_2](OTf)_2$ in 5 mL acetic acid. The reaction was complete after 10 minutes and after purification 37 mg (28%) of a pale yellowish-white solid was isolated. m.p. 101.5-102.5°C. IR (neat): 3514, 2947, 2936, 2859, 1714, 1614, 1515, 1462, 1445, 1375, 1357, 1301, 1275, 1247, 1180, 1145, 1086, 1032, 984, 971, 947, 865, 817, 806, 722 cm^{-1}. ^1H NMR (400 MHz, $CDCl_3$) δ 7.38-7.33 (m, 2H), 6.87-8.82 (m, 2H), 5.24 (dd, *J* = 5.4Hz, *J* = 10.4Hz, 1H), 3.77 (s, 3H), 2.22-2.20 (m, 1H), 1.92-1.84 (m, 3H), 1.82 (s, 3H), 1.80-1.40 (m, 5H). ^{13}C NMR (75 MHz, $CDCl_3$) δ 169.8, 158.4, 138.1, 125.8, 113.5, 76.2, 74.9, 55.2, 39.8, 27.2, 24.1, 21.1, 20.9. HRMS (EI) *m*/*e* calcd. for $C_{15}H_{20}O_4$ $[M-H]^+$: 264.1362; found: 264.1364.

(1*S*,2*S*)-2-(4-methylphenyl)-2-hydroxycyclohexyl acetate

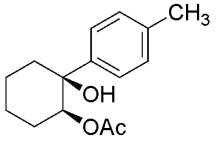

The dioxygenation was carried out with 86 mg of 1-methyl-4-cyclohexenylbenzene (0.5 mmol), 177 mg of $PhI(OAc)_2$, 27 μL of H_2O, and 8.5 mg of $[Pd(dppp)(H_2O)_2](OTf)_2$ in 5 mL acetic acid. The reaction was complete after 10 minutes and after purification 67 mg (48%) of a white solid was isolated. m.p. 91-92°C. IR (neat): 3531, 2938, 2927, 2857, 1721, 1518, 1445, 1375, 1355, 1244, 1141, 1082, 1033, 993, 974, 867, 815, 790, 722 cm^{-1}. ^1H NMR (400 MHz, $CDCl_3$) δ 7.34-7.30 (m, 2H), 7.15-7.10 (m, 2H), 5.27 (dd, *J* = 5.3Hz, *J* = 10.6Hz, 1H), 2.32 (s, 3H), 2.19 (d, *J* = 2.1Hz, 1H), 1.93-1.83 (m, 3H), 1.82 (s, 3H), 1.80-1.40 (m, 5H). ^{13}C NMR (100 MHz, $CDCl_3$) δ 170.0, 143.2, 136.7, 136.7, 129.1, 124.8, 76.4, 75.4, 40.0, 31.1, 27.4, 24.4, 21.3, 21.2. HRMS (EI) *m*/*e* calcd. for $C_{15}H_{20}O_3$ $[M-H]^+$: 248.1412; found: 248.1409.

(1*S*,2*S*)-2-(4-fluorophenyl)-2-hydroxycyclohexyl acetate

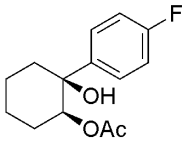

The dioxygenation was carried out with 88 mg of 1-fluoro-4-cyclohexenylbenzene (0.5 mmol), 177 mg of $PhI(OAc)_2$, 27 μL of H_2O, and 8.5 mg of $[Pd(dppp)(H_2O)_2](OTf)_2$ in 5 mL acetic acid. The reaction was complete after 2 hours and after purification 74 mg (58%) of a white solid was isolated. m.p. 107-108°C. IR (neat): 3534, 3490, 2952, 2938, 2865, 1712, 1599, 1507, 1376, 1244, 1225, 1162, 1142, 1081, 1032, 984, 952, 852, 833, 827, 724 cm^{-1}. ^1H NMR (400 MHz, $CDCl_3$) δ 7.44-7.38 (m, 2H), 7.03-6.96 (m, 2H), 5.25 (dd, J = 5.1Hz, J = 10.7Hz, 1H), 2.22 (d, J = 2.0Hz, 1H), 1.94-1.83 (m, 3H), 1.82 (s, 3H), 1.80-1.40 (m, 5H). ^{13}C NMR (75 MHz, $CDCl_3$) δ 169.7, 161.7 (d, J = 244 Hz), 141.7 (d, J = 3Hz), 126.4 (d, J = 8Hz), 114.9 (d, J = 21Hz), 76.1, 75.0, 39.8, 27.2, 24.1, 21.0, 20.8. HRMS (EI) *m*/*e* calcd. for $C_{14}H_{17}FO_3$ $[M-H]^+$: 252.1162; found: 252.1165.

(1*S*,2*S*)-2-(4-chlorophenyl)-2-hydroxycyclohexyl acetate

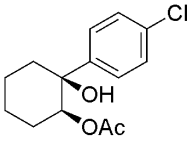

The dioxygenation was carried out with 96 mg of 1-chloro-4-cyclohexenylbenzene (0.5 mmol), 177 mg of $PhI(OAc)_2$, 27 μL of H_2O, and 8.5 mg of $[Pd(dppp)(H_2O)_2](OTf)_2$ in 5 mL acetic acid. The reaction was complete after 2 hours and after purification 106 mg (79%) of a white solid was isolated. m.p. 109-110°C. IR (neat): 3519, 2942, 2858, 1719, 1494, 1376, 1243, 1219, 1142, 1082, 1036, 994, 975, 866, 843, 821, 796, 748 cm^{-1}. ^1H NMR (400 MHz, $CDCl_3$) δ 7.40-7.36 (m, 2H), 7.32-7.26 (m, 2H), 5.24 (dd, J = 5.0Hz, J = 10.8Hz, 1H), 2.23-2.21 (m, 1H), 1.94-1.83 (m, 3H), 1.82 (s, 3H), 1.80-1.40 (m, 5H). ^{13}C NMR (75 MHz, $CDCl_3$) δ 169.6, 144.5, 132.7, 128.3, 126.2, 76.0, 75.1, 39.7, 27.1, 24.1, 20.9, 20.8. HRMS (EI) *m*/*e* calcd. for $C_{14}H_{17}ClO_3$ $[M-H]^+$: 268.0866; found: 268.0869.

(1*S*,2*S*)-2-(4-(trifluoromethyl)phenyl)-2-hydroxycyclohexyl acetate

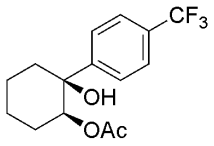

The dioxygenation was carried out with 113 mg of 1-trifluoromethyl-4-cyclohexenylbenzene (0.5 mmol), 177 mg of $PhI(OAc)_2$, 27 μL of H_2O, and 8.5 mg of $[Pd(dppp)(H_2O)_2](OTf)_2$ in 5 mL acetic acid. The reaction was complete after 16 hours and after purification 54 mg (36%) of a white solid was isolated. m.p. 115-116°C. IR (neat): 3513, 2944, 2862, 1724, 1619, 1411, 1379, 1324, 1240, 1219, 1144, 1114, 1073, 1037, 1018, 996, 976, 869, 832, 800, 728 cm^{-1}. ^1H NMR (400 MHz, $CDCl_3$) δ 7.58 (s, 2H), 7.26 (s, 2H), 5.31 (dd, *J* = 4.9Hz, *J* = 10.9Hz, 1H), 2.30 (d, *J* = 2.1Hz, 1H), 1.98-1.83 (m, 3H), 1.81 (s, 3H), 1.80-1.42 (m, 5H). ^{13}C NMR (75 MHz, $CDCl_3$) δ 169.6, 150.1, 129.2 (d, *J* = 32Hz), 124.1 (d, *J* = 269 Hz), 125.20 (d, *J* = 3Hz), 125.19 (d, J = 11Hz), 75.9, 75.3, 39.6, 27.1, 24.0, 20.8, 20.7. HRMS (EI) *m*/*e* calcd. for $C_{15}H_{17}F_3O_3$ $[M-H]^+$: 302.1130; found: 302.1131.

(1*S*,2*S*)-2-(4-*tert*-butylphenyl)-2-hydroxycyclohexyl acetate

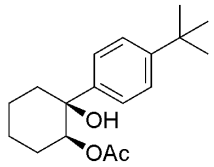

The dioxygenation was carried out with 107 mg of 1-*tert*-butyl-4-cyclohexenylbenzene (0.5 mmol), 177 mg of $PhI(OAc)_2$, 27 μL of H_2O, and 8.5 mg of $[Pd(dppp)(H_2O)_2](OTf)_2$ in 5 mL acetic acid. The reaction was complete after 10 minutes and after purification 96 mg (66%) of a white solid was isolated. m.p. 89.5-90.5°C. IR (neat): 3531, 2958, 2862, 1718, 1509, 1374, 1362, 1347, 1291, 1254, 1241, 1202, 1109, 1080, 1031, 991, 973, 952, 873, 852, 824, 804, 699 cm^{-1}. ^1H NMR (400 MHz, $CDCl_3$) δ 7.37-7.32 (m, 4H), 5.28 (dd, J = 5.2Hz, J = 10.6Hz, 1H), 2.21 (d, J = 2.1Hz, 1H), 1.96-1.84 (m, 3H), 1.83 (s, 3H), 1.80-1.40 (m, 5H), 1.30 (s, 9H). ^{13}C NMR (100 MHz, $CDCl_3$) δ 169.9, 149.7, 142.9, 125.1, 124.3, 76.1, 75.0, 39.8, 34.3, 31.2, 27.2, 24.1, 21.1, 20.9. HRMS (EI) *m*/*e* calcd. for $C_{18}H_{26}O_3$ $[M-H]^+$: 290.1882; found: 290.1874.

1.4.4.4 General Procedure for Reaction Kinetics Experiments

In an oven dried, argon purged 1DR vial with a magnetic stir bar, 1-phenyl-1-cyclohexene (15.8 mg, 0.1 mmol) and dodecane (17.0 mg, 0.1 mmol) was added with a microsyringe. While adding all reagents to the vial a septa with an argon balloon was kept on the vial. Next, anhydrous acetic acid (0.8 mL, 0.1 M) was added, followed by H_2O (10.8 μL, 0.6 mmol), and lastly $PhI(OAc)_2$ (35.4 mg, 0.11 mmol). The capped mixture was stirred in an oil bath at 20°C for approximately 5 minutes at 700 rpm in order to dissolve all of the reagents. Before adding the catalyst solution, one aliquot (time = 0 min) of 20 μL was taken out of the reaction mixture and quenched in 2 mL of a saturated $NaHSO_3$ solution. At the exact moment the $[Pd(dppp)(H_2O)_2](OTf)_2$ solution (0.01mmol/mL in AcOH, 0.2 mL, 0.002 mmol) was added to the vial, a timer was started. 20 μL aliquots were taken out of the reaction at exactly 30 sec, 1, 2, 5, 7, 10, 15, 21, 28, and 36 minutes. Immediately after their removal from the reaction the aliquots were quenched in 2 mL of a saturated $NaHSO_3$ solution. These aqueous mixtures were extracted with HPLC grade EtOAc, dried over Na_2SO_4 and filtered into GC vials. Each of the samples was analyzed by GC-FID to determine the amount of hydroxyacetate product that was formed at each time interval (by comparison to the dodecane internal standard). When plotting the concentration of product formed with respect to time in a graph, the slope of the tangent to the curve from 0 to about 2 minutes (first 10% of the reaction) represents the initial rate of reaction. All reaction kinetics were determined by using the initial rate of reaction method. Each experiment was repeated a minimum of three times in order to perform an average of the values obtained.

1.4.4.5 General Procedure for Hammett Plot Kinetic Experiments

In this scenario, initial rates of reaction were required for the different aryl substituted 1-phenyl-1-cyclohexene derivatives. However, to avoid repeating the kinetic experiments three times and to increase accuracy, competitive kinetic experiments were done between the two substituted substrates with the closest reactivity. In other words, the initial rates of reaction were determined in the same procedure as outlined in section 1.4.4.4, but *two* reacting substrates were used in each reaction. The substrates were tested in the following pairs: (a) 1-phenyl-1-cyclohexene (10.0 equiv) with 1-methyl-4-cyclohexenylbenzene (1.0 equiv), (b) 1-methyl-4-cyclohexenylbenzene (1.0 equiv) with 1-*tert*-butyl-4-cyclohexenylbenzene (1.0 equiv), (c) 1-phenyl-1-cyclohexene (1.0 equiv) with 1-chloro-4-cyclohexenylbenzene (1.0 equiv), (d) 1-chloro-4-

cyclohexenylbenzene (1.0 equiv) with 1-fluoro-4-cyclohexenylbenzene (1.0 equiv), (e) 1-chloro-4-cyclohexenylbenzene (1.0 equiv) with 1-trifluoromethyl-4-cyclohexenylbenzene (10.0 equiv). All other reagent equivalents are the same as in section 1.4.4.4, with the exception of reaction (a) where a 5x dilution was applied (ie. 4.8 mL solvent). The log of the initial rates obtained was graphed versus the σ_p parameter obtained from literature[28] to complete the Hammett plot.

The following was determined with graphing analysis:

(a) *p*-Me substituted substrate reacts 11.83 times faster than 1-phenyl-1-cyclohexene

(b) *p*-Me substituted substrate reacts 1.43 times faster than *p*-*t*Bu substituted substrate

(c) 1-phenyl-1-cyclohexene reacts 4.06 times faster than *p*-Cl substituted substrate

(d) *p*-F substituted substrate reacts 3.81 times faster than *p*-Cl substituted substrate

(e) *p*-Cl substituted substrate reacts 19.27 times faster than *p*-CF_3 substituted substrate

1.4.4.6 General Procedure for ^{18}O Labelling in the Dioxygenation of 1-Phenyl-1-cyclohexene

To a solution of 1-phenyl-1-cyclohexene (33.2 mg, 0.2 mmol), $PhI(OAc)_2$ (180 mg, 1.1 equiv.), $H_2{}^{18}O$ (97 atom % from Isotec, 10 equiv.) in anhydrous HOAc (2 mL) was added $[Pd(dppp)(H_2O)_2](OTf)_2$ (2 mol %). The reaction was stirred at room temperature for 3 hours. HOAc was removed directly on rotary evaporator. Flash column chromatography afforded 28.4 mg (61%) of hydroxyacetate as white solid. The NMR matched the one without labeling.[14] Labelled product IR (neat): 3579.78, 3532.14, 3055.96, 2942.24, 2858.25, **1689.10**, 1494.69, 1446.11, 1373.21, 1264.15, 1249.96, 1141.05, 1034.22, 989.20, 737.93, 702.70 cm^{-1}. Unlabeled product IR (neat): 3494.35, 3060.03, 3027.13, 2940.78, 2861.98, **1724.38**, 1494.93, 1446.37, 1373.13, 1244.14, 1073.96, 1038.95, 990.40, 865.18, 758.18, 700.91 cm^{-1}.

---

[28] Hansch, C.; Leo, A.; Taft, R. W. *Chem. Rev.* **1991**, *91*, 165.

1.4.4.7 General Procedure for the Synthesis of 5-Arylpent-4-yn-1-ol Derivatives

Prepared based on a literature procedure.[29] In a flame dried and argon purged flask equipped with a magnetic stir bar, aryl iodide (1.2 equiv), 4-pentyne-1-ol (1.0 equiv), CuI (0.02 equiv), Et_3N (20 equiv), and anhydrous THF were combined in no particular order. The $PdCl_2(PPh_3)_2$ catalyst (0.01 equiv) was added last to the stirring mixture, which was left to react at room temperature for 16 hours under an argon atmosphere. After the reaction was complete, the crude mixture was washed with 1M HCl (3x). The organic layer was subsequently dried over Na_2SO_4, filtered, and concentrated under reduced pressure. The crude products were purified by silica gel chromatography. (To remove trace palladium from the products, the substrates were dissolved in toluene and an equal amount of 20% $NaHSO_3$ and then heated to 60°C for 1 hour with vigorous stirring. The organic layer was then separated and dried over $MgSO_4$, filtered and concentrated under reduced pressure.)[30]

5-phenylpent-4-yn-1-ol

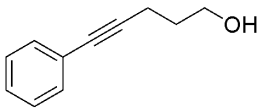

Clear oil prepared by Dr. Yang Li. ^1H NMR spectrum was in accordance with literature sources.[31]

5-*p*-tolylpent-4-yn-1-ol

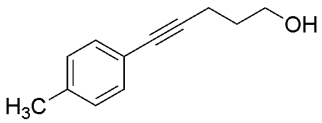

Prepared with 500 mg of 4-pentyne-1-ol (5.94 mmol), 1.55 g of 4-iodotoluene, and 41 mg of $PdCl_2(PPh_3)_2$ catalyst. After purification (15-50% Et_2O-hexanes), 910 mg (88%) of a light yellow oil which crystallized upon standing into a colourless solid was isolated. ^1H NMR spectrum was in accordance with literature sources.[29]

---

[29] Gericke, K. M.; Chai, D. I.; Lautens, M. *Tetrahedron* **2008**, *64*, 6002.

[30] Bullock, K. M.; Mitchell, M. B.; Toczko, J. F. *Org. Proc. Res. & Dev.* **2008**, *12*, 896.

[31] Fuji, K.; Morimoto, T.; Tsutsumi, K.; Kakiuchi, K. *Chem. Commun*. **2005**, 3295.

5-(4-methoxyphenyl)pent-4-yn-1-ol

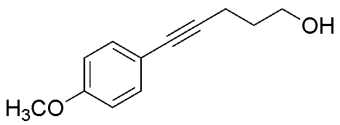

White solid prepared by Dr. Yang Li. m.p. 39-40.5°C. IR (neat): 3287, 2936, 2873, 2838, 1607, 1569, 1509, 1464, 1441, 1373, 1289, 1244, 1173, 1109, 1064, 1030, 902, 836, 824, 798 cm^{-1}. ^{1}H NMR (400 MHz, $CDCl_3$) δ 7.34-7.29 (m, 2H), 6.83- 6.78 (m, 2H), 3.82-3.77 (m, 2H), 3.78 (s, 3H), 2.51 (t, J = 6.9Hz, 2H), 2.0 (br, 1H), 1.84 (qn, J = 6.6Hz, 2H). ^{13}C NMR (100 MHz, $CDCl_3$) δ 159.1, 132.8, 115.9, 113.8, 87.7, 80.8, 61.8, 55.2, 31.4, 15.9. HRMS (EI) *m*/*e* calcd. for $C_{12}H_{14}O_2$ $[M-H]^+$: 190.0994; found: 190.0998.

5-(naphthalen-1-yl)pent-4-yn-1-ol

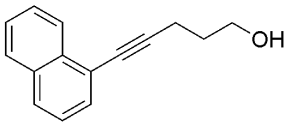

Prepared with 276 mg of 4-pentyne-1-ol (3.28 mmol), 1.0 g of 1-iodonaphthalene, and 23 mg of $PdCl_2(PPh_3)_2$ catalyst. After purification (15-30% EtOAc-hexanes), 556 mg (81%) of a colourless oil was isolated. ^{1}H NMR spectrum was in accordance with literature sources.[29]

1.4.4.8 General Procedure for the Synthesis of (*E*)-5-Arylpent-4-en-1-ol Derivatives

To a flame dried and argon purged flask equipped with a magnetic stir bar was added the appropriate 5-arylpent-4-yn-1-ol derivative (1.0 equiv) and anhydrous THF (0.05M). After dissolving, the flask was cooled to 0°C in an ice bath and stirred for 10 minutes to equilibrate. $LiAlH_4$ (5.0 equiv) was added slowly and upon completion the flask was fitted with a condenser. The solution was refluxed for 72 hours with an argon balloon and then quenched slowly by adding EtOAc dropwise into the stirring mixture, followed by H_2O. The mixture and extracted with Et_2O (3x) and the combined organic layers were dried over Na_2SO_4, filtered and concentrated under reduced pressure. Products were purified by silica gel chromatography.

(*E*)-5-phenylpent-4-en-1-ol

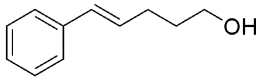

Prepared with 200 mg of 5-phenylpent-4-yn-1-ol (1.25 mmol) and 238 mg of $LiAlH_4$. After column chromatography (20% EtOAc-hexanes), 150 mg (74%) of a colourless oil was isolated. ^{1}H NMR spectrum was in accordance with literature sources.[32]

(*E*)-5-*p*-tolylpent-4-en-1-ol

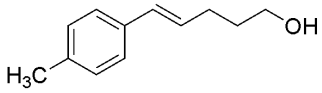

Prepared with 155 mg of 5-*p*-tolylpent-4-yn-1-ol (0.89 mmol) and 169 mg of $LiAlH_4$. After column chromatography (20% EtOAc-hexanes), 109 mg (69%) of a colourless oil was isolated. ^{1}H NMR spectrum was in accordance with literature sources.[33]

(*E*)-5-(4-methoxyphenyl)pent-4-en-1-ol

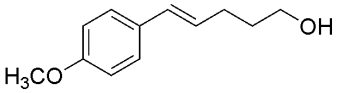

Prepared with 181 mg of 5-(4-methoxyphenyl)pent-4-yn-1-ol (0.95 mmol) and 181 mg of $LiAlH_4$. After column chromatography (20-35% EtOAc-hexanes), 67 mg (37%) of a colourless solid was isolated. ^{1}H NMR spectrum was in accordance with literature sources.[33]

---

[32] Seiders, II, J. R.; Wang, L.; Floreancig, P. E. *J. Am. Chem. Soc.* **2003**, *125*, 2406.

[33] Belanger, G.; Levesque, F.; Paquet, J.; Barbe, G. *J. Org. Chem.* **2005**, *70*, 291.

(*E*)-5-(naphthalen-1-yl)pent-4-en-1-ol

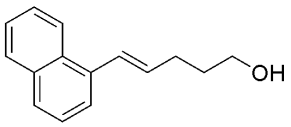

Prepared with 295 mg of 5-(naphthalen-1-yl)pent-4-yn-1-ol (1.40 mmol) and 267 mg of $LiAlH_4$. After column chromatography (15-30% EtOAc-hexanes), 158 mg (53%) of a colourless oil was isolated. IR (neat): 3305, 3043, 2935, 1689, 1590, 1508, 1434, 1394, 1169, 1057, 966, 791, 776 cm^{-1}. ^1H NMR (400 MHz, $CDCl_3$) δ 8.10 (d, J = 7.8Hz, 1H), 7.80-7.85 (m, 1H), 7.73 (d, J = 8.1Hz, 1H), 7.38-7.56 (m, 4H), 7.14 (d, J = 15.6Hz, 1H), 6.23 (td, J = 6.9Hz, J = 15.5Hz, 1H), 3.74 (t, J = 6.5Hz, 2H), 2.37-2.45 (m, 2H), 1.81 (td, J = 6.7Hz, J = 13.8Hz, 2H), 1.64 (br, 1H). ^{13}C NMR (100 MHz, $CDCl_3$) δ 135.5, 133.6, 133.3, 131.1, 128.4, 127.6, 127.3, 125.6, 123.9, 124.5, 62.4, 32.3, 29.7. HRMS (EI) *m*/*e* calcd. for $C_{15}H_{16}O$ $[M-H]^+$: 212.1201; found: 212.1198.

1.4.4.9 General Procedure for Intramolecular Pd-Catalyzed Olefin Dioxygenation

In a flame dried and argon purged 1DR vial equipped with a magnetic stir bar, the appropriate (*E*)-5-arylpent-4-en-1-ol (1.0 equiv) derivative was dissolved in anhydrous toluene (0.1M). $PhI(OAc)_2$ (1.5 equiv) and [Pd(*R*)-BINAP(μ-OH_2)]$_2$(OTf)$_2$ (0.01 equiv) catalyst were added and allowed to dissolve. The mixture was then heated to 50°C in an oil bath or heating block for 16 hours. After concentration under reduced pressure the crude mixture was purified by preparative TLC (15% EtOAC-hexanes). Two diastereomeric products were isolated for each reaction. The products were dissolved in *i*PrOH and analyzed by chiral HPLC to determine the enantiomeric excess.

phenyl(tetrahydrofuran-2-yl)methyl acetate

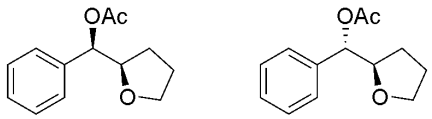

threo *erythro*

Prepared with 20 mg of (*E*)-5-phenylpent-4-en-1-ol (0.12 mmol), 59 mg of $PhI(OAc)_2$, and 2 mg of [Pd(*R*)-BINAP(μ-OH_2)]$_2$(OTf)$_2$. After purification by prep-TLC, 20 mg (75%) of two

colourless oils was isolated. Using the chiral OJ column on an HPLC (15 μL injection, 2 mL/min, 10% *i*PrOH-hexanes, 30 min), it was determined that the *threo* product had 36% ee and the *erythro* product had 22% ee. ^{1}H NMR spectrum was in accordance with literature sources.[14]

(tetrahydrofuran-2-yl)(p-tolyl)methyl acetate

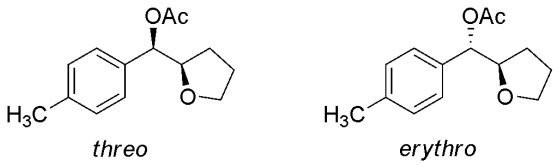

Prepared with 20 mg of (*E*)-5-*p*-tolylpent-4-en-1-ol (0.11 mmol), 55 mg of $PhI(OAc)_2$, and 2 mg of $[Pd(R)\text{-}BINAP(\mu\text{-}OH_2)]_2(OTf)_2$. After purification by prep-TLC, 1.3 and 1.1 mg (total 9%) of two colourless oils was isolated. Using the chiral OJ column on an HPLC (15 μL injection, 2 mL/min, 10% *i*PrOH-hexanes, 20 min), it was determined that the *threo* product had 9% ee and the *erythro* product had 9% ee. *threo* IR (neat): 2925, 2856, 1740, 1511, 1447, 1370, 1236, 1071, 1028, 968, 812 cm^{-1}. *erythro* IR (neat): 2925, 2857, 1742, 1515, 1458, 1369, 1234, 1181, 1071, 1021, 968, 810 cm^{-1}. *threo* ^{1}H NMR (300 MHz, $CDCl_3$) δ 7.28-7.23 (m, 2H), 7.17-7.12 (m, 2H), 5.60 (d, *J* = 7.9Hz, 1H), 4.22 (dd, *J* = 7.3Hz, *J* = 14.8Hz, 1H), 3.92-3.79 (m, 2H), 2.33 (s, 3H), 2.09 (s, 3H), 1.88-1.80 (m, 1H), 1.72-1.65 (m, 1H), 1.60-1.54 (m, 2H). ^{13}C NMR (100 MHz, $CDCl_3$) δ 170.3, 138.1, 134.9, 129.1, 127.4, 80.7, 77.9, 68.6, 28.4, 25.7, 21.3, 21.2. *erythro* ^{1}H NMR (300 MHz, $CDCl_3$) δ 7.27 (d, *J* = 8.0Hz, 2H), 7.15 (d, *J* = 7.9Hz, 2H), 5.73 (d, *J* = 5.2Hz, 1H), 4.18-4.24 (m, 1H), 3.73-3.79 (m, 2H), 2.33 (s, 3H), 2.1 (s, 3H), 1.95-1.92 (m, 1H), 1.84-1.75 (m, 3H). ^{13}C NMR (100 MHz, $CDCl_3$) δ 170.0, 137.8, 134.7, 129.0, 127.4, 80.7, 77.2, 68.9, 27.5, 25.6, 21.2, 21.1. HRMS (ESI) *m*/*e* calcd. for $C_{14}H_{18}O_3$ $[M\text{-}H]^+$: 234.1256; found: 257.1 $[M\text{-}Na]^+$.

(4-methoxyphenyl)(tetrahydrofuran-2-yl)methyl acetate

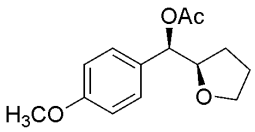

threo

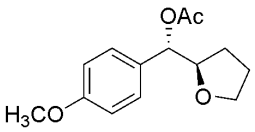

erythro

Prepared with 20 mg of (*E*)-5-(4-methoxyphenyl)pent-4-en-1-ol (0.10 mmol), 50 mg of $PhI(OAc)_2$, and 2 mg of $[Pd(R)\text{-}BINAP(\mu\text{-}OH_2)]_2(OTf)_2$. After purification by prep-TLC, 4.2 and 3.7 mg (total 30%) of two pale yellow oils was isolated. Using the chiral HPLC, it was determined that the *threo* product had 5% ee (OJ column, 15 μL injection, 1 mL/min, 1% *i*PrOH-hexanes, 80 min) and the *erythro* product had 16% ee (OD-H column, 4 μL injection, 1 mL/min, 1% *i*PrOH-hexanes, 30 min). *threo* IR (neat): 2923, 2870, 1732, 1612, 1515, 1463, 1370, 1304, 1235, 1175, 1069, 1027, 965, 829 cm^{-1}. *erythro* IR (neat): 2928, 2858, 1741, 1612, 1514, 1463, 1370, 1233, 1175, 1070, 1026, 967, 827 cm^{-1}. *threo* ^1H NMR (300 MHz, $CDCl_3$) δ 8.32 (d, *J* = 8.4Hz, 1H), 7.84 (dd, *J* = 8.2Hz, *J* = 12.3Hz, 2H), 7.62-7.42 (m, 4H), 6.42 (d, *J* = 7.9Hz, 1H), 4.53 (q, *J* = 7.3Hz, 1H), 4.00-3.81 (m, 2H), 2.12 (s, 3H), 1.94-1.76 (m, 2H), 1.66-1.50 (m, 2H). ^{13}C NMR (75 MHz, $CDCl_3$) δ 170.4, 133.9, 133.8, 131.1, 129.0, 128.8, 126.4, 125.8, 125.7, 125.2, 123.7, 80.8, 75.1, 68.6, 28.4, 25.8, 21.5. ery*thro* ^1H NMR (400 MHz, $CDCl_3$) δ 8.18 (d, *J* = 8.4Hz, 1H), 7.86 (d, *J* = 8.7Hz, 1H), 7.80 (d, *J* = 8.2Hz, 1H), 7.62-7.43 (m, 4H), 6.70 (d, *J* = 4.5Hz, 1H), 4.47-4.40 (m, 1H), 3.89-3.82 (m, 1H), 3.80-3.74 (m, 1H), 2.16 (s, 3H), 1.98-1.80 (m, 4H). ^{13}C NMR (100 MHz, $CDCl_3$) δ 169.9, 133.9, 133.7, 130.9, 128.8, 128.6, 126.3, 125.6, 125.2, 124.3, 123.3, 80.4, 73.5, 69.0, 26.9, 25.9, 21.2. HRMS (EI) *m*/*e* calcd. for $C_{14}H_{18}O_4$ $[M\text{-}H]^+$: 250.1205; found: 250.1202.

naphthalen-1-yl(tetrahydrofuran-2-yl)methyl acetate

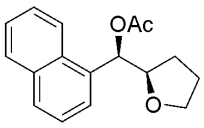

threo

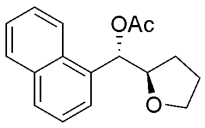

erythro

Prepared with 14 mg of (*E*)-5-(naphthalen-1-yl)pent-4-en-1-ol (0.06 mmol), 31 mg of $PhI(OAc)_2$, and 1.6 mg of $[Pd(R)\text{-}BINAP(\mu\text{-}OH_2)]_2(OTf)_2$. After purification by prep-TLC, 3.6 and 2.8 mg (total 37%) of two pale yellow oils was isolated. Using the chiral AD-H column on an HPLC (4 μL injection, 1 mL/min, 1% *i*PrOH-hexanes, 60 min), it was determined that the *erythro* product had 19% ee and the ee was inconclusive for the *threo* product. *threo* IR (neat): 2947, 2870, 1738, 1598, 1512, 1443, 1230, 1168, 1069, 1025, 965, 888, 801, 779 cm^{-1}. *erythro* IR (neat): 2926, 2870, 1742, 1598, 1511, 1444, 1368, 1228, 1166, 1069, 1025, 966, 937, 798, 777 cm^{-1}. *threo* ^1H NMR (400 MHz, $CDCl_3$) δ 7.31-7.27 (m, 2H), 6.89-6.85 (m, 2H), 5.59 (d, *J* = 7.9Hz, 1H), 4.22 (q, *J* = 7.3Hz, 1H), 3.92-3.82 (m, 2H), 3.80 (s, 3H), 2.09 (s, 3H), 1.89-1.78 (m, 2H), 1.74-1.64 (m, 1H), 1.56-1.46 (m, 1H). ^{13}C NMR (100 MHz, $CDCl_3$) δ 170.3, 159.6, 130.1, 128.8, 113.9, 80.7, 77.7, 68.6, 55.2, 28.4, 25.7, 21.3. ery*thro* ^1H NMR (400 MHz, $CDCl_3$) δ 7.33-7.30 (m, 2H), 6.90-6.85 (m, 2H), 5.70 (d, *J* = 5.2Hz, 1H), 4.21 (dd, *J* = 6.6Hz, *J* = 12.1Hz, 1H), 3.79 (s, 3H), 3.78-3.73 (m, 2H), 2.09 (s, 3H), 1.98-1.90 (m, 1H), 1.80-1.70 (m, 3H). mixture of *threo* and *erythro* ^{13}C NMR (100 MHz, $CDCl_3$) δ 170.1, 159.4, 129.8, 128.9, 125.8, 113.7, 113.5, 80.7, 68.7, 55.2, 39.0, 27.7, 25.6, 25.5, 22.3, 21.2. HRMS (EI) *m*/*e* calcd. for $C_{17}H_{18}O_3$ $[M\text{-}H]^+$: 270.1256; found: 270.1263.

Chapter 2
Indole Functionalization

2.1 Introduction

2.1.1 C–H Bond Activation

To functionalize an organic molecule can require multi-step synthetic sequences in order to install a new moiety at a predetermined position. Thus, for many chemists it has been their goal to directly convert unactivated C–H bonds into more valuable C–O, C–N, or even C–C bonds with the generation of a minimal amount of waste. This strategy can not only reduce the amount of reactions toward a target molecule, but also allow the preparation of compounds that would otherwise be inaccessible. However, due to the inertness of C–H bonds, functionalizing such a bond becomes difficult. One popular strategy to overcome this issue is to use transition metal-catalysis.[34] Metal catalysts can insert into C–H bonds (C–H metallation) to form organometallic reagents which can be trapped by reactive species to furnish newly functionalized derivatives. Another challenge in C–H bond activation is to ensure regioselectivity in cases where there are multiple C–H bonds that can potentially be functionalized. To circumvent this concern, directing group- or chelation-assisted C–H bond functionalizations were created.

2.1.2 Chelate-Assisted C–H Bond Activation

Chelate-assisted C–H bond activations employ functional groups to control the regioselectivity of C–H bond activation via coordination to the transition metal catalyst. Generally, directing groups are oxygen- or nitrogen-centered due to their ability to donate a lone pair of electrons. The strategy of using a functional group to direct transition metal insertion into a C–H bond was devised over two decades ago by Kleinman and Dubek (eq 24).[35]

---

[34] Alberico, D.; Scott, M. E.; Lautens, M. *Chem. Rev*. **2007**, *107*, 174.

[35] Kleinman, J. P.; Dubeck, M. *J. Am. Chem. Soc.* **1963**, *85*, 1544.

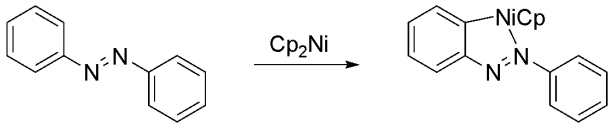

(24)

As depicted in Scheme 10, the directing group will coordinate to the transition metal catalyst so that the subsequent C–H bond insertion occurs via the formation of the kinetically or thermodynamically favoured five- or six-membered cycle.[34] The final product will have a new functionality installed *ortho* to the directing group. Thus in symmetrical substrates the possibility for both mono- and di-functionalization exists, while in unsymmetrical substrates sterics will guide functionalization to the more accessible *ortho* position.

Scheme 10. General scheme for chelate-assisted C–H bond functionalization.

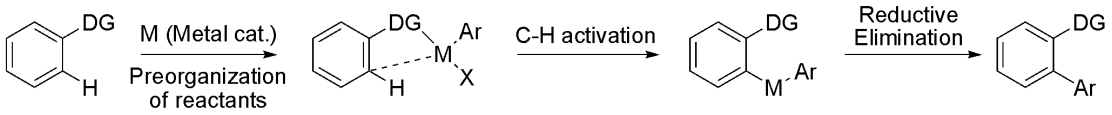

Some of the most common directing groups include the following organic moieties: phenols, ketones, aldehydes, amides, imines, pyridines, oxazolines and imidazolines.[34] While there are many more directing groups that could be discussed, only amide and urea functional groups will be examined in more detail.

2.1.2.1 Amide Directed C–H Bond Activation

After the successful implementation of phenol and ketone directed arylation, Miura was able to extend this methodology to the C–H bond functionalization of benzanilides as well.[36] The palladium-catalyzed direct arylation of benzanilides with aryl triflates and bromides afforded the diarylated product selectively, in very good yields (eq 25). Mechanistically, the proposed key step of this reaction would be the coordination of the amidate ion (generated *in-situ*) with the intermediary arylpalladium species.

---

[36] Oi, S.; Fukita, S.; Inoue, Y. *Chem. Commun.* **1998**, 2439.

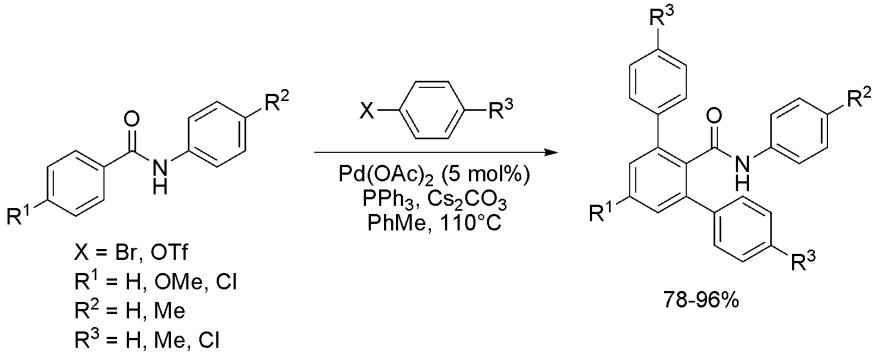

(25)

On the other hand, the Sanford group was able to circumvent the use of strong bases and expensive ligands by developing a palladium-catalyzed oxidative C–H bond arylation that could be carried out in the presence of moisture and air. In this amide-directed C–H bond functionalization hypervalent iodine substrates are used as the oxidizing arylation reagents or coupling partners (eq 26).[37] As described in their report, a $Pd^{II/IV}$ catalytic cycle is presumed to be involved in the reaction mechanism.

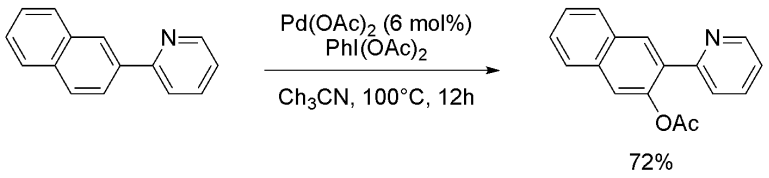

(26)

Another important account of amide-directed arylation was reported by Daugulis. Simple benzamide derivatives could undergo direct *ortho*-arylation with aryl iodide coupling reagents in the presence of a $Pd(OAc)_2$ catalyst, in trifluoroacetic acid and a stoichiometric amount of silver acetate (eq 27).[38]

---

[37] Kalyani, D.; Deprez, N. R.; Desai, L. V.; Sanford, M. S. *J. Am. Chem. Soc.* **2005**, *127*, 7330.

[38] Shabashov, D.; Daugulis, O. *Org. Lett.* **2006**, *8*, 4947.

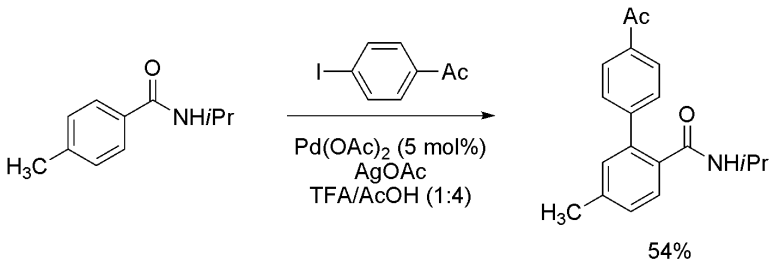

(27)

2.1.2.2 Urea Directed C–H Bond Activation

In 2009, the joint efforts of Lloyd-Jones and Booker-Milburn on the urea-directed *ortho*-carbonylation of aniline derivatives were published.[39] The *o*-carbonylation proceeded efficiently with 1 atm of CO, benzoquinone, TsOH and 5% [$Pd(OTs)_2(CH_3CN)_2$] catalyst loading at room temperature to produce cyclic imidate or methyl anthranilate derivatives (eq 28). It was noted by X-ray crystallography that the [$Pd(OTs)_2(CH_3CN)_2$] catalyst had a powerful activating effect on the aryl-urea moiety, in that the urea carbonyl was fully coordinated to the catalyst in a six-membered palladacycle.

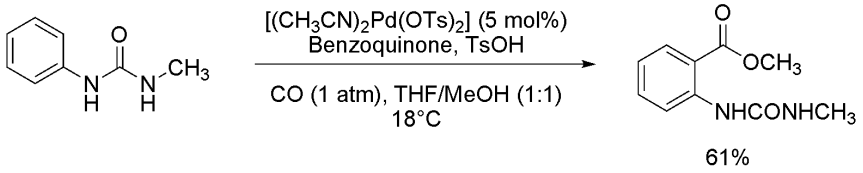

(28)

2.1.2.3 Directing Group-Assisted C–H Bond Halogenation

Generally, creating carbon–halogen bonds is a sought after goal in organic chemistry because it is an important way to establish a "handle" on an organic molecule so that it can further be functionalized to build up complexity and value with other existing methodologies. In their report on the *ortho*-carbonylation of aryl-urea substrates, Lloyd-Jones and Booker-Milburn identified other potential coupling reagents that could be used to functionalize aryl-ureas.[39] The

---

[39] Houlden, C. E.; Hutchby, M.; Bailey, C. D.; Ford, J. G.; Tyler, S. N. G.; Gagne, M. R.; Lloyd-Jones, G. C.; Booker-Milburn, K. I. *Angew. Chem. Int. Ed.* **2009**, *48*, 1830.

list of reagents included NBS and NCS, which under the reported conditions would install a bromine or chlorine atom, respectively at the *ortho* positions (eq 29).

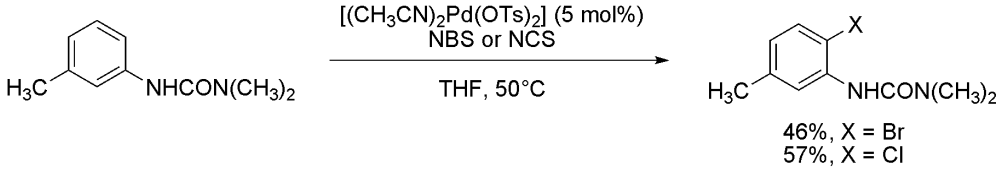

(29)

Sanford has also utilized the various *N*-halosuccinimide reagents in the halogenation of C–H bonds. A mild and simple $Pd(OAc)_2$ catalyzed method for the regioselective chlorination, bromination, and iodination of arenes was achieved with chelate-assisted C–H bond activation.[40] Selective mono-halogenation was shown to proceed in very good yields with pyridine (eq 30), oxime ether, isoquinoline, amide, and isoxazoline directing group moieties.

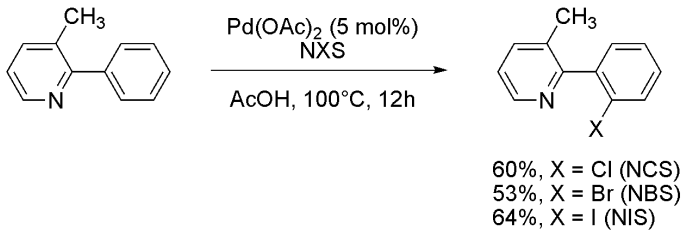

(30)

2.1.2.4 Directing Group-Assisted C–H Bond Oxygenation

As described in Section 1.1.3, Sanford was able to extend their previously developed C–H bond functionalization strategies to include C–H bond oxygenation. The oxidative functionalization was carried out with a $Pd(OAc)_2$ catalyst and a hypervalent iodine oxidant in acetic acid at 100°C.[12] With the use of chelation-assistance, excellent regioselectivity was achieved for a variety of aryl substrates, including pyridines and imines (eq 10).

---

[40] Kalyani, D.; Dick, A. R.; Anani, W. Q.; Sanford, M. S. *Org. Lett.* **2006**, *8*, 2523.

2.1.3 C–H Bond Activation of Indoles

Indoles have long been identified as valuable motifs in medicinal chemistry and have been marked as "privileged" structures due to their persistent appearance in natural products and pharmaceutical agents.[41] The synthesis of indoles and their functionalized derivatives has thus been an important endeavour for organic chemists. Prior to the use of direct arylation or C–H bond functionalization, the synthesis of substituted indoles was done by beginning with the appropriately functionalized starting materials before the construction of the indole core. However, it would be desirable to functionalize positions on the heterocycle after the construction of the indole scaffold, in order to gain access to a large variety of functionalized substrates in a short period of time, as would be necessary in an SAR (Structure Activity Relationship) study of indole derivatives. Currently, C–H bond activation approaches have been employed to functionalize the indole C2, C3 and C7 positions.

2.1.3.1 Indole C2 C–H Bond Activation

The first report of an intermolecular indole C–H bond functionalization was in 1989 when Ohta carried out the direct arylation of indoles with chloropyrazines (eq 31).[42]

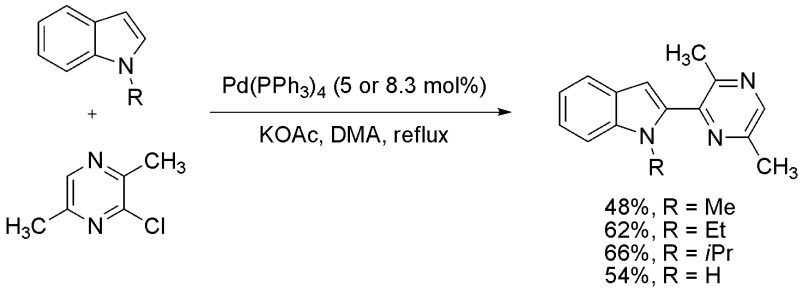

(31)

Since then, the Sames group has developed a number of reaction systems to selectively activate the C2 C–H bond. One of their first reports was a highly functional group tolerant palladium-catalyzed arylation of *N*-substituted indoles (eq 32).[43] Careful consideration of reaction conditions allowed for minimization of the competing homocoupling of the aryl iodide. Also, the

---

[41] Austin, J. F.; MacMillan, D. W. C.; *J. Am. Chem. Soc*. **2002**, 124, 1172.

[42] Akita, Y.; Itagaki, Y.; Takizawa, S.; Ohta, A. *Chem. Pharm. Bull.***1989**, *37*, 1477.

[43] Lane, B. S.; Sames, D. *Org. Lett.* **2004**, *6*, 2897.

substrate scope was found to be tolerant of alkyl and aryl substituents on the indole nitrogen, as well as various substituted aryl iodide coupling reagents.

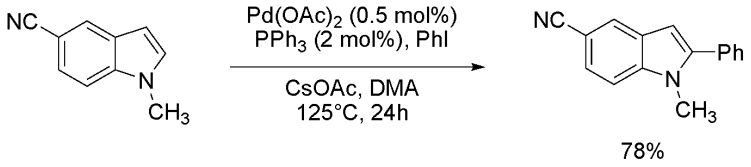

(32)

As an extension of his previous work, Sames later showed that the C2 arylation of free (N–H)-indoles and pyrroles could also be catalyzed by palladium under phosphine-free conditions.[44] However, another solution to this problem was to utilize an entirely different transition metal catalyst. Due to the high reactivity and selectivity of aryl-rhodium(III) complexes, the direct arylation of free (N–H)-indoles and pyrroles can be achieved with only a mild base (eq 33).[45] Interestingly, it was noted that the cesium pivalate base activates the rhodium catalyst by acting as a ligand, which is important in the C–H metalation step.

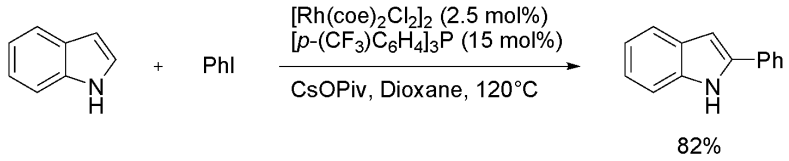

(33)

In attempts of combating some of the down falls of other indole C2 arylation approaches, such as the need for elevated temperatures, differing reaction conditions for protected and unprotected indoles, and variable levels of selectivity, scope and functional group tolerance, Sanford developed a new technique to arylate indoles. In her new oxidative approach, the use of an $IMesPd(OAc)_2$ catalyst allowed for the effective coupling of iodine(III) reagents with various indole substrates to furnish 2-arylindole products in high yields and under very mild conditions (eq 34).[46]

---

[44] Wang, X.; Gribkov, D. V.; Sames, D. *J. Org. Chem.* **2007**, *72*, 1476.

[45] Wang, X.; Lane, B. S.; Sames, D. *J. Am. Chem. Soc.* **2005**, *127*, 4996.

[46] Deprez, N. R.; Kalyani, D.; Krause, A.; Sanford, M. S. *J. Am. Chem. Soc.* **2006**, *128*, 4972.

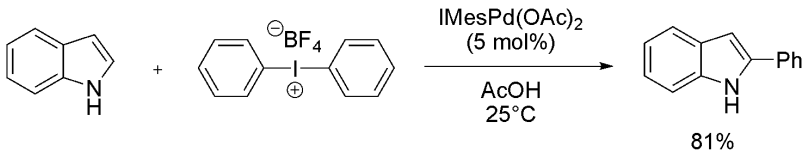

(34)

Other key research in this field has been completed by the Fagnou group, whereby they have shown that the regioselective palladium-catalyzed oxidative cross-coupling of *N*-pivalylindoles and unactivated arenes, such as benzene (eq 35) could be achieved.[47] Effectively, this example represents a transformation in which two C–H activation events are successfully accomplished.

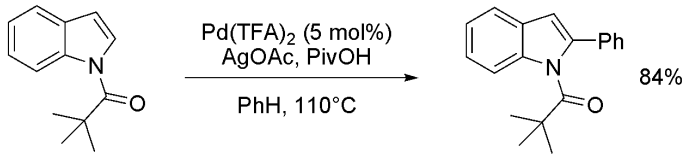

(35)

In addition to the direct arylation of indoles, efforts have been directed towards developing other methods for functionalization, for instance the palladium-catalyzed 2-alkenylation of indoles with methyl acrylate.[48]

2.1.3.2 Indole C3 C–H Bond Activation

One method for inverting the regioselectivity of indole C–H bond functionalization from the C2 to the C3 position is to use steric hindrance. Sames illustrated that this was possible by using indole Grignard salts in a palladium-catalyzed arylation reaction.[49] Presumably, under these conditions the steric demand of the magnesium coordination sphere affects the arylation regioselectivity. It was found that the identity of the Grignard salt could have a profound effect on the regioselectivity, where bulkier magnesium salts such as the MeMgCl-TMEDA treated indole had the best C3 selectivity (eq 36).

---

[47] Stuart, D. R.; Villemure, E.; Fagnou, K. *J. Am. Chem. Soc.* **2007**, *129*, 12072.

[48] Capito, E.; Brown, J. M.; Ricci, A. *Chem. Commun.* **2005**, 1854.

[49] Lane, B. S.; Brown, M. A.; Sames, D. *J. Am. Chem. Soc.* **2005**, *127*, 8050.

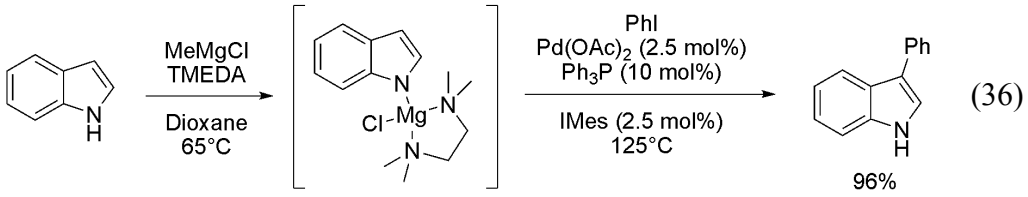

(36)

On the other hand, Fagnou developed a novel palladium(II)-catalyzed cross-coupling of *N*-acetylindoles with unactivated arenes.[50] This methodology utilizes a $Pd(TFA)_2$ catalyst, $Cu(OAc)_2$ as an oxidant, catalytic amounts of 3-nitropyridine and cesium pivalate. It is also effective for a variety of electron rich and poor indoles or arenes (eq 37).

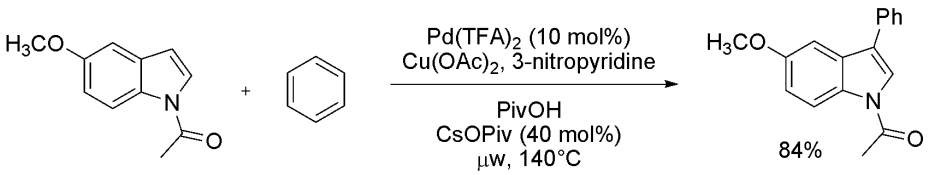

(37)

2.1.3.3 Indole C7 C–H Bond Activation

To date, there is very little precedence for C7 C–H bond functionalization of indoles. In 2006, one account on the iridium-catalyzed borylation of 2-substituted indoles at the 7-position was reported with pinacolborane (eq 38).[51] This transformation is believed to be directed through transition metal coordination with the indole nitrogen.

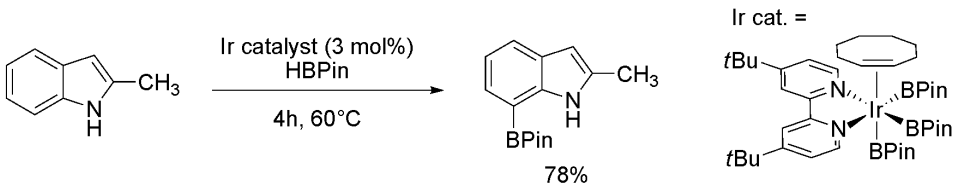

(38)

---

[50] Stuart, D. Fagnou, K. Science 2007,

[51] Paul, S.; Chotana, G. A.; Holmes, D.; Reichle, R. C.; Maleczka, R. E.; Smith, M. R. III *J. Am. Chem. Soc.* **2006**, *128*, 15552.

Other, less related accounts include an aluminum anilide mediated ethylene insertion into the C7 C–H bond of 2-methylindole at elevated temperatures,[52] and a low-yielding rhodium-catalyzed carbene insertion into the C7 C–H bond of a 3-substituted indole.[53]

2.1.4 Research Goals

Although there are ample literature reports on the C–H bond functionalization of indoles, very few examples of C7 indole functionalization exist. It was imagined that with directed C–H bond activation a transition metal would be able to insert into the C7 C–H bond via a five- or six-membered ring intermediate (eq 39). This could also be extended to the C1 C–H bond functionalization of carbazole substrates. The directing groups that were of interest in this application were electron rich amide and urea moieties at the *N*-position. Thus, the initial step was to generate the appropriately substituted indole and carbazole substrates. Subsequently, a variety of transition metal catalysts and coupling partners (arylating, halogenating, and oxygenating reagents) could be tested for reactivity. Overall, this strategy would allow rapid access to 7-functionalized indole and 1-functionalized carbazole compounds which represent and intriguing class of natural products.[54]

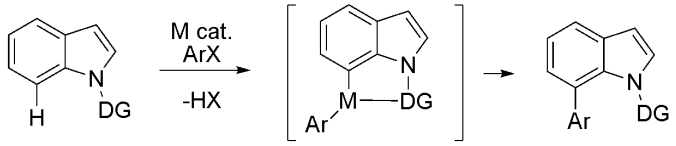

(39)

---

[52] Stroh, R.; Hahn, W. *Justus Liebigs Ann. Chem.* **1959**, *623*, 176.

[53] Kennedy, A. R.; Taday, M. H.; Rainier, J. D. *Org. Lett.* **2001**, *3*, 2407.

[54] For some examples see: (a) Govek, S. P.; Overman, L. E. *J. Am. Chem. Soc.* **2001**, *123*, 9468. (b) Deng, H. B.; Jung, J. K.; Liu, T.; Kuntz, K. W.; Snapper, M. L.; Hoveyda, A. H. *J. Am. Chem. Soc.* **2003**, *125*, 9032. (c) Nicolaou, K. C.; Chen, D. Y. K.; Huang, X. H.; Ling, T. T.; Bella, M.; Snyder, S. A. *J. Am. Chem. Soc.* **2004**, *126*, 12888. (d) Garg, N. K.; Sarpong, R.; Stoltz, B. M. *J. Am. Chem. Soc.* **2002**, *124*, 13179. (e) Lin, S.; Yang, Z.-Q.; Kwok, B. H. B.; Koldobskiy, M.; Crews, C. M.; Danishefsky, S. J. *J. Am. Chem. Soc.* **2004**, *126*, 6347.

2.2 Results and Discussion

2.2.1 C–H Activation of the Indole C7 Position

To begin examining the possibility of activating the C7 C–H bond of an indole scaffold, the appropriate indole substrate had to be synthesized. Ideally, the nitrogen of the indole was to be functionalized with a directing group for the subsequent C–H activation, and the position at C2 should be occupied with a bulky group in order to prevent functionalization at that C–H bond. Thus, 2-methylindole was the starting material of choice which was subjected to various conditions to install a carbamyl directing group on the indole nitrogen (Table 9). It was hypothesized that the *N,N*-dimethyl urea moiety would be electron rich enough to direct activation of the C7 C–H bond through coordination of a metal to the urea carbonyl lone pairs followed by insertion into the C–H bond. After many attempts at functionalizing the indole nitrogen, it was found that a strong base, such as *n*-BuLi was required for the reaction between 2-methylindole and *N,N*-dimethylcarbamyl chloride to occur.

Table 9. Synthesis of *N,N*,2-trimethyl-1*H*-indole-1-carboxamide.

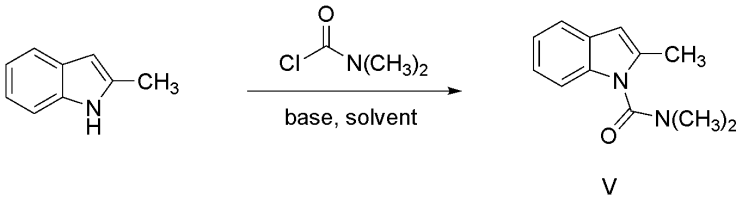

V

Entry	Base	Solvent	Yield V
1	DMAP	CH_2Cl_2	NR
2	NaOH	CH_2Cl_2	NR
3	NaH	CH_2Cl_2	NR
4	*n*-BuLi	THF	77%

Subsequently, the direct arylation at the C7 position of the *N,N*,2-trimethyl-1*H*-indole-1-carboxamide was tested. With a 5 mol% loading of $Pd(OAc)_2$ and bromobenzene as the coupling partner, multiple bases were screened for direct arylation in dioxane at 130°C. Some of the most

commonly employed bases in C–H bond activation were used; however, no arylation at the C7 carbon of *N,N*,2-trimethyl-1*H*-indole-1-carboxamide was observed (Table 10).

Table 10. Examining direct arylation of *N,N*,2-trimethyl-1*H*-indole-1-carboxamide by varying the identity of the base under palladium catalysis.

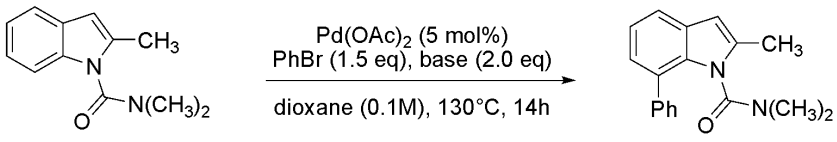

Entry	Base	Product
1	Na_2CO_3	NR
2	NaOAc	NR
3	AgOAc	NR
4	NaOMe	NR
5	K_3PO_4	NR

Since direct arylation was not observed under the standard palladium catalysis conditions (Table 10), other previously published methodologies were investigated. In Table 11, entries 1 to 4 exemplify the strategy used by Lloyd-Jones[39] in directing group assisted C–H bond activations. However, this was not effective in activating the C7 C–H bond of *N,N*,2-trimethyl-1*H*-indole-1-carboxamide. Other approaches that were explored included the work of Fagnou (entries 5 and 6)[47] and Daugulis (entry 7)[38]. Unfortunately, none of the desired product was furnished in either of these cases. However, as shown in entry 6, the C–H bond activation at C3 was possible (as determined by ^{1}H NMR). In this reaction the main product detected was *N,N*,2-trimethyl-3-phenyl-1*H*-indole-1-carboxamide which may indicate that the activation of the C2 C–H bond was not directed by the urea carbonyl, rather it was an electrophilic aromatic substitution type activation.

Table 11. Attempts at arylating C7 of *N,N*,2-trimethyl-1*H*-indole-1-carboxamide with published methodologies.

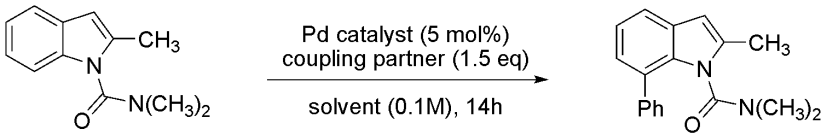

Entry	Catalyst	Coupling Partner	Additives	Solvent	Temp. (°C)	Product
1	$Pd(OAc)_2$	PhI	1,4-benzoquinone, *p*-TSA	CH_2Cl_2	70	NR
2	$PdCl_2$	PhI	1,4-benzoquinone, *p*-TSA	CH_2Cl_2	70	NR
3	$Pd(OAc)_2$	PhI	K_2CO_3	CH_2Cl_2	70	NR
4	$Pd(OAc)_2$	PhBr	*p*-TSA, AgOAc	CH_2Cl_2	110	NR
5	$Pd(OAc)_2$	PhBr	K_2CO_3	DMA	110	NR
6[a]	$Pd(OAc)_2$	PhBr	K_2CO_3, PivOH	DMA	110	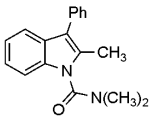
7	$Pd(OAc)_2$	PhBr	AgOAc	TFA	130	NR
8	$Pd(OAc)_2$	PhH	$Na_2S_2O_8$, TFA	PhH	rt	NR

[a] Undesired product was not isolated; Structure determined by crude ^{1}H NMR

In addition to arylating at the indole C7 position, we were also interested in brominating the C–H bond. The bromination strategies that were attempted are outlined in Table 12. All of the strategies involve the use of *N*-bromosuccinimide as the brominating agent. Entries 1 to 3 exemplify chemistry developed by Lloyd-Jones,[39] while the brominating strategy in entry 4 is an example from the Sanford[40] group. As in the case with the arylation of *N,N*,2-trimethyl-1*H*-indole-1-carboxamide, the desired C7 bromination was not achieved. Though, when 5% $Pd(OAc)_2$ was used in combination with a K_2CO_3 base, bromination at C3 of the indole scaffold was detected by ^{1}H NMR. Once again, this product is most likely generated through an electrophilic aromatic substitution mechanism as opposed to a true directed C–H bond activation.

Table 12. Attempts at brominating C7 of *N,N*,2-trimethyl-1*H*-indole-1-carboxamide with published methodologies.

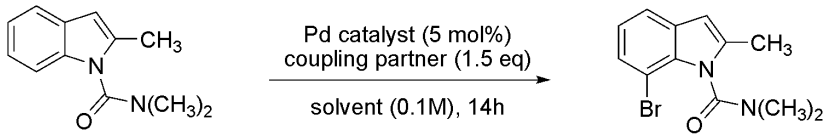

Entry	Catalyst	Coupling Partner	Additives	Solvent	Temp. (°C)	Product
1	$Pd(OAc)_2$	NBS	1,4-benzoquinone, *p*-TSA	CH_2Cl_2	70	NR
2	$PdCl_2$	NBS	1,4-benzoquinone, *p*-TSA	CH_2Cl_2	70	NR
3[a]	$Pd(OAc)_2$	NBS	K_2CO_3	CH_2Cl_2	70	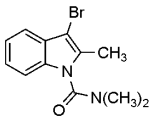
4	$Pd(OAc)_2$	NBS	-	AcOH	130	NR

[a] Undesired product was not isolated; Structure determined by crude ^1H NMR

2.2.2 C–H Activation of the Carbazole C1 Position

The unsuccessful arylation and bromination of the indole C7 C–H bond may be due to the electronic bias for the C2 and C3 positions to be more reactive. Thus, one way to circumvent this issue is to start with a symmetrical starting material such as a carbazole. With a directing group on the carbazole nitrogen, the activation of the C1 C–H bond could be feasible. In hopes of utilizing this strategy, two carbazole derivatives were synthesized, each with a functional group that could direct the metal catalyst insertion into the appropriate C–H bond. *N*-ethylidene-9*H*-carbazol-9-amine was generated by treating carbazole with sodium nitrite in a sulfuric acid solution to afford the *N*-nitrosocarbazole followed by a one-pot procedure to reduce the nitroso moiety to an amine which then could be condensed with acetaldehyde to yield the final product (eq 40). Also, in the same way *N,N*,2-trimethyl-1*H*-indole-1-carboxamide was synthesized, *N,N*-dimethyl-9*H*-carbazole-9-carboxamide was furnished by reaction with *N,N*-dimethylcarbamyl chloride under strongly basic conditions (eq 41).

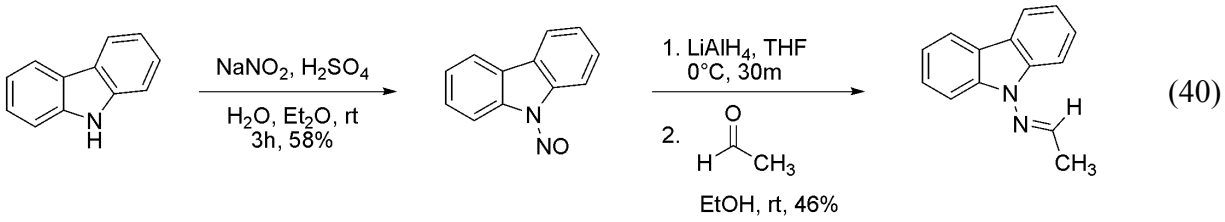

(40)

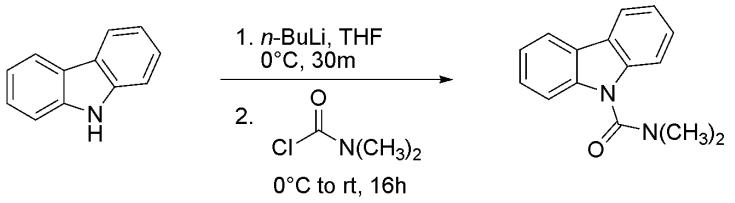

(41)

Both new carbazole derivatives have the ability to direct C–H bond functionalization by ensuring coordination of the metal catalyst with either the imine nitrogen or carbamyl carbonyl oxygen lone pairs. After coordination to the directing groups, the metal can insert into the C1 C–H bond to form either a five or six-membered ring intermediate, as shown in Scheme 11.

Scheme 11. Directed metal insertion into the C1 C–H bond of functionalized carbazoles.

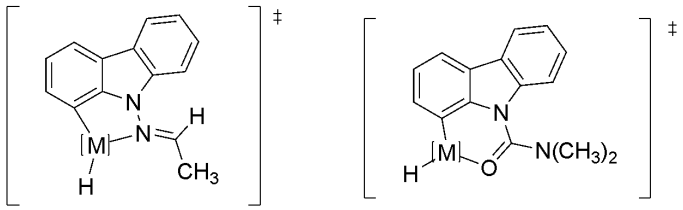

N,N-dimethyl-9*H*-carbazole-9-carboxamide was subsequently used in C–H bond activation reactions with various coupling partners, in order to generate diverse products (Scheme 12). To brominate the C1 position a 5 mol% loading of $Pd(OAc)_2$ was used in combination with NBS and K_2CO_3 as the base. With these conditions a trace amount of the desired 1-bromo-*N,N*-dimethyl-9*H*-carbazole-9-carboxamide product was detected by GC-MS; however, since the starting material and product have the same Rf by TLC, the product was not isolable. Conversely, more success was found with the arylation and acetoxylation of *N,N*-dimethyl-9H-carbazole-9-carboxamide. Again with a $Pd(OAc)_2$ catalyst, but with an oxidizing agent and under

acidic conditions, the simultaneous C–H bond activation of benzene and the carbazole substrate was found to proceed in 16% conversion (by GC-FID) to yield the desired product. With some further optimization, the yield of this reaction could be improved rendering it more synthetically useful.

Scheme 12. Exploring the bromination, arylation and acetoxylation of *N,N*-dimethyl-9*H*-carbazole-9-carboxamide through C–H bond activation strategies.

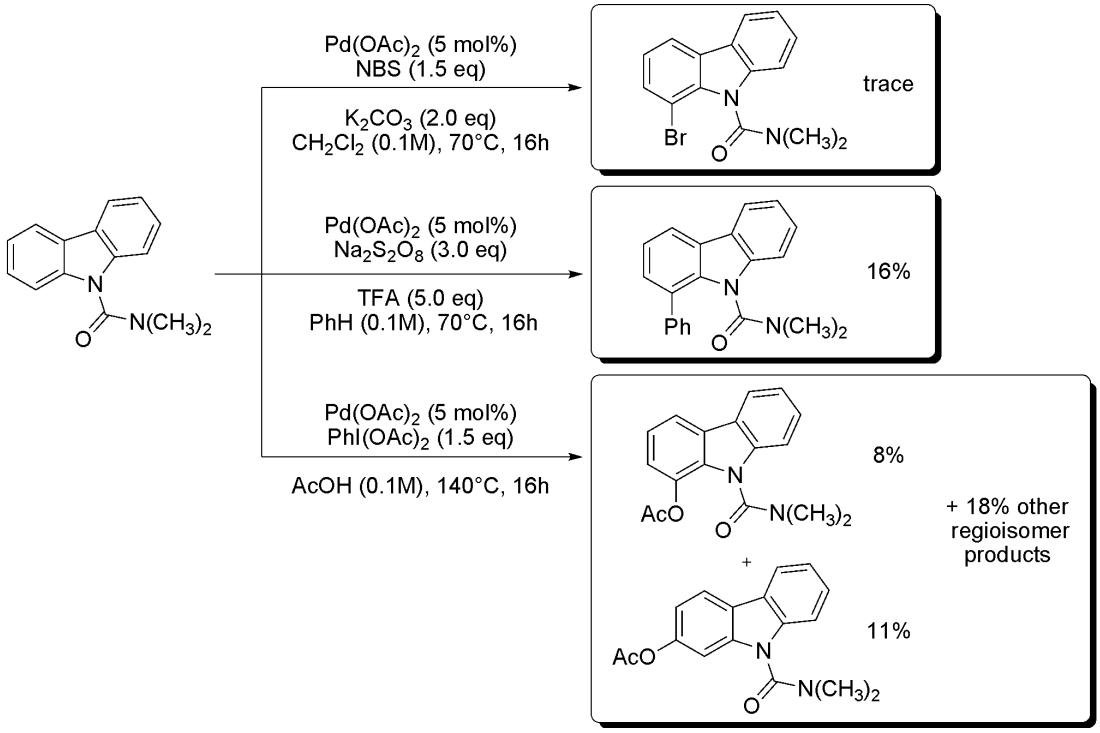

The final palladium-catalyzed reaction conditions that were probed involved the use of $PhI(OAc)_2$ in acetic acid, in hopes of acetoxylating the functionalized carbazole C1 position. GC-FID analysis revealed that a number of acetoxylated products had been generated, of which the most discernable ones were where the C1 and C2 C–H bonds had undergone activation. These products were produced in 8% and 11%, respectively. Due to the difficulty of separating these isomeric products by chromatography and the large number of products produced, this transformation still requires optimization of yield and selectivity. Lastly, the product array that was furnished may also indicate that this C–H bond functionalization was not actually influenced by the directing group rather it was an electrophilic aromatic substitution reaction.

2.3 Conclusion

Different *N*-substituted indole and carbazole substrates were successfully synthesized and tested in chelate-assisted C–H bond arylation, halogenation, and oxygenation. Although the C7 C–H bond activation of *N,N*,2-trimethyl-1*H*-indole-1-carboxamide was not achieved with various literature procedures, promising results were obtained for the C1 C–H bond activation of *N,N*-dimethyl-9*H*-carbazole-9-carboxamide. The direct arylation of *N,N*-dimethyl-9*H*-carbazole-9-carboxamide with a $Pd(OAc)_2$ catalyst, with $Na_2S_2O_8$, TFA, and in benzene was found to proceed in 16% yield (by GC-FID). Also, palladium-catalyzed oxygenation of the same substrate with $PhI(OAc)_2$ in acetic acid could yield the C1 (8%), C2 (11%) acetoxylated, and other regioisomeric products (18%). Further optimization of the reaction conditions could allow for synthetically useful yields of the functionalized products to be acquired.

2.4 Experimental Procedures

For General Experimental, Materials, or Instrumentation, please see sections 1.4.1, 1.4.2, and 1.43, respectively.

2.4.1 General Procedure for the Synthesis of *N*-substituted Indole and Carbazoles

To a flask equipped with a magnetic stir bar was added the appropriate indole or carbazole substrate (1.0 equiv) and dissolved in anhydrous THF (0.23M). The mixture was cooled to 0°C in an ice bath and *n*-BuLi (1.5 equiv) was added dropwise to the stirring solution. The colour of the solution became dark burgundy red and was stirred for a total of 30 minutes. While still cold, *N,N*-dimethylcarbamyl chloride (1.5 equiv) was added dropwise and the reaction was allowed to stir at room temperature over night. When the reaction was complete, water was added slowly to quench the excess *n*-BuLi and then extracted with EtOAc (3x). The combined organic layers were dried over Na_2SO_4, filtered, and concentrated by reduced pressure. Lastly, the products were purified by column chromatography (10-20% EtOAc-hexanes).

***N,N*,2-trimethyl-1*H*-indole-1-carboxamide**

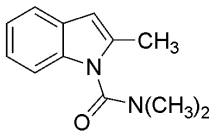

The reaction was carried out with 5.0 g of 2-methylindole (38.1 mmol), 36 mL of *n*-BuLi (1.6 M, 57.2 mmol), and 5.3 mL of *N,N*-dimethylcarbamyl chloride (57.2 mmol). After purification 5.9 g (77%) of a red oil was isolated. IR (neat): 2924, 1680, 1562, 1489, 1456, 1390, 1327, 1301, 1258, 1225, 1188, 1147, 1113, 1063, 1017, 785, 743 cm^{-1}. ^1H NMR (400 MHz, $CDCl_3$) δ 7.51-7.45 (m, 1H), 7.21-7.07 (m, 3H), 6.3 (s, 1H), 2.99 (s, 6H), 2.44 (d, *J* = 1.0Hz, 3H). ^{13}C NMR (100 MHz, $CDCl_3$) δ 154.3, 136.2, 135.6, 128.7, 122.1, 121.1, 120.0, 111.0, 104.0, 37.7, 13.2. HRMS (EI) *m*/*e* calcd. for $C_{12}H_{14}N_2O$ $[M-H]^+$: 202.1106; found: 202.1102.

_N,N_-dimethyl-9_H_-carbazole-9-carboxamide

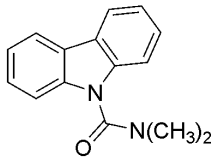

The reaction was carried out with 550 mg of carbazole (3.0 mmol), 3.8 mL of *n*-BuLi (1.6 M, 6.0 mmol), and 0.5 mL of *N,N*-dimethylcarbamyl chloride (5.4 mmol). After purification 556 mg (78%) of an orange oil was isolated. IR (neat): 3061, 2930, 1675, 1599, 1478, 1444, 1384, 1312, 1297, 1254, 1225, 1161, 1107, 1060, 1026, 934, 749, 725, 655 cm^{-1}. ^{1}H NMR (400 MHz, $CDCl_3$) δ 8.03 (d, *J* = 7.7Hz, 2H), 7.56 (d, *J* = 8.3Hz, 2H), 7.45 (ddd, *J* = 1.2Hz, *J* = 7.2Hz, *J* = 8.3Hz, 2H), 7.30 (m, 2H), 3.09 (s, 6H). ^{13}C NMR (75 MHz, $CDCl_3$) δ 154.8, 138.6, 126.5, 124.3, 121.4, 120.1, 112.6, 38.1. HRMS (EI) *m*/*e* calcd. for $C_{15}H_{14}N_2O$ $[M-H]^+$: 238.1106; found: 238.1100.

9-nitroso-9_H_-carbazole

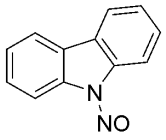

Based on a literature procedure.[55] In a flask equipped with a magnetic stir bar, 5.0 g (30.0 mmol) carbazole was dissolved in Et_2O (60 mL, 0.5M). 17 mL of a 50% v/v H_2SO_4 solution (1.79M with respect to carbazole) was added to the solution followed by a dropwise addition of a solution containing 248 mg (3.6 mmol) of sodium nitrite in 1 mL of water. The reaction was stirred for 3 hours at room temperature after which the two phases were separated and the aqueous layer was extracted with Et_2O (3x). The combined organic phases were washed with 2% Na_2CO_3, dried over Na_2SO_4, filtered and concentrated under reduced pressure. The yellow crystals obtained were recrystallized in a minimum amount of hot Et_2O, to afford 3.23g (55%) of golden yellow needles. m.p. 78.5-80°C. IR (neat): 3052, 1483, 1469, 1425, 1312, 1245, 1221, 1203, 1149, 1121, 1057, 1032, 1015, 973, 931, 777, 743, 716, 697 cm^{-1}. ^{1}H NMR (400 MHz, $CDCl_3$) δ 8.57-8.52 (m, 1H), 8.22 (d, J = 7.9Hz, 1H), 7.94-7.87 (m, 2H), 7.57-7.43 (m, 4H). ^{13}C

[55] Winter, A. H.; Gibson, H. H.; Falvey, D. E. *J. Org. Chem.* **2007**, *72*, 8186.

NMR (100 MHz, $CDCl_3$) δ 138.6, 132.7, 128.6, 128.1, 127.4, 126.2, 125.3, 124.8, 120.4, 119.9, 116.5, 112.3. HRMS (EI) *m*/*e* calcd. for $C_{12}H_8N_2O$ $[M-H]^+$: 196.0637; found: 196.0636.

_N_-ethylidene-9_H_-carbazol-9-amine

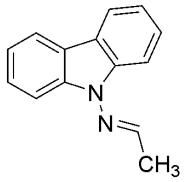

The first step of this reaction was based on a literature procedure.[55] To a round bottom flask equipped with a stir bar was added 3.0 g (15.3 mmol) of 9-nitroso-9*H*-carbazole and dissolved in 150 mL of anhydrous THF (0.1M). While stirring, 2.9 g of $LiAlH_4$ (76.5 mmol) was added slowly to the mixture at 0°C and the colour of the solution turned from yellow to dark orange-red. After stirring at room temperature for 15 minutes, EtOAc was added dropwise to the reaction mixture to quench the excess reducing agent, followed by the slow addition of water. The aqueous layer was extracted with EtOAc (3x), dried with Na_2SO_4, and filtered. A burgundy coloured solid (2.7 g) was obtained after concentration under reduced pressure. The second step of this reaction was based on a different literature procedure.[56] Without purification, the crude solid (2.7 g, 14.8 mmol) was dissolved in absolute EtOH (100 mL) in a flask with a magnetic stir bar, and 1.66 mL of acetaldehyde (29.6 mmol) was added. The reaction was stirred at room temperature for 16 hours after which it was directly concentrated under reduced pressure to afford a dark red solid. The product was purified by column chromatography (2-10% Et_2O-hexanes) to yield 1.41 g (46%) of a light beige solid. m.p. 56-57°C. IR (neat): 3053, 1598, 1428, 1437, 1335, 1306, 1238, 1221, 1203, 1150, 1116, 1056, 1031, 1003, 930, 869, 776, 741, 716, 698 cm^{-1}. ^1H NMR (400 MHz, $CDCl_3$) δ 8.43-8.35 (m, 1H), 8.06-8.00 (m, 2H), 7.64-7.58 (m, 2H), 7.45-7.38 (m, 2H), 7.27-7.20 (m, 2H), 2.27 (d, *J* = 5.3Hz, 3H). ^{13}C NMR (100 MHz, $CDCl_3$) δ 153.8, 138.1, 126.1, 122.0, 120.2, 120.1, 109.9, 19.4. HRMS (EI) *m*/*e* calcd. for $C_{14}H_{12}N_2$ $[M-H]^+$: 208.1000; found: 208.0999.

---

[56] Entwistle, I. D.; Johnstone, R. A. W.; Wilby, A. H. *Tetrahedron* **1982**, *38*, 419.

2.4.2 General Procedure for the Synthesis of 1-Phenyl-9*H*-carbazole.

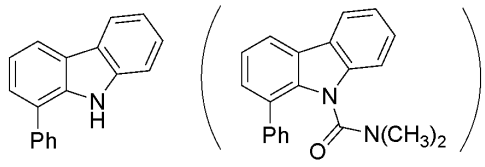

In a 1DR vial containing a magnetic stir bar, 20 mg of *N,N*-dimethyl-9*H*-carbazole-9-carboxamide (0.08 mmol) was dissolved in 1 mL of benzene (0.1M). Subsequently, 32 μL of trifluoroacetic acid (0.42 mmol), 60 mg of $Na_2S_2O_8$ (0.25 mmol), and 0.9 mg of $Pd(OAc)_2$ (0.0042 mmol) were added to the solution and allowed to dissolve. The reaction was heated to 70°C for 16 hours. After completion, the mixture was filtered through a plug of silica and concentrated under reduced pressure. Since the crude could not be purified by silica gel chromatography to afford the *N,N*-dimethyl-1-phenyl-9*H*-carbazole-9-carboxamide product (due to no separation by TLC), the mixture was reduced with $LiAlH_4$ (6.4 mg, 0.17 mmol) in anhydrous THF at 0°C. The reduction was allowed to proceed for 22 hours at room temperature upon which it was quenched with the slow addition of EtOAc and water. The organic phase was dried over Na_2SO_4, filtered and concentrated. The crude oil was purified by prep-TLC (15% benzene-hexanes) to yield 1.9 mg (9.3%) of 1-phenyl-9*H*-carbazole as a light yellow oil. IR (neat): 3434, 3056, 2922, 2853, 1723, 1601, 1506, 1489, 1413, 1321, 1232, 1177, 1124, 750, 702 cm^{-1}. ^1H NMR (400 MHz, $CDCl_3$) δ 8.31 (br, 1H), 8.13-8.06 (m, 2H), 7.72-7.67 (m, 2H), 7.59-7.53 (m, 2H), 7.48-7.40 (m, 4H), 7.33 (t, *J* = 7.6Hz, 1H), 7.29-7.22 (m, 1H). ^{13}C NMR (100 MHz, $CDCl_3$) δ 139.5, 139.1, 137.3, 129.3, 129.0, 128.4, 127.5, 127.4, 125.9, 125.7, 125.1, 123.7, 123.6, 120.5, 119.9, 119.6, 119.5, 110.7. HRMS (EI) *m/e* calcd. for $C_{18}H_{13}N$ $[M-H]^+$: 243.1048; found: 243.1041.

2.4.3 General Procedure for the Acetoxylation of Carbazole Derivatives

In a 1DR vial with a magnetic stir bar 20 mg of *N,N*-dimethyl-9*H*-carbazole-9-carboxamide (0.08 mmol) was dissolved in 1 mL of acetic acid (0.1M). 41 mg of $PhI(OAc)_2$ (0.13 mmol) was added to the solution and thoroughly dissolved before 0.9 mg of $Pd(OAc)_2$ (0.0042 mmol) was added. The reaction was heated to 140°C for 16 hours and then concentrated under reduced pressure. Purification by prep-TLC (30% EtOAc-hexanes) allowed for the various isomeric

products to be isolated as a mixture. Another prep-TLC (15% benzene-hexanes) separated the individual acetoxylated carbazole products.

9-(dimethylcarbamoyl)-9*H*-carbazol-2-yl acetate

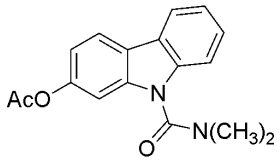

Obtained light yellow oil in 11% GC-FID yield, and 0.8 mg (3.2%) isolated yield. IR (neat): 2924, 2855, 1769, 1687, 1601, 1482, 1449, 1387, 1306, 1199, 1175, 1154, 1115, 747, 724 cm^{-1}. ^{1}H NMR (400 MHz, $CDCl_3$) δ 8.01-7.96 (m, 1H), 7.57-7.53 (m, 1H), 7.51-7.42 (m, 3H), 7.31 (ddd, *J* = 1.0Hz, *J* = 7.3Hz, *J* = 8.0Hz, 1H), 7.13-7.07 (m, 1H), 3.11 (s, 6H), 2.53 (s, 3H). ^{13}C NMR (100 MHz, $CDCl_3$) δ 171.0, 154.4, 145.7, 143.7, 140.2, 138.5, 126.8, 126.7, 122.2, 121.8, 120.0, 114.7, 112.4, 110.1, 38.1 (*N*-methyl carbon of other rotamer), 30.0, 29.7, 21.3. HRMS (EI) *m*/*e* calcd. for $C_{17}H_{16}N_2O_3$ $[M-H]^+$: 296.1161; found: 296.1156.

9-(dimethylcarbamoyl)-9*H*-carbazol-1-yl acetate

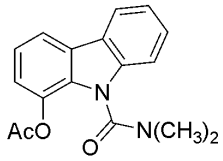

Obtained light yellow oil in 8% GC-FID yield, and 2.4 mg (9.6%) isolated yield. IR (neat): 2928, 2855, 1760, 1689, 1580, 1485, 1453, 1429, 1390, 1324, 1286, 1192, 1168, 1089, 1010, 914, 753 cm^{-1}. ^{1}H NMR (400 MHz, $CDCl_3$) δ 8.07-8.03 (m, 1H), 7.95-7.91 (m, 1H), 7.47 (ddd, *J* = 1.2Hz, *J* = 7.2Hz, *J* = 8.3Hz, 1H), 7.35-7.27 (m, 3H), 7.21 (dd, *J* = 1.1Hz, *J* = 7.9Hz, 1H), 3.26 (s, 3H), 2.93 (s, 3H), 2.37 (s, 3H). ^{13}C NMR (100 MHz, $CDCl_3$) δ 168.9, 153.8, 138.7, 136.4, 130.6, 127.2, 127.0, 123.9, 121.6, 121.5, 120.6, 120.3, 117.9, 111.0, 30.0, 29.7, 20.8. HRMS (EI) *m*/*e* calcd. for $C_{17}H_{16}N_2O_3$ $[M-H]^+$: 296.1161; found: 296.1161.

Chapter 3
Towards a Phosphine Helical Ligand

3.1 Introduction

[*n*]Helicenes are organic, ortho-fused polycyclic aromatic compounds that adopt nonplanar conformations similar to that of a winding helix. Due to their structure, these compounds have unique optical and electronic properties as well as an intrinsic chirality, which makes them important synthetic targets in the field of organic chemistry.[57] The first synthesis of [6]helicene (hexahelicene) was achieved in a twelve step route in 1956 by Newman.[58]

3.1.1 Select Recent Approaches Towards the Synthesis of Racemic [*n*]Helicenes

Traditionally, helicene scaffolds were built by oxidative photocyclization based on stilbene-type precursors[59]; however, due to many drawbacks other methodologies have become more popular in recent years. The first non-photocyclization route towards a helicene was reported by Dubois.[60] In this approach a five-step carbenoid coupling strategy was used in which the key dibromide intermediate (eq 42) could cyclize in very good yield to afford the [7]helicene.

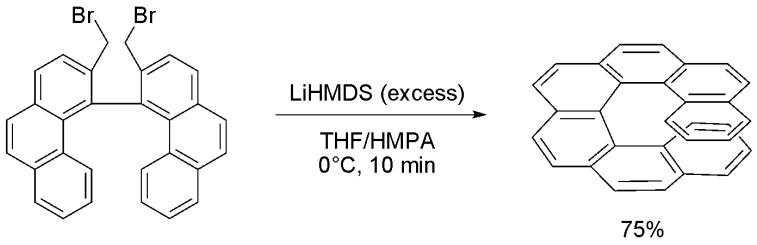

(42)

---

[57] Urbano, A. *Angew. Chem. Int. Ed.* **2003**, *42*, 3986.

[58] Newman, M. S.; Lednicer, D. *J. Am. Chem. Soc.*, **1956**, *78*, 4765.

[59] Liu, L.; Yang, B.; Katz, T. J.; Poindexter, M. K. *J. Org. Chem.* **1991**, *56*, 3769.

[60] Gingras, M.; Dubois, F. *Tetrahedron Lett.* **1999**, *40*, 1309.

Considered as a breakthrough in the field, in 2002 Stara, Stary and co-workers presented a transition-metal catalyzed isomerization of aromatic *cis,cis* dienetriynes in an innovative and atom-economical synthesis of helicenes.[61] Under mild conditions, the [2+2+2] cycloisomerization of the *cis,cis* dienetriynes could be carried out with a nickel(0) catalyst to furnish numerous substituted [5], [6] (eq 43), and [7]helicenes.

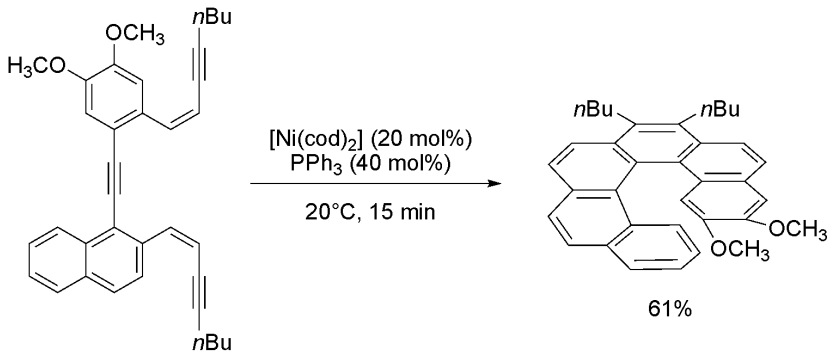

(43)

Routes towards the synthesis of diverse helicene structures, such as that of azahelicenes with pyrrole rings or oxahelicenes with furan rings have also been studied. One recent example utilizes a palladium catalyst to complete the sterospecific synthesis of hetero[7]helicenes by a double *N*-arylation and intramolecular *O*-arylation.[62] However, higher yields and decreased reaction times can be achieved with other methodologies such as the olefin metathesis route developed by the Collins group (eq 44).[63] With the synthesis of 1,1'-binaphthyl frameworks, the subsequent ring-closing metathesis under ruthenium-catalyzed conditions could be carried out with microwave heating or at 40°C (for sensitive functionalities).

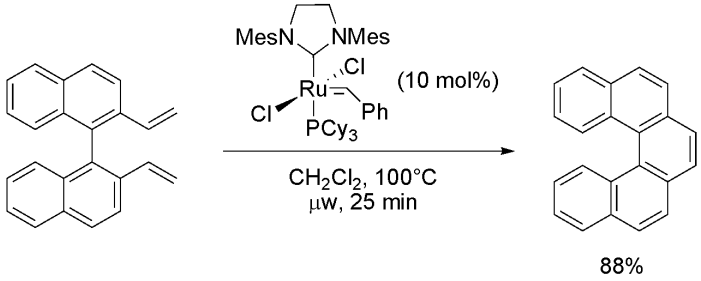

(44)

---

[61] Teply, F.; Stara, I. G.; Stary, I.; Kollarovic, A.; Saman, D.; Rulisek, L.; Fiedler, P. *J. Am. Chem. Soc.* **2002**, *124*, 9175.

[62] Nakano, K.; Hidehira, Y.; Takahashi, K.; Hiyama, T.; Nozaki, K. *Angew, Chem. Int. Ed.* **2005**, *44*, 7136.

[63] Collins, S. K.; Grandbois, A.; Vachon, M. P.; Cote, J. *Angew. Chem. Int. Ed.* **2006**, *45*, 2923.

Another interesting approach that utilizes pyridine directed C–H bromination (described by Sanford and co-workers) was reported by Takenaka in the preparation of helical pyridine *N*-oxides.[64] Their synthesis was reliant on two sequences of a *Z*-selective Wittig reaction followed by Stille-Kelly reaction (eq 45).

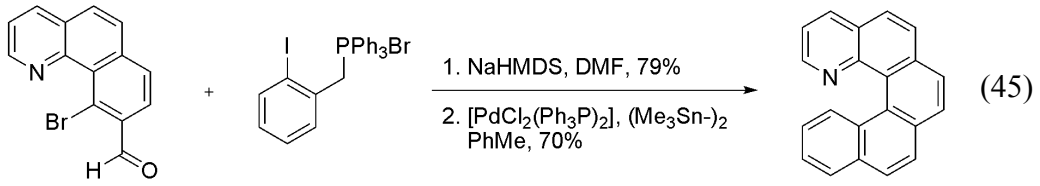

(45)

Also published in 2008 was a very unique approach to the synthesis of helicenes via a Friedel–Crafts-type cyclization of 1,1-difluoro-1-akenes (eq 46).[65]

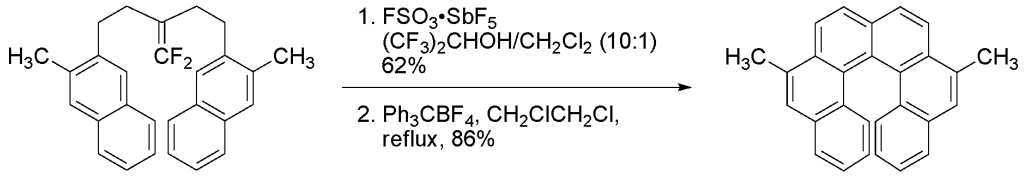

(46)

3.1.2 Research Goals

Decades ago, [*n*]helicenes were built out of the curiosity of organic chemists; however, recent reports show that [*n*]helicenes can be very effective chiral ligands or additives in a broad spectrum of reactions, including enantioselective hydrogenation,[66] addition of alkylzinc reagents to aldehydes,[67] and kinetic resolution.[68] Thus, our goal was to synthesize a [5]helicene backbone with a mono-diphenylphosphine substitution so that the substrate would be utilized as a ligand in a transition-metal catalyzed process. Some inspiration for this target was drawn from a helical

---

[64] Takenaka, N.; Sarangthem, R. S.; Captain, B. *Angew. Chem. Int. Ed*. **2008**, *47*, 9708.

[65] Ichikawa, J.; Yakota, M.; Kudo, T.; Umezaki, S. *Angew. Chem. Int. Ed.* **2008**, *47*, 4870.

[66] Nakano, D.; Yamaguchi, M. *Tetrahedron Lett.* **2003**, *44*, 4969.

[67] Sato, I.; Yamashima, R.; Kadowaki, K.; Yamamoto, J.; Shibata, T.; Soai, K. *Angew. Chem. Int. Ed.* **2001**, *40*, 1096.

[68] Reetz, M. T.; Sostmann, S. *J. Organomet. Chem.* **2000**, *603*, 105.

diphosphane (PHelix) which was shown to be valuable in enantioselective rhodium-catalyzed hydrogenation.[69] Also, it was hypothesized that a helical phosphine ligand could encourage a palladium-arene chelating interaction to stabilize $L_1Pd^{(0)}$, an interaction known to be beneficial with the Buchwald ligands (Scheme 13).[70]

Scheme 13. Proposal for [5]helicene ligand.

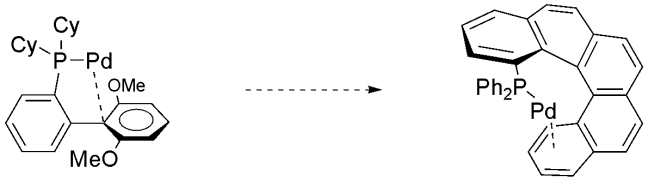

[69] Reetz, M. T.; Beuttenmuller, E. W.; Goddard, R. *Tetrahedron Lett.* **1997**, *38*, 3211.

[70] Barder, T. E.; Walker, S. D.; Martinelli, J. R.; Buchwald, S. L. *J. Am. Chem. Soc.* **2005**, *127*, 4685.

3.2 Results and Discussion

3.2.1 Approach via Olefin Metathesis

Initially, our route to access a phosphine helicene ligand involved the key steps shown in the retrosynthetic analysis in Scheme 14 (which was drafted in collaboration with Peter Dornan). After the synthesis of Fragments A and B, a Kumada type coupling of the aryl triflate and the metallated aryl bromide would be the next step in the synthesis. From the resulting dialdehyde species, a Wittig olefination would be able to afford the diene, which could undergo olefin metathesis under ruthenium-catalyzed conditions to cyclize the fifth and final ring of the helicene backbone. Following this, the oxygen handle on the helicene would be reduced to the alcohol so that it could be triflated and via transition metal catalysis, transformed to the diphenylphosphine helical ligand.

Scheme 14. Approach towards a helical phosphine ligand with a key olefin metathesis reaction.

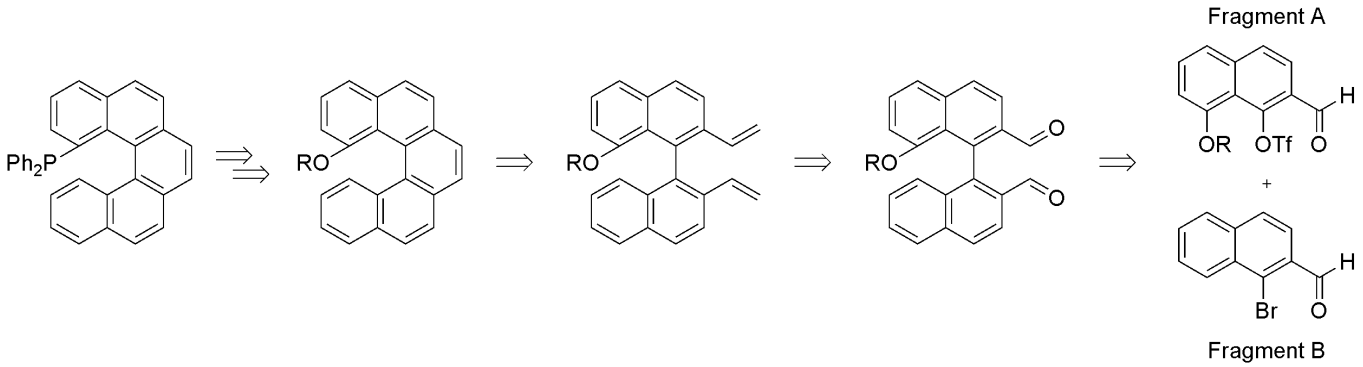

To access Fragment B, a convenient two step procedure was devised. Starting with the commercially available 1-bromo-2-methylnaphthalene, a benzylic bromination with NBS and benzoyl peroxide was carried out under reflux to afford 1-bromo-2-(dibromomethyl)naphthalene (eq 47). Subsequently, treatment with $AgNO_3$ would oxidize the dibromomethyl group to an aldehyde, effectively producing 1-bromo-2-naphthaldehyde (Fragment B) in satisfactory yield (eq 48).

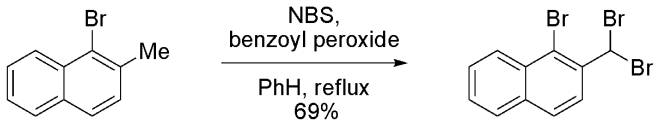

(47)

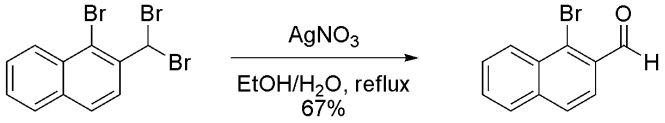

(48)

8-(benzyloxy)-1-hydroxy-2-naphthaldehyde was synthesized in hopes of directly triflating the free alcohol to furnish Fragment A in the helicene retrosynthesis (Peter Dornan). However, we found that under numerous conditions the triflate group could not be installed on the oxygen of C1 successfully. It was hypothesized that the bulky benzyl protecting group on the oxygen of C8 was preventing the triflation from occurring due to increased steric hindrance around the free alcohol. With this in mind, we decided to synthesize the same naphthaldehyde derivative but with a methoxy group at the C8 position. Under standard alkylating conditions with iodomethane, naphthalene-1,8-diol (prepared by Peter Dornan) was selectively mono methylated in good yield (eq 49). 8-methoxynaphthalen-1-ol was then converted to 1-hydroxy-8-methoxy-2-naphthaldehyde by an ortho directed formylation with paraformaldehyde and $MgCl_2$ (eq 50). The last step in order to complete the synthesis of Fragment A was to once again triflate the alcohol of 1-hydroxy-8-methoxy-2-naphthaldehyde. The most common literature procedures for triflating were not effective in this case, in that the starting material could not react in good yield (eq 51). Also, it was found that the triflated product was not very stable to decomposition. Thus, our strategy to change the C8 alcohol protecting group to a methoxy group was not very useful in making the subsequent triflating step any more facile.

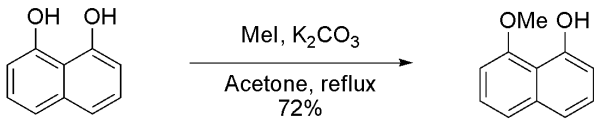

(49)

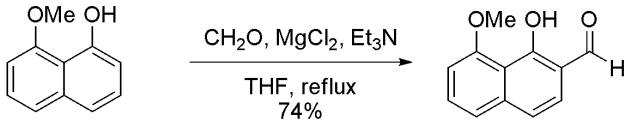

(50)

(51)

Reaction Conditions	Product
Tf_2O, DMAP, Py	NR
Tf_2O, *n*-BuLi, THF	NR
Tf_2O, 30% K_3PO_4 in PhMe	18%

One possible explanation as to why the synthesis of Fragment A is so difficult is that there is hydrogen-bond assisted stabilization of the precursor naphthaldehyde, making the alcohol proton less acidic (Scheme 15). The stability gained from the internal H-bond between the alcohol and aldehyde moieties may prevent the triflate group from being installed.

Scheme 15. Internal H-bond presumed to occur in 1-hydroxy-8-methoxy-2-naphthaldehyde.

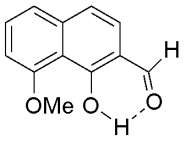

3.2.2 Approach via Radical Photocyclization

Our second approach involved the use of a different strategy to generate the helicene backbone; one which involved a photoinduced cyclization (Scheme 16). We envisioned that starting with Fragments C and D a Heck reaction could be done to tether the two fragments with a double bond. Next, with UV irradiation the intermediate would cyclize and form the five ring helicene backbone. Then in a similar fashion to our first attempted helicene synthesis approach, the methoxy handle on the helicene ring would be deprotected to the alcohol so that it could be triflated and via transition metal catalysis, transformed to the diphenylphosphine helicene.

Scheme 16. Approach towards a helical phosphine ligand with a key photocyclization reaction.

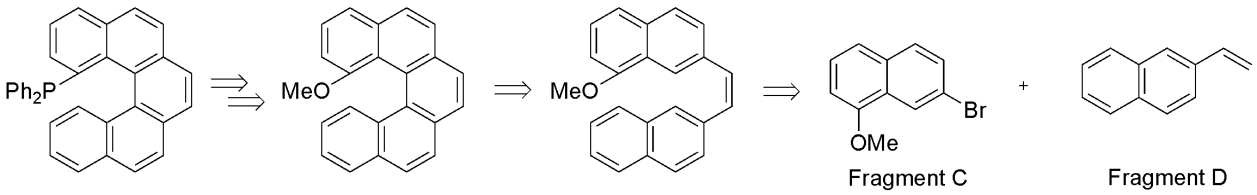

Since 2-vinylnaphthalene (Fragment D) is commercially available, only Fragment C had to be synthesized from simpler precursors. First, a Fridel-Crafts bromination of α-tetralone was completed which produced a 1:1 mixture of the desired 7-bromo-3,4-dihydronaphthalen-1(2*H*)-one product and the undesired isomer, 5-bromo-3,4-dihydronaphthalen-1(2*H*)-one (eq 52). Although difficult, these isomers could be separated by column chromatography. Benzylic bromination of 7-bromo-3,4-dihydronaphthalen-1(2*H*)-one at C4 enabled the following one step aromatization and methylation of the intermediate 7-bromonaphthalen-1-ol alcohol to produce 7-bromo-1-methoxynaphthalene (or Fragment C) in very good yield (eq 53).

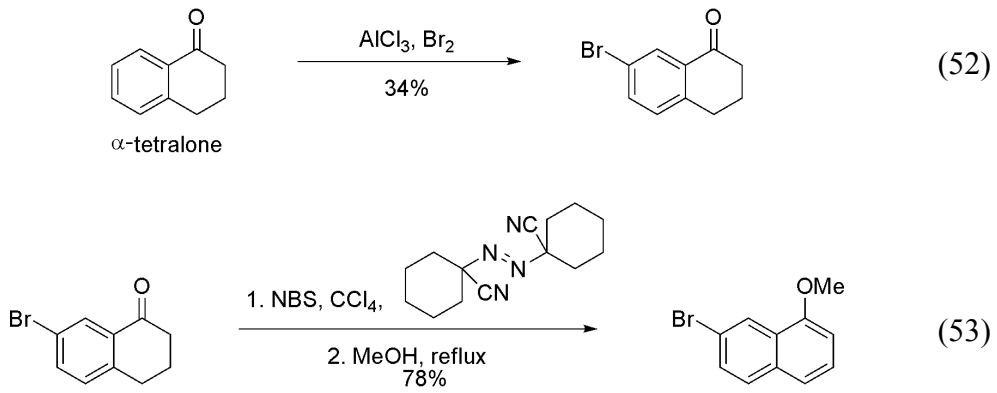

The Heck reaction of 7-bromo-1-methoxynaphthalene and 2-vinylnaphthalene was carried out with a catalytic amount of $Pd(OAc)_2$, K_3PO_4 base, and at 140°C (eq 54). While the yield was relatively poor, enough product was isolated to test the next crucial photocyclization step. In eq 55, the attempted cyclization of 1-methoxy-7-(2-(naphthalen-2-yl)vinyl)naphthalene is shown. Presumably, under these conditions UV irradiation would propagate iodine radicals which would then initiate the cyclization of the desired substrate. However, no reaction was observed when either 350nm UV light or visible light was used as the irradiation source. In order to complete the helicene backbone further optimization of this reaction is required, for at the moment it is unclear what is impeding the transformation. There are two distinct possibilities as to why no reaction was observed: either poor isomerization of the *trans* alkene starting material to the required *cis* isomer, or no iodine radical initiation occurred at the wavelengths of light that were examined.

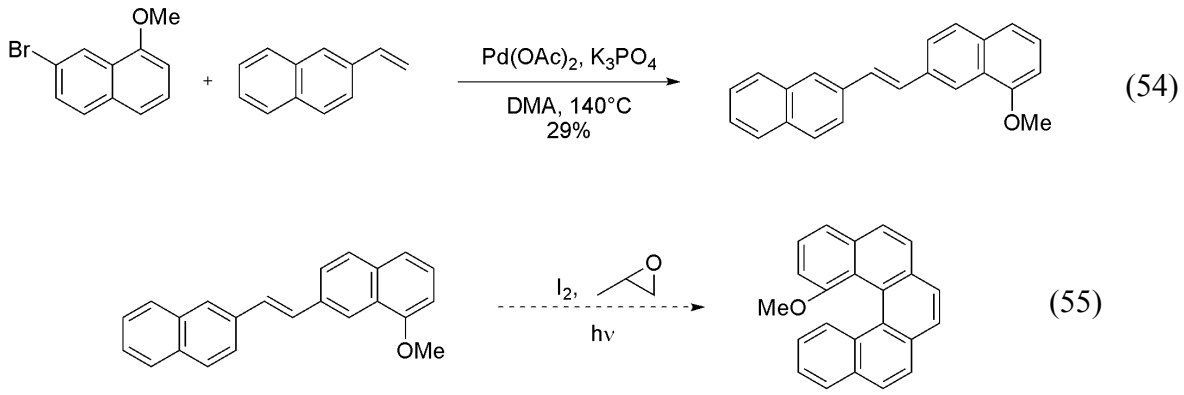

3.3 Conclusion

Towards the synthesis of a [5]helical phosphine ligand, two different approaches were attempted. The first strategy involved a key olefin metathesis reaction which required the synthesis of two precursor naphthalene derivatives: 1-bromo-2-naphthaldehyde and a triflated 1-hydroxy-8-methoxy-2-naphthaldehyde. 1-Bromo-2-naphthaldehyde was furnished in two steps from the commercially available 1-bromo-2-methylnaphthalene, while 1-hydroxy-8-methoxy-2-naphthaldehyde was synthesized in two steps from naphthalene-1,8-diol. However, the triflation of 1-hydroxy-8-methoxy-2-naphthaldehyde was not efficient under a variety of reaction conditions and thus, a new route toward the target helicene was attempted.

The second strategy towards the [5]helical phosphine ligand was a more traditional approach using a key photocyclization step. For this route, the photocyclization precursor was generated by a Heck reaction between 7-bromo-1-methoxynaphthalene and 2-vinylnaphthalene (commercially available). 7-Bromo-1-methoxynaphthalene was synthesized in two steps from α-tetralone. Unfortunately, the photoinduced cyclization did not proceed to furnish the necessary helicene backbone. Thus, currently new strategies toward the desired helicene are required to continue the synthesis.

3.4 Experimental Procedures

For General Experimental, Materials, or Instrumentation, please see sections 1.4.1, 1.4.2, and 1.43, respectively.

3.4.1 General Procedure for the Synthesis of 1-Bromo-2-(dibromomethyl) naphthalene

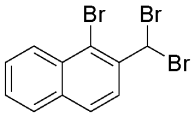

Based on a literature procedure.[71] In a flask equipped with a magnetic stir bar, 1.0 g of 1-bromo-2-methyl naphthalene (4.5 mmol) and 2.33 g of *N*-bromosuccinimide (13.1 mmol) were dissolved in benzene (50 mL, 0.09M). Note, the NBS was not completely soluble in benzene at room temperature. Next, 190 mg of benzoyl peroxide (75% w/w, 0.59 mmol) was added to the solution and it was refluxed at 95°C over night (16 hours). The reaction had changed colour from light yellow to orange. The solids in the reaction were filtered off and the solution was concentrated under reduced pressure to obtain a yellow-orange solid. The compound was purified by column chromatography (2% EtOAc-hexanes) to obtain 1.18 g (69%) of a very light yellow solid. ^{1}H NMR spectrum was in accordance with literature sources.[71]

3.4.2 General Procedure for the Synthesis of 1-Bromo-2-naphthaldehyde

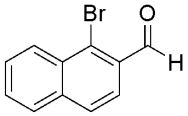

Based on a literature procedure.[71] In a flask equipped with a magnetic stir bar, 137 mg of 1-bromo-2-(dibromomethyl)naphthalene (0.36 mmol) was dissolved in EtOH (14.4 mL, 0.025M). In a separate vial 122 mg of $AgNO_3$ (0.72 mmol) was dissolved in water (3.6 mL, 0.2M with

---

[71] Demir, A. S.; Reis, O. *Tetrahedron* **2004**, *60*, 3803.

respect to $AgNO_3$). The $AgNO_3$ solution was added to the organic mixture upon which the entire solution became milky. The mixture was refluxed for 75 minutes (progressively becoming clearer in colour) and while still hot, it was suction filtered to remove the lime green precipitate. The remaining clear solution was concentrated under reduced pressure to obtain a white solid. The solid was washed with cold 4:1 EtOH:H_2O under suction filtration and then dried under vacuum to afford 51 mg (67%) of a fluffy white solid. ^{1}H NMR spectrum was in accordance with literature sources.[72]

3.4.3 General Procedure for the Synthesis of 8-Methoxynaphthalen-1-ol

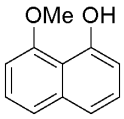

500 mg of naphthalene-1,8-diol (3.12 mmol) and 560 mg of K_2CO_3 (4.06 mmol) was dissolved in acetone (31 mL, 0.1M) in a flask containing a magnetic stir bar (the mixture was brown-purple in colour). At room temperature, iodomethane (193 μL, 440 mg, 3.12 mmol) was added to the stirring mixture dropwise. The solution was subsequently refluxed for 60 minutes and then concentrated under reduced pressure to remove the acetone. The crude was dissolved in EtOAc and washed with a 10% HCl solution and brine. The organic layer was dried with $MgSO_4$, filtered, and then concentrated to obtain a black oil. The product was purified by column chromatography (3-5% EtOAc-hexanes) to afford 389 mg (72%) of a light yellow oil which solidified to a light yellow solid under vacuum. m.p. 54-55°C. IR (neat): 3350, 1630, 1610, 1581, 1514, 1450, 1397, 1307, 1228, 1196, 1158, 1074, 1028, 963, 811, 751, 671 cm^{-1}. ^{1}H NMR (400 MHz, $CDCl_3$) δ 9.32 (s, 1H), 7.45-7.28 (m, 4H), 6.88 (dd, J = 1.3Hz, J = 7.4Hz, 1H), 6.78 (d, J = 7.6Hz, 1H), 4.06 (s, 3H). ^{13}C NMR (75 MHz, $CDCl_3$) δ 156.1, 154.4, 136.7, 127.7, 125.6, 121.8, 118.8, 115.0, 110.4, 103.8, 56.0. HRMS (EI) *m*/*e* calcd. for $C_{11}H_{16}O_2$ $[M-H]^+$: 174.0681; found: 174.0685.

---

[72] Moleele, S. S.; Michael, J. P.; de Koning, C. B. *Tetrahedron* **2006**, *62*, 2831.

3.4.4 General Procedure for the Synthesis of 1-Hydroxy-8-methoxy-2-naphthaldehyde

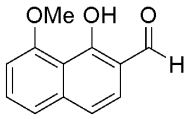

Prepared according to a literature procedure.[73] 350 mg of 8-methoxynaphthalen-1-ol (2.0 mmol) was dissolved in anhydrous THF (20 mL, 0.1M) in a flame dried and argon purged flask equipped with a magnetic stir bar. 288 mg of $MgCl_2$ (3.0 mmol), 1.1 mL of Et_3N (7.5 mmol), and 241 mg of paraformaldehyde (8.0 mmol) were added (in that order) to the solution and the reaction was refluxed for 60 minutes under an argon atmosphere. The colour had changed from bright lime green, to canary yellow, and finally to orange. The reaction was allowed to cool, upon which EtOAc was added and the mixture and was washed with a 10% HCl solution. The aqueous layer was extracted with EtOAc (3x), and the combined organic layers were dried over Na_2SO_4, filtered, and concentrated under reduced pressure. The resulting dark brown-yellow oil was purified by column chromatography (20% EtOAc-hexanes) to obtain 300 mg (74%) of a dark golden yellow solid. m.p. 88-89°C. IR (neat): 3314, 1670, 1651, 1626, 1593, 1509, 1466, 1454, 1380, 1232, 1130, 1067, 968, 894, 816, 783, 751, 695 cm^{-1}. ^1H NMR (400 MHz, $CDCl_3$) δ 11.14 (br, 1H), 10.42 (s, 1H), 7.69 (d, J = 8.6Hz, 1H), 7.50 (t, J = 8.0Hz, 1H), 7.39 (dd, J = 0.6Hz, J = 8.2Hz, 1H), 7.28 (d, J = 8.6Hz, 1H), 6.93-6.87 (m, 1H), 4.10 (s, 3H). ^{13}C NMR (75 MHz, $CDCl_3$) δ 191.1, 161.9, 158.2, 139.9, 129.9, 125.1, 121.6, 119.3, 117.2, 115.1, 105.7, 56.4 (methoxy with H-bond), 30.9 (methoxy without H-bond). HRMS (EI) *m*/*e* calcd. for $C_{12}H_{10}O_3$ $[M-H]^+$: 202.0630; found: 202.0626.

---

[73] Hofslokken, N. U.; Skattebol, L. *Acta Chemica Scandinavica* **1999**, *53*, 258.

3.4.5 General Procedure for the Synthesis of 7-Bromo-3,4-dihydronaphthalen-1(2*H*)-one

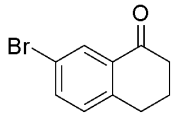

Based on a literature procedure.[74] To a flame dried and argon purged flask equipped with a magnetic stir bar was added 4.17 g of aluminum trichloride (31.3 mmol). While stirring, 1.66 mL of α-tetralone (12.5 mmol) was added slowly over 1 minute and a white gas was evolved ($HCl_{(g)}$). The mixture became darker in colour until it turned into a dark brown sludge. (Note, sometimes gentle heating was required to lower the viscosity and allow the stir bar to rotate.) The mixture was stirred at room temperature for 30 minutes before the dropwise addition of 2.40 g of bromine (15.0 mmol) was carried out (maximum stirring is important at this step). After all of the bromine had been added, the flask was equipped with a condenser and the brown mixture was heated to 80°C for 5 minutes. A little bit of a 10% $Na_2S_2O_3$ solution was added to the flask to quench excess bromine and the entire mixture was poured into a seperatory funnel containing ice and 10% HCl. The mixture was extracted with Et_2O (3x) and the combined organic layers were washed with water and brine, dried over Na_2SO_4, and concentrated under reduced pressure. The resulting dark yellow oil was purified by column chromatography (0-7% EtOAc-hexanes) to afford 958 mg (34%) of a yellow solid. ^{1}H NMR spectrum was in accordance with literature sources.[75]

---

[74] Cornelius, L. A. M.; Combs, D. W. *Synth. Commun*. **1994**, *24*, 2777.

[75] Heller, D. P.; Goldberg, D. R.; Wu, H.; Wulff, W. D. *Can. J. Chem.* **2006**, *84*, 1487.

3.4.6 General Procedure for the Synthesis of 7-Bromo-1-methoxynaphthalene

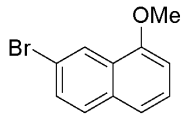

Based on a literature procedure.[76] To a flask equipped with a magnetic stir bar was added 100 mg of 7-bromo-3,4-dihydronaphthalen-1(2*H*)-one (0.44 mmol), 87 mg of *N*-bromosuccinimide (0.49 mmol), 5.4 mg of 1,1-azobis(cyclohexanecarbonitrile) (0.022 mmol), and 2 mL of CCl_4 (0.25M). After dissolution, the solution was refluxed for 30 minutes, after which 5.5 mL of MeOH was added to the solution and the refluxing continued for 16 hours. The solution was then concentrated under reduced pressure and purified by column chromatography (0-10% EtOAc-hexanes) to afford 81 mg (78%) of a light red oil. IR (neat): 1585, 1497, 1455, 1432, 1386, 1358, 1267, 1234, 1207, 1107, 1068, 994, 885, 819, 739, 708 cm^{-1}. ^1H NMR (300 MHz, $CDCl_3$) δ 8.42 (d, *J* = 1.9Hz, 1H), 7.66 (d, *J* = 8.7Hz, 1H), 7.55 (dd, *J* = 2.0Hz, *J* = 8.7Hz, 1H), 7.41-7.37 (m, 2H), 6.84 (dd, *J* = 3.0Hz, *J* = 5.6Hz, 1H), 4.00 (s, 3H). ^{13}C NMR (75 MHz, $CDCl_3$) δ 154.5, 132.8, 129.7, 129.1, 126.6, 126.3, 124.6, 120.0, 119.3, 104.7, 55.6. HRMS (EI) *m*/*e* calcd. for $C_{11}H_9BrO$ $[M-H]^+$: 235.9837; found: 235.9836.

3.4.7 General Procedure for the Synthesis of 1-Methoxy-7-(2-(naphthalen-2-yl)vinyl)naphthalene

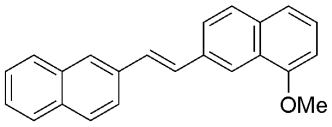

Based on a literature procedure.[77] To a flame dried and argon purged 1DR vial equipped with a magnetic stir bar was added 23.4 mg of 7-bromo-1-methoxynaphthalene (0.1 mmol) and 0.5 mL of DMA. Subsequently, 29.4 mg of K_3PO_4 (0.14 mmol), 18.3 mg of 2-vinylnaphthalene (0.12 mmol), and 0.02 mg of $Pd(OAc)_2$ (0.0001 mmol) were added and dissolved. The vial was capped and heated to 140°C for 16 hours. The reaction was then concentrated under reduced pressure

---

[76] Akbarzadeh, T.; Shafiee, A. *Synth. Commun.* **2004**, *34*, 1455.

[77] Yao, Q.; Kinney, E. P.; Yang, Z. *J. Org. Chem.* **2003**, *68*, 7528.

and purified by prep-TLC (5% EtOAc-hexanes) to obtain 9 mg (29%) of a dark yellow solid. m.p. 142-143.5°C. IR (neat): 1597, 1569, 1505, 1460, 1431, 1385, 1269, 1239, 1216, 1097, 1066, 997, 961, 889, 863, 848, 821, 783, 741 cm^{-1}. ^{1}H NMR (400 MHz, $CDCl_3$) δ 8.36 (s, 1H), 7.92-7.77 (m, 7H), 7.52-7.34 (m, 6H), 6.84 (dd, *J* = 0.9Hz, *J* = 7.4Hz, 1H), 4.05 (s, 3H). ^{13}C NMR (100 MHz, $CDCl_3$) δ 155.6, 135.0, 134.2, 134.1, 133.8, 133.0, 129.5, 128.7, 128.3, 128.0, 127.9 127.7, 126.6, 126.3, 126.0, 125.8, 125.7, 124.1, 123.5, 120.9, 120.1, 104.3, 55.6. HRMS (EI) *m*/*e* calcd. for $C_{23}H_{18}O$ $[M-H]^+$: 310.1358; found: 310.1352.

Appendix A. NMR Spectra

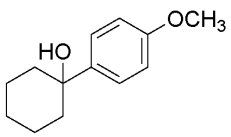

^{1}H NMR in $CDCl_3$

^{13}C NMR in $CDCl_3$

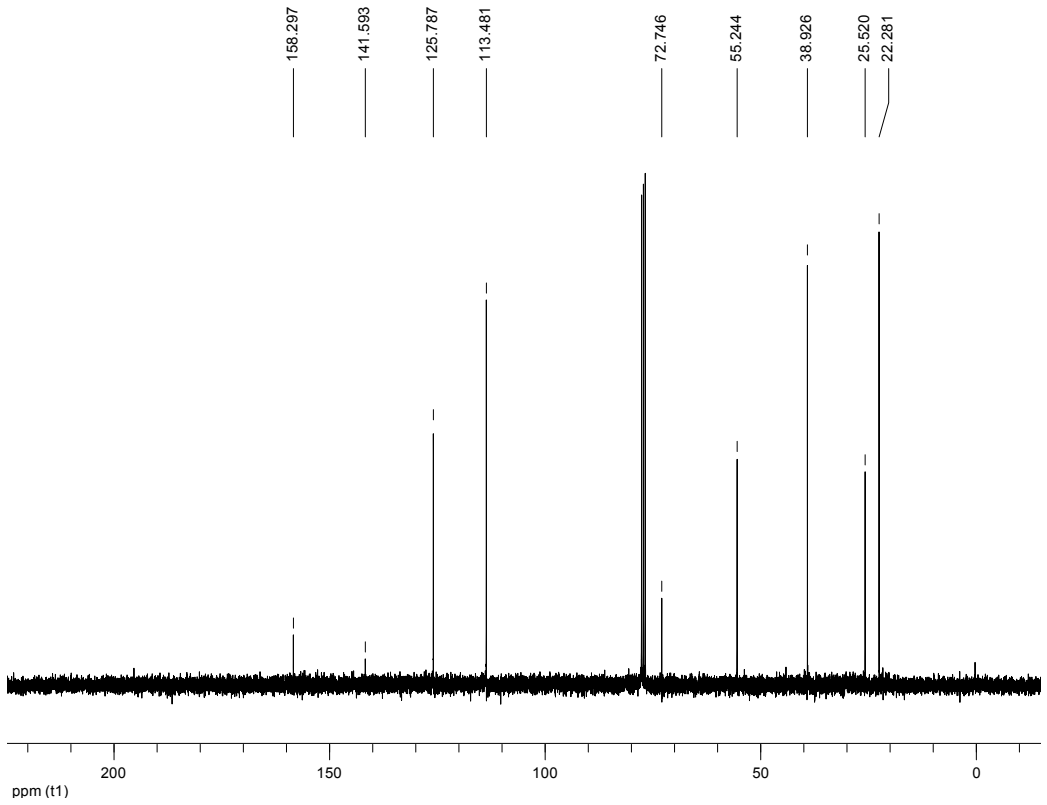

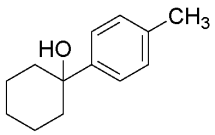

^{1}H NMR in $CDCl_3$

^{13}C NMR in $CDCl_3$

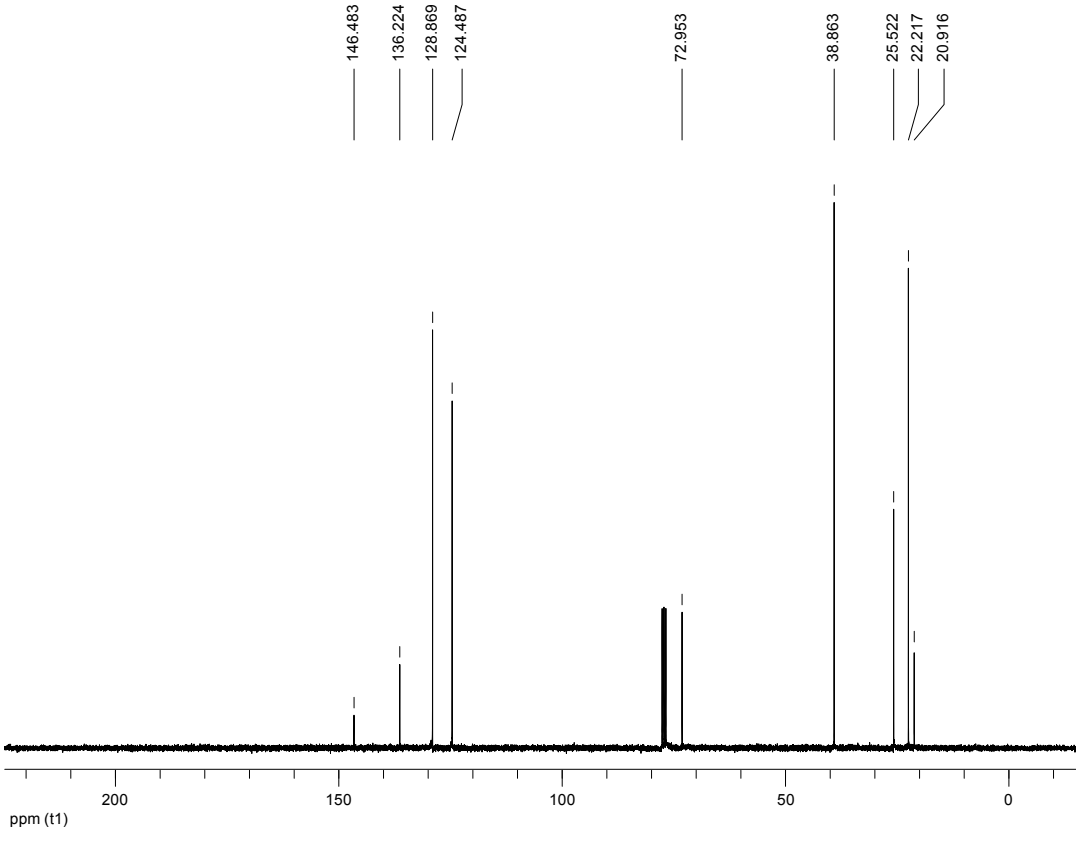

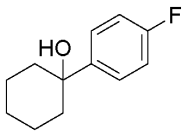

^{1}H NMR in $CDCl_3$

^{13}C NMR in $CDCl_3$

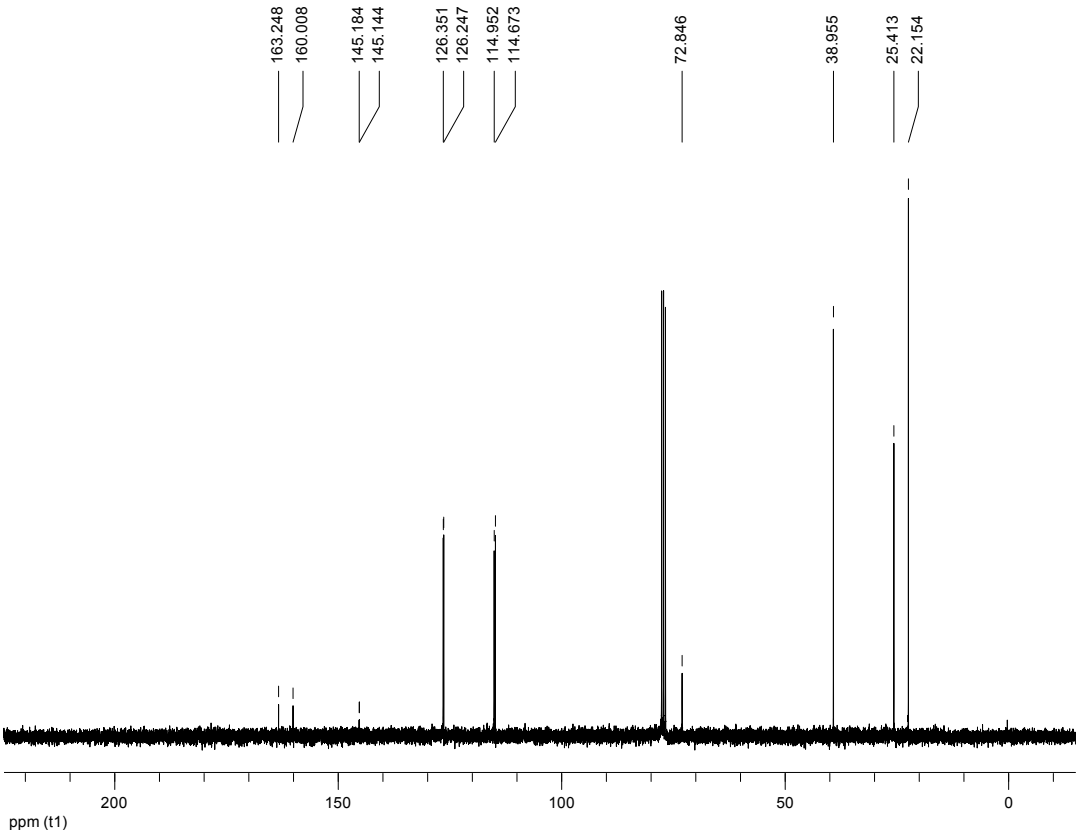

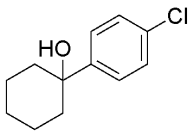

^{1}H NMR in $CDCl_3$

^{13}C NMR in $CDCl_3$

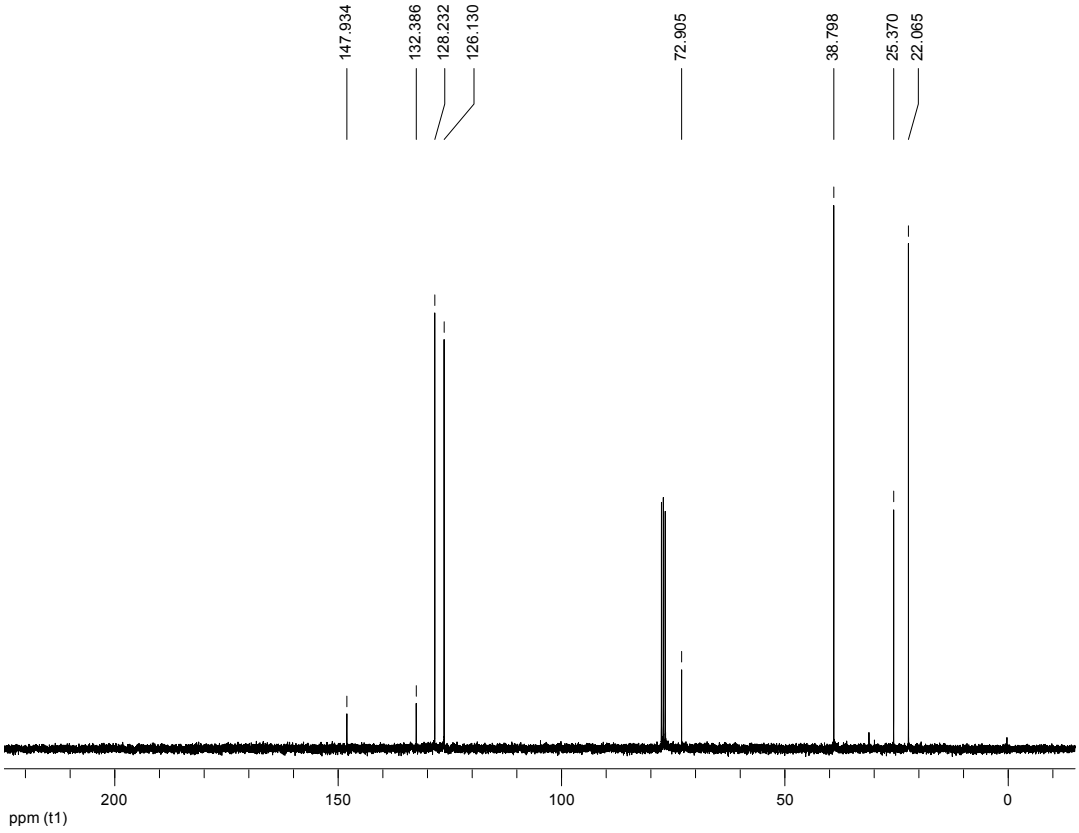

^{1}H NMR in $CDCl_3$

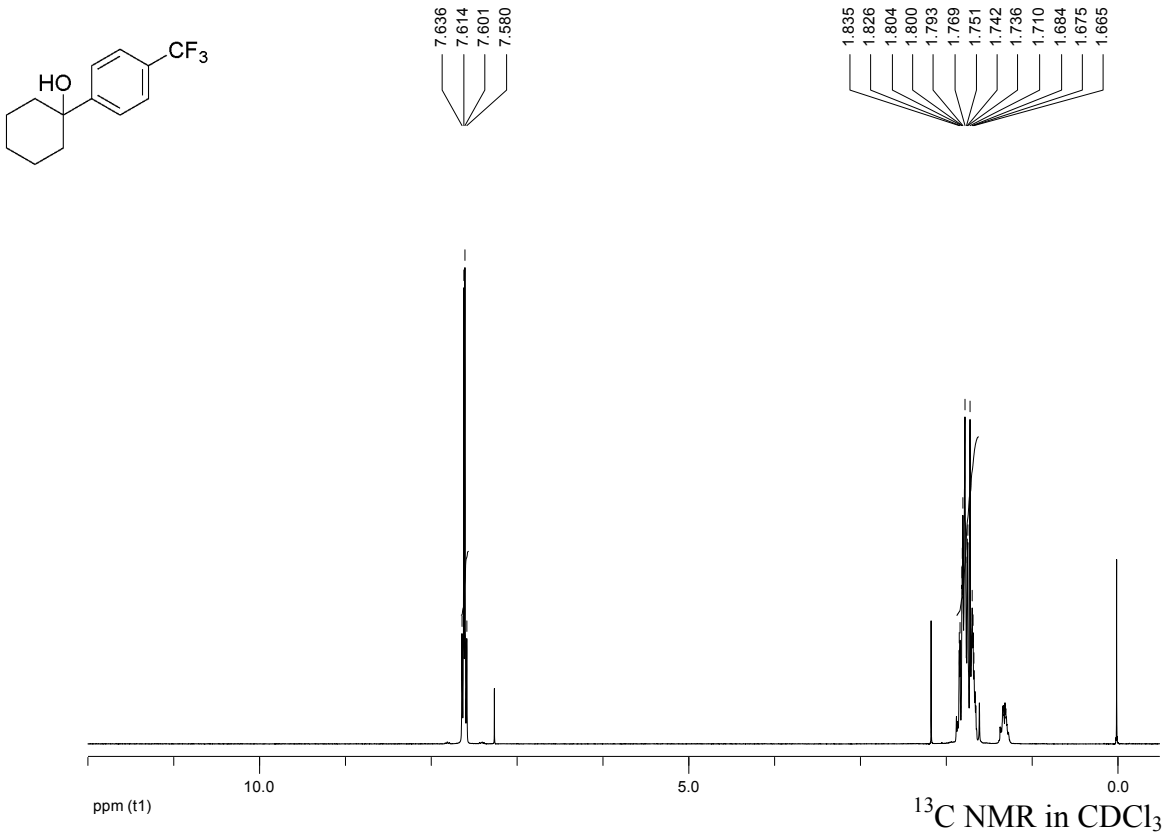

^{13}C NMR in $CDCl_3$

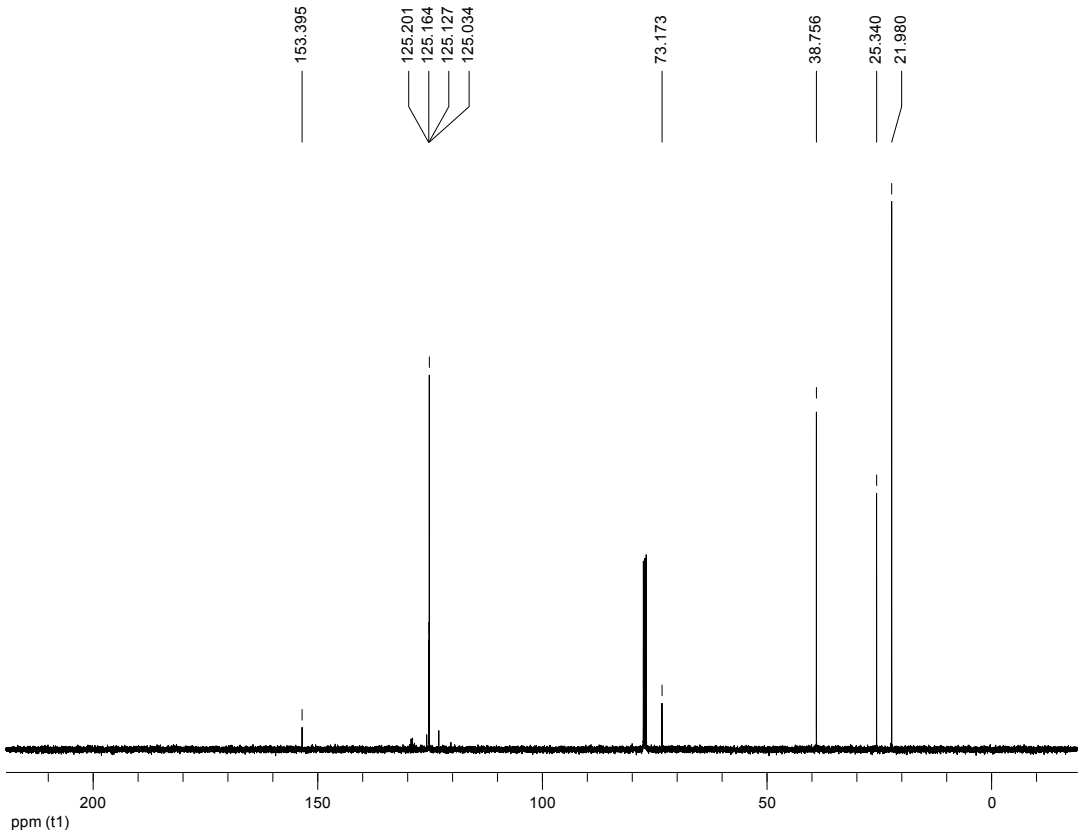

^{1}H NMR in $CDCl_3$

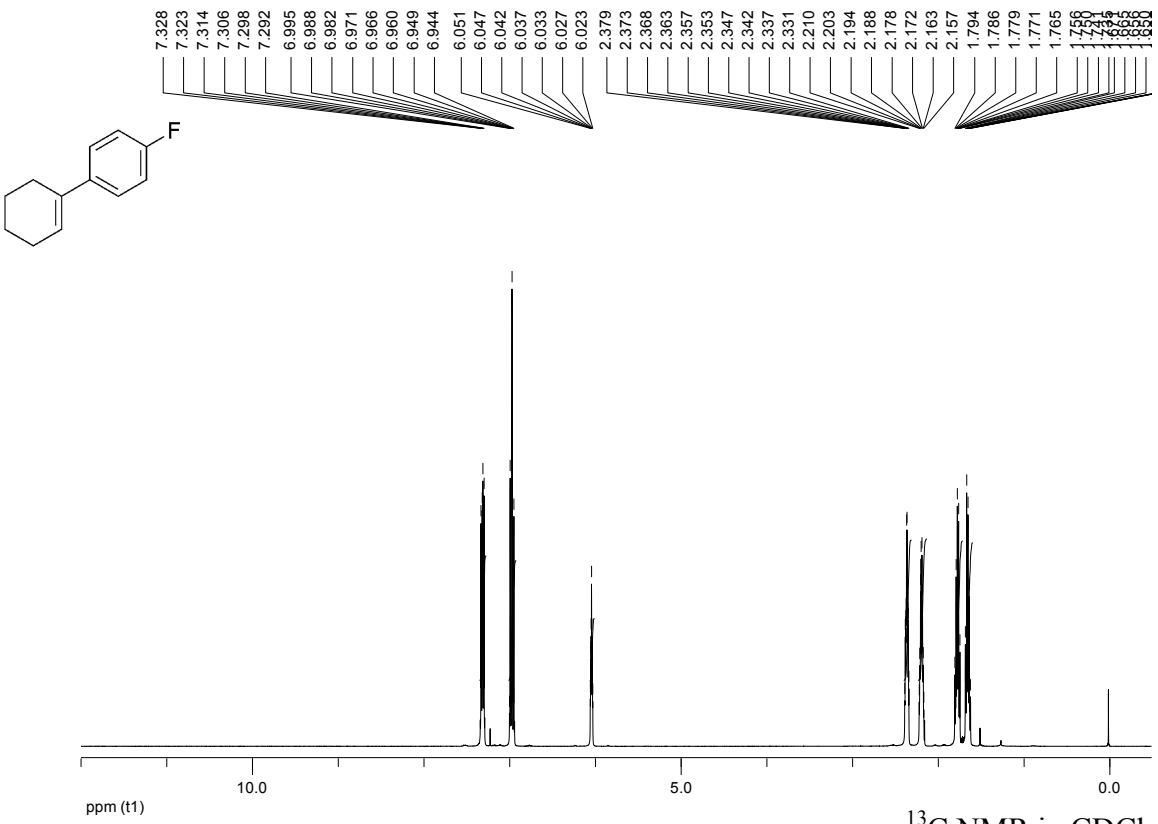

^{13}C NMR in $CDCl_3$

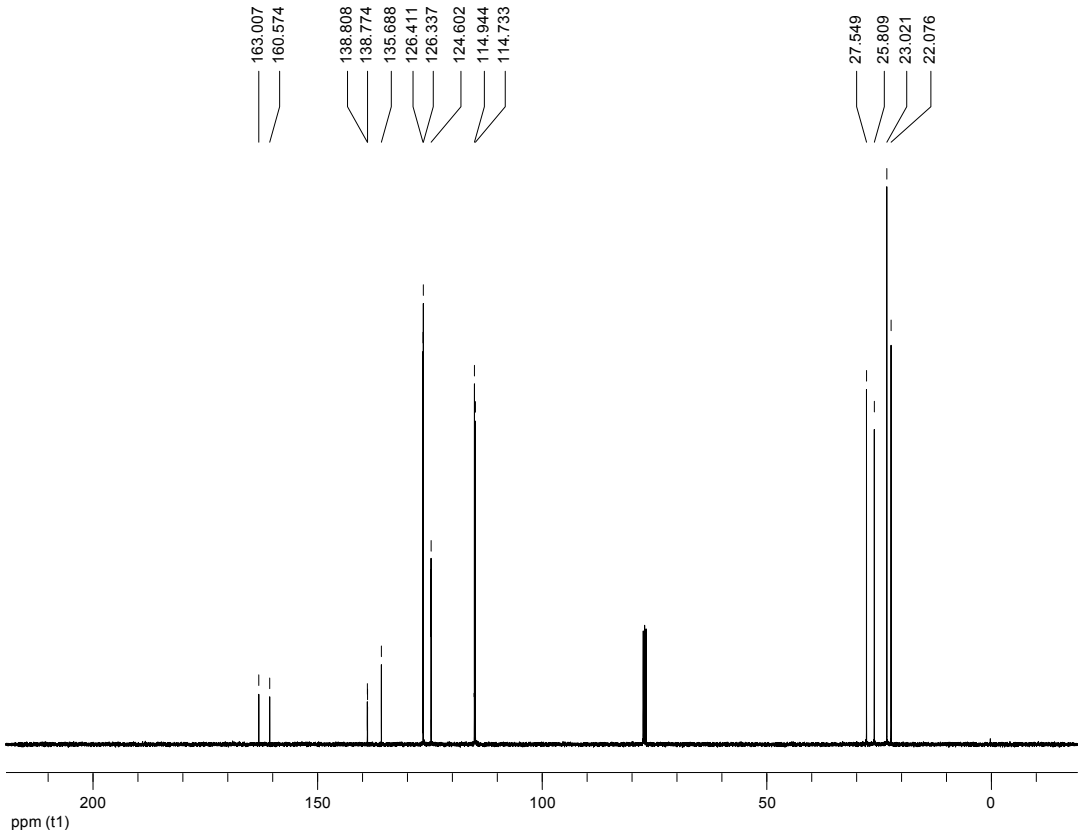

^{1}H NMR in $CDCl_3$

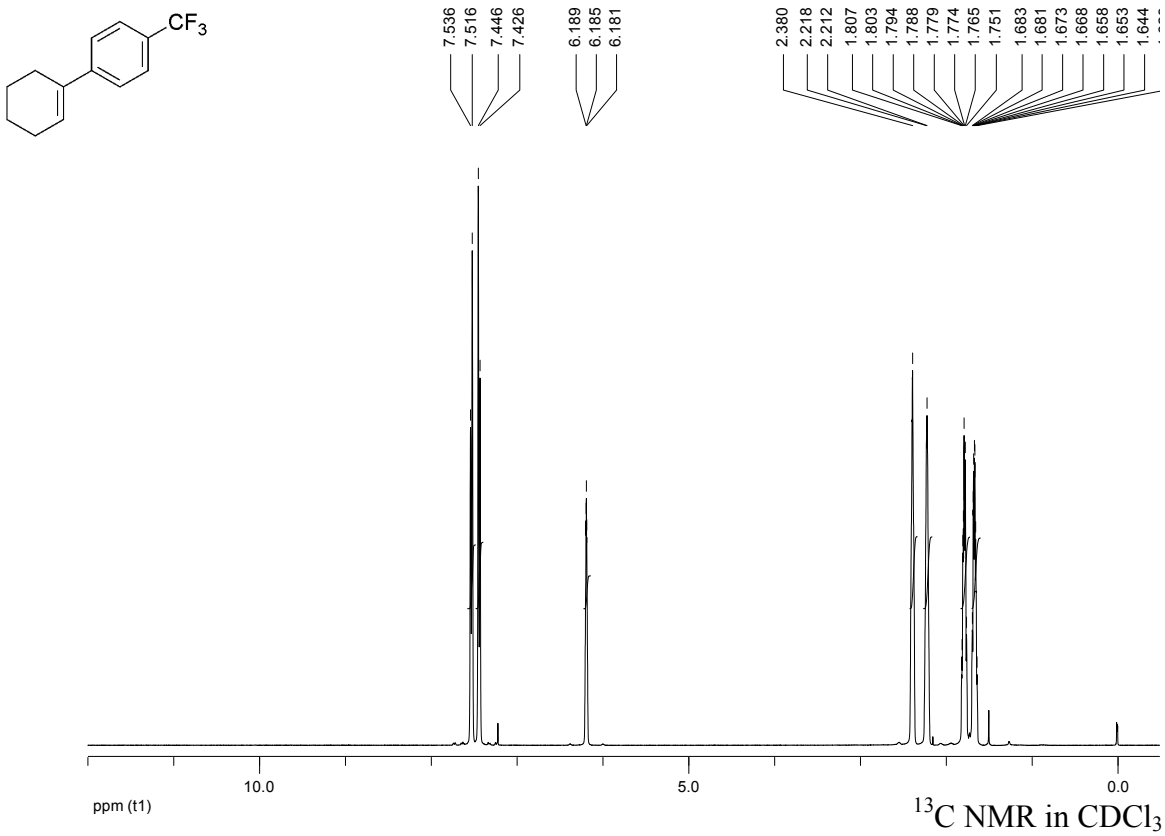

^{13}C NMR in $CDCl_3$

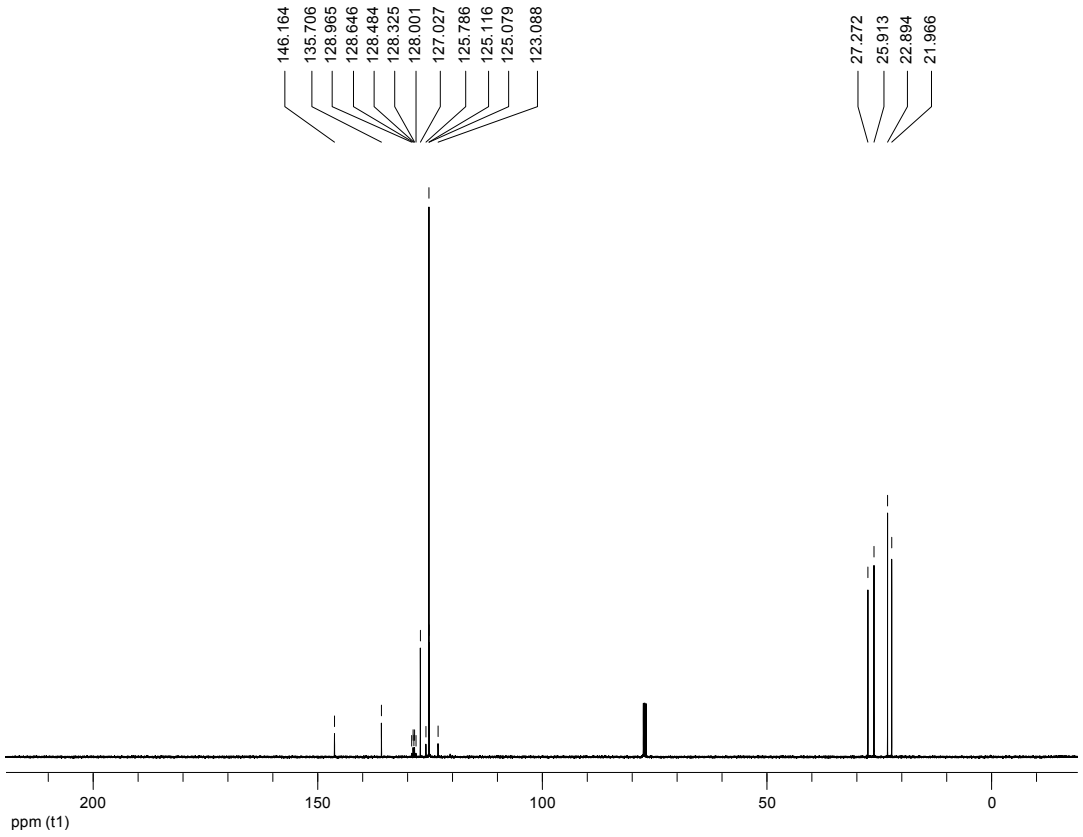

^{1}H NMR in $CDCl_3$

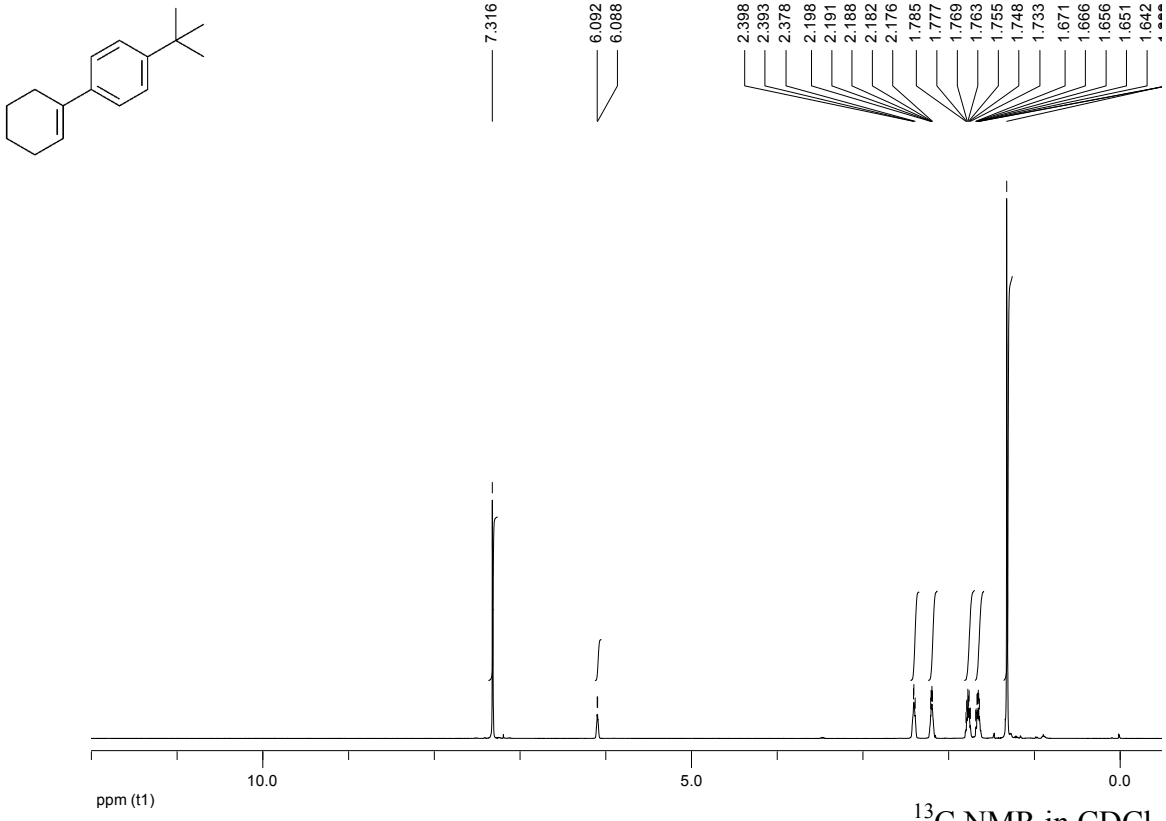

^{13}C NMR in $CDCl_3$

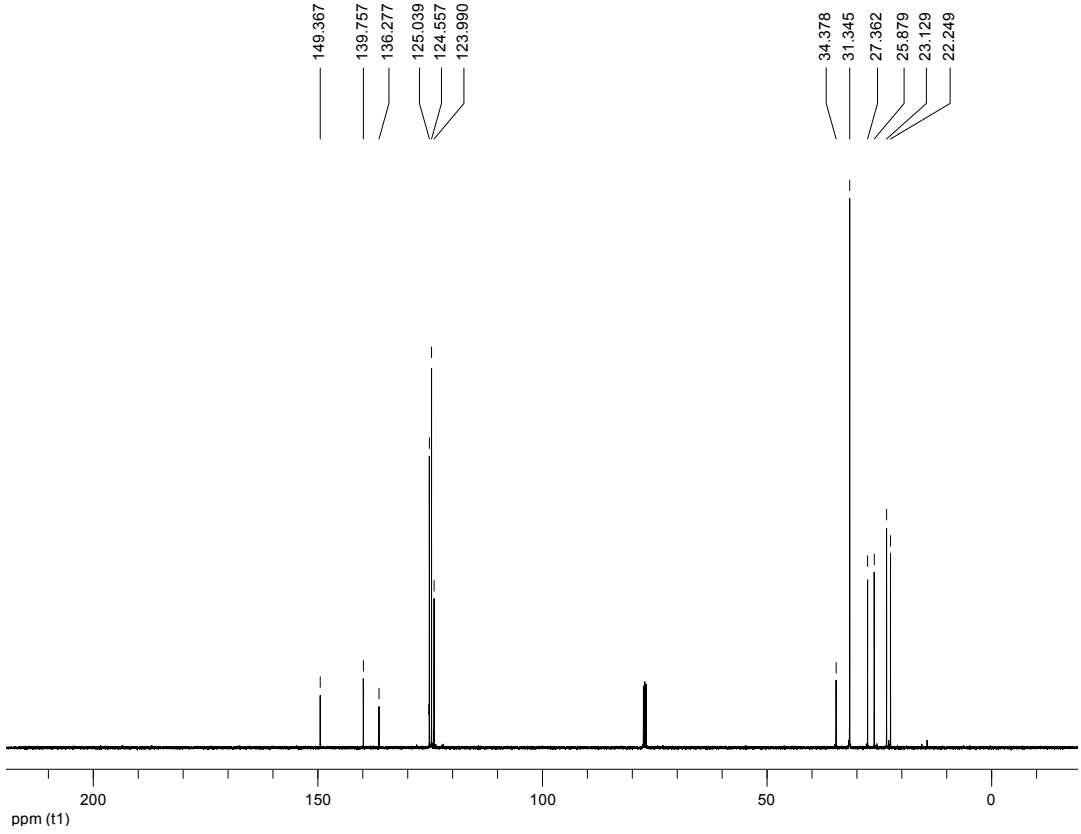

^{1}H NMR in $CDCl_3$

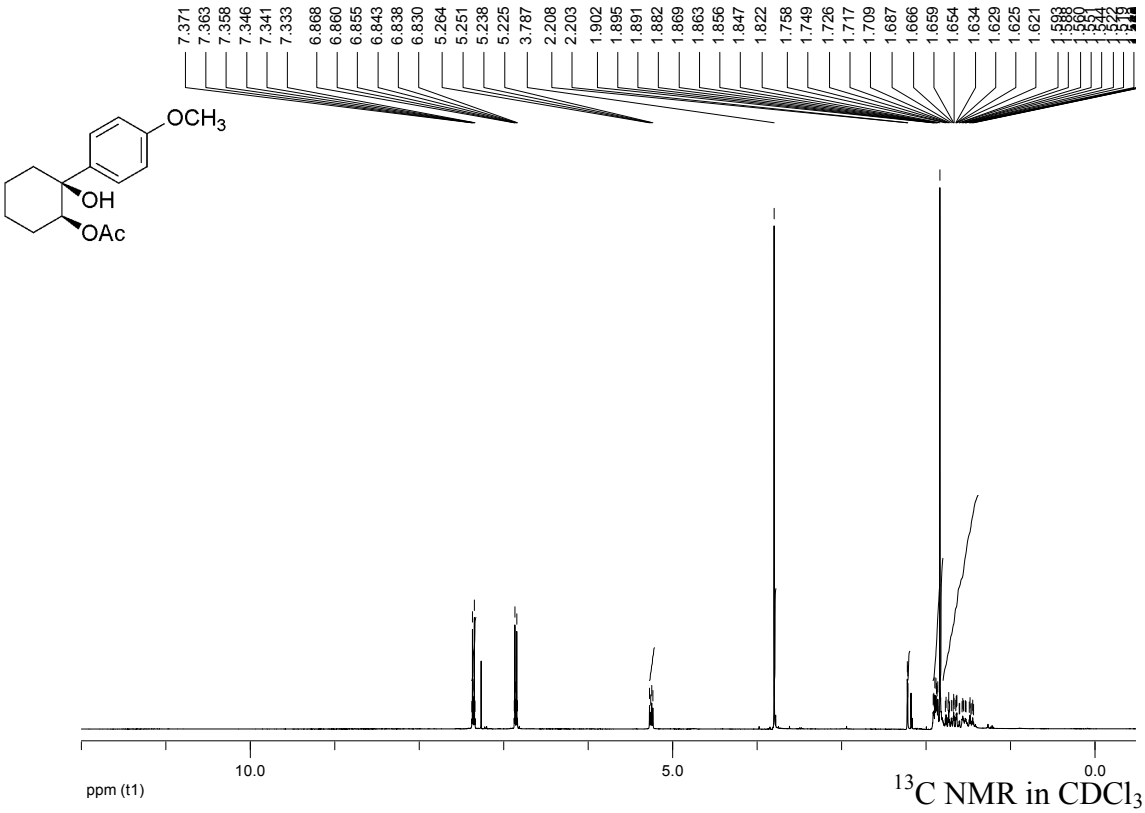

^{13}C NMR in $CDCl_3$

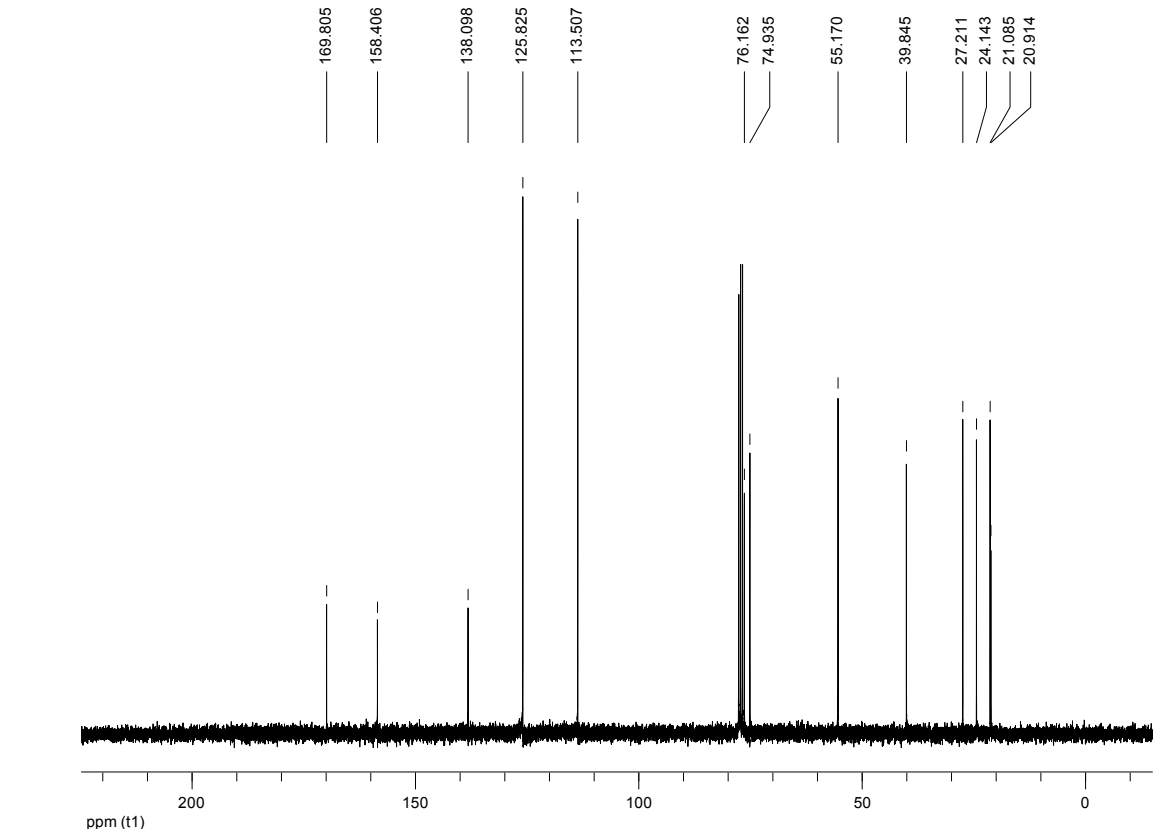

^{1}H NMR in $CDCl_3$

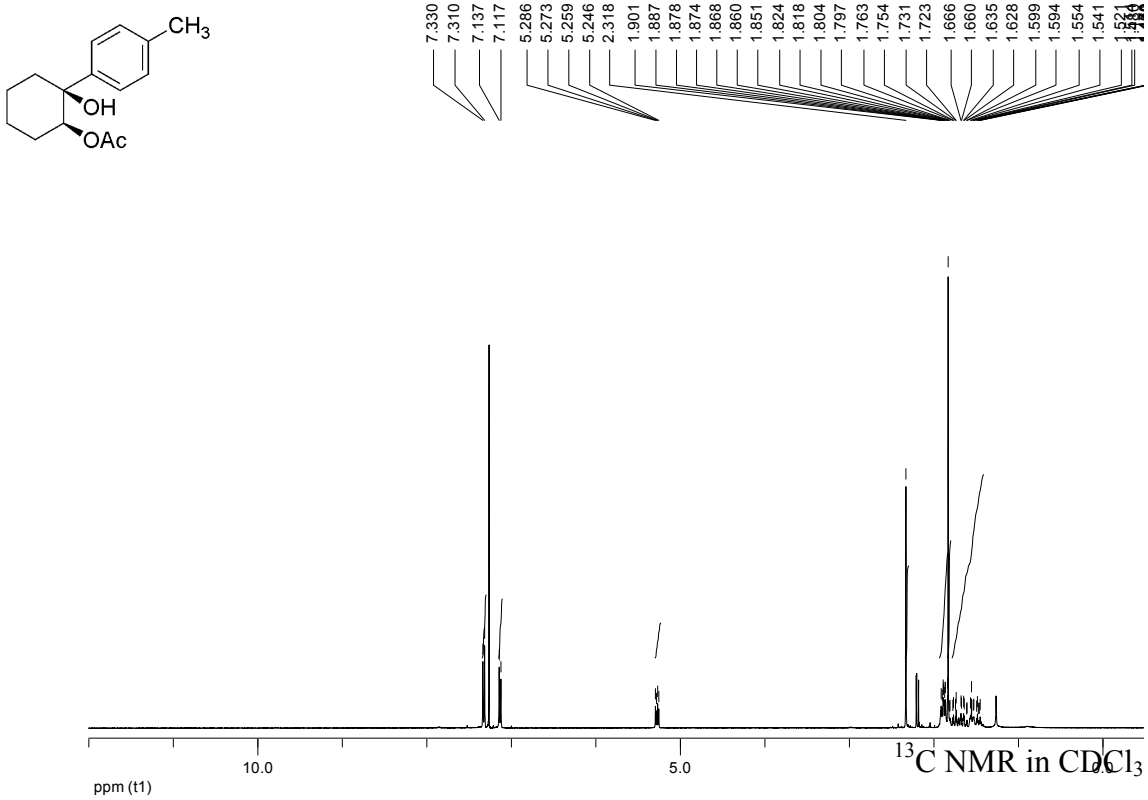

^{13}C NMR in $CDCl_3$

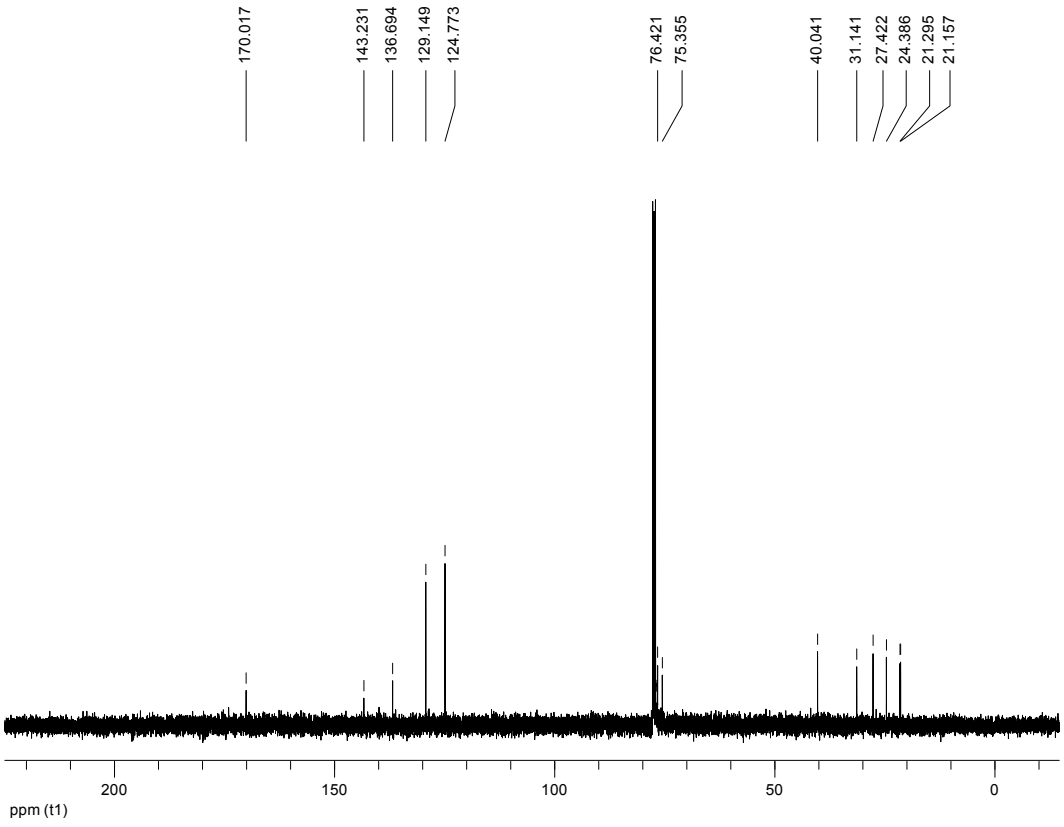

^{1}H NMR in $CDCl_3$

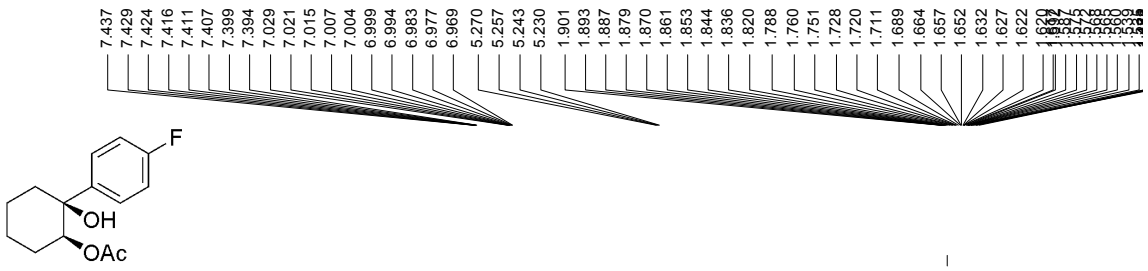

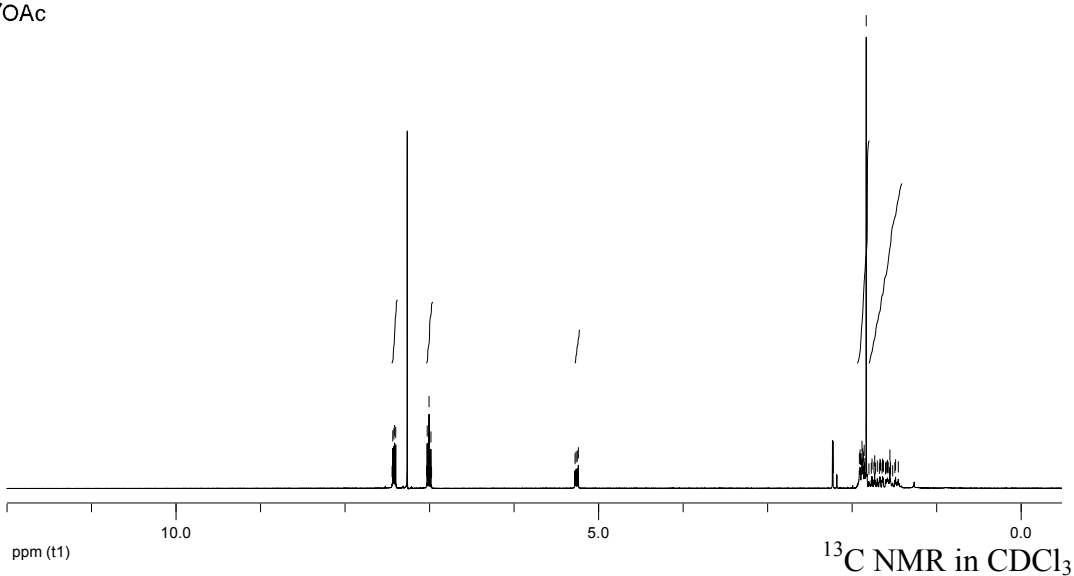

^{13}C NMR in $CDCl_3$

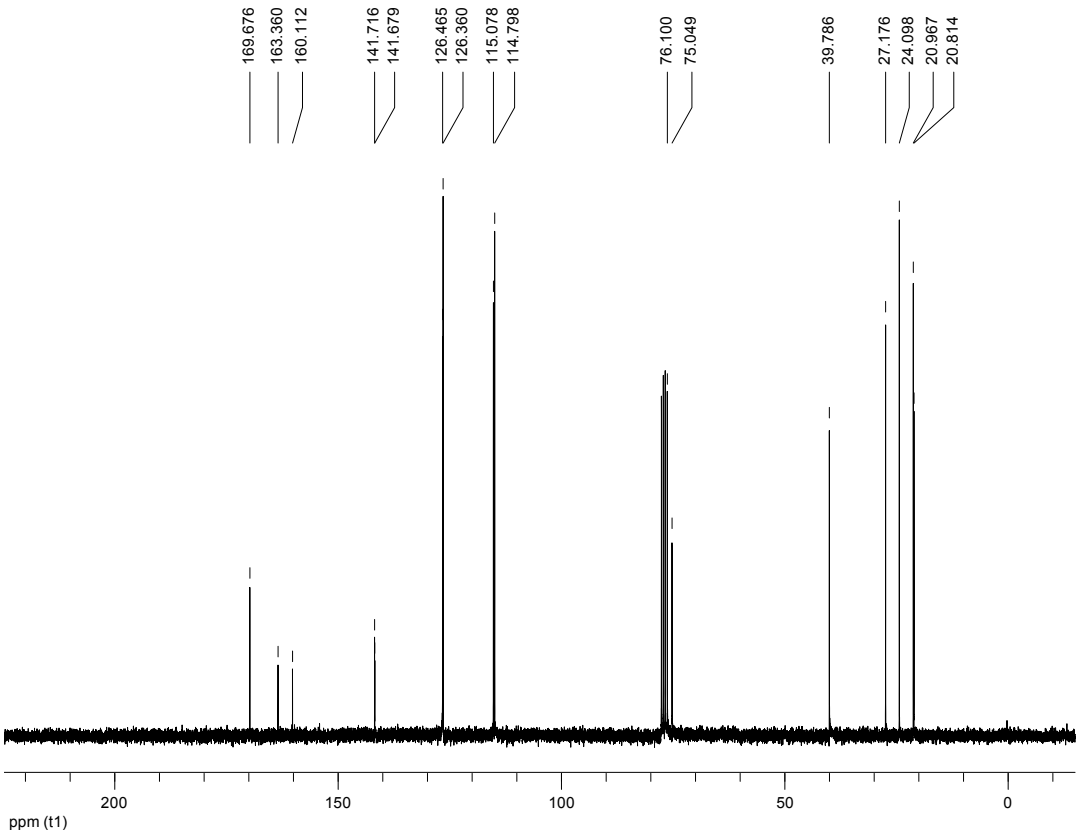

^{1}H NMR in $CDCl_3$

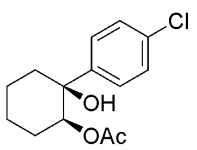

^{13}C NMR in $CDCl_3$

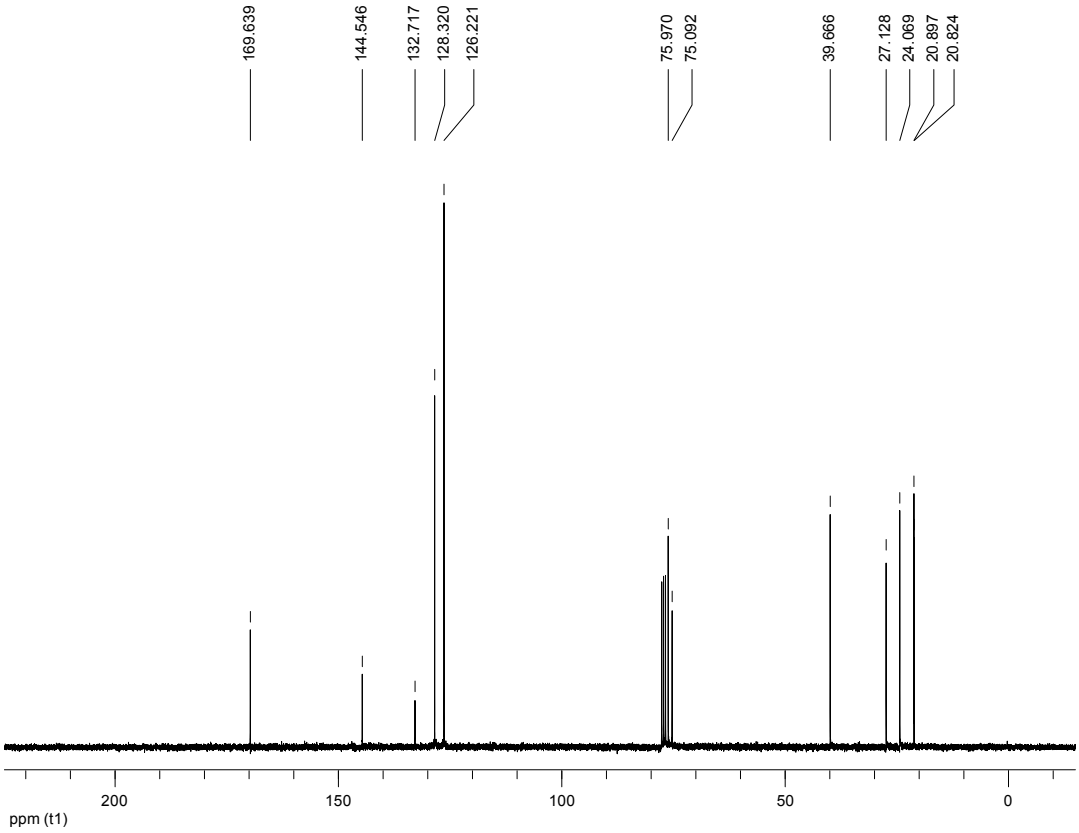

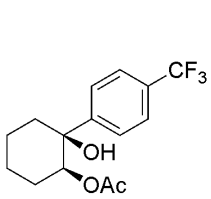

^{1}H NMR in $CDCl_3$

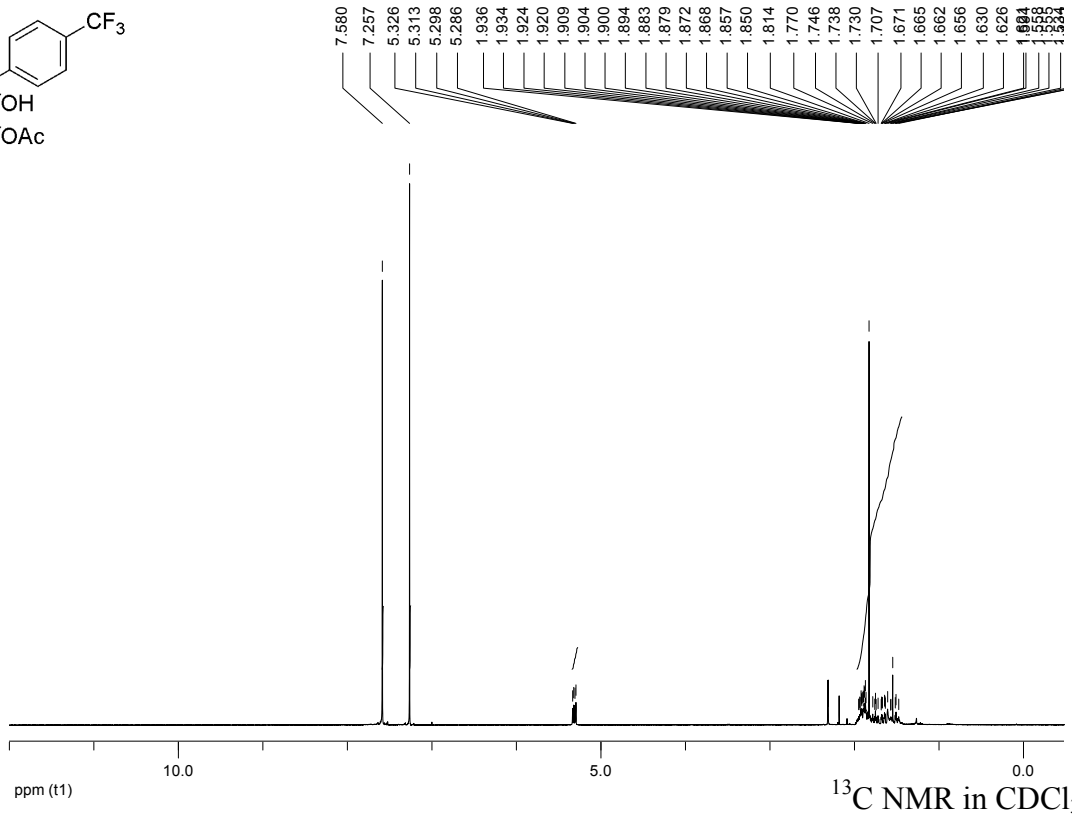

^{13}C NMR in $CDCl_3$

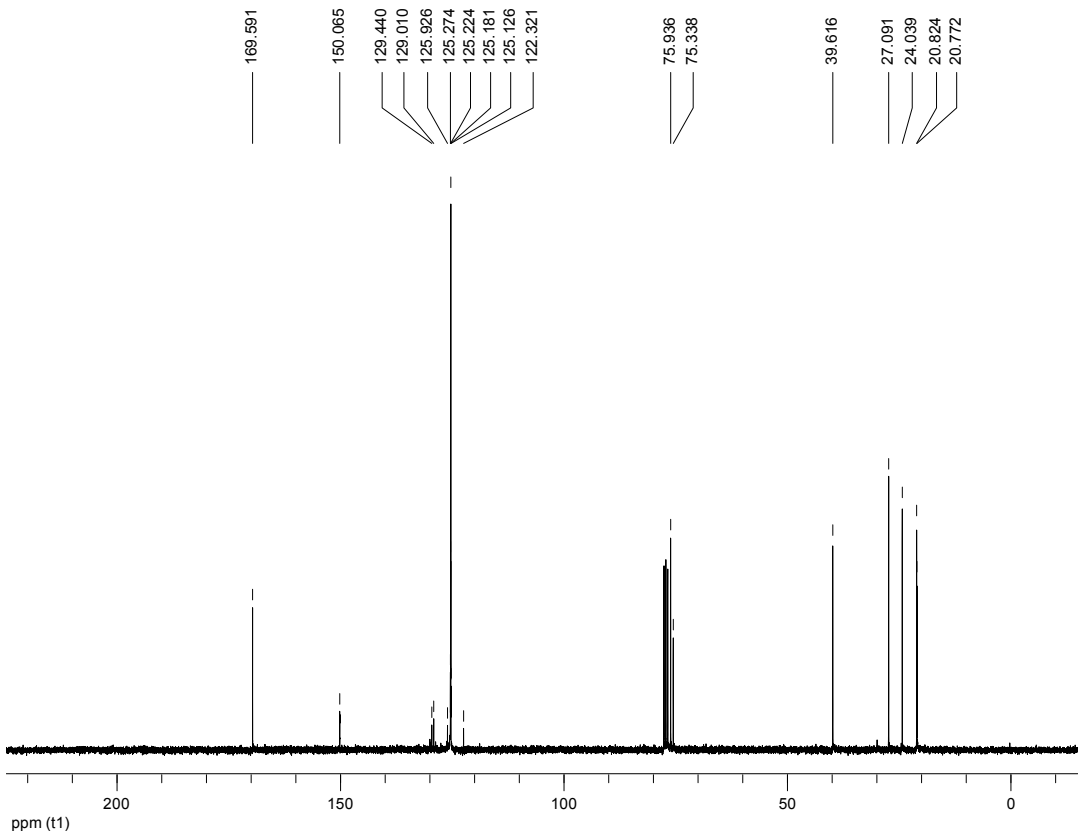

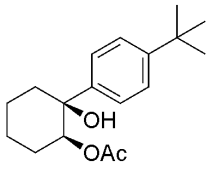

^{1}H NMR in $CDCl_3$

^{13}C NMR in $CDCl_3$

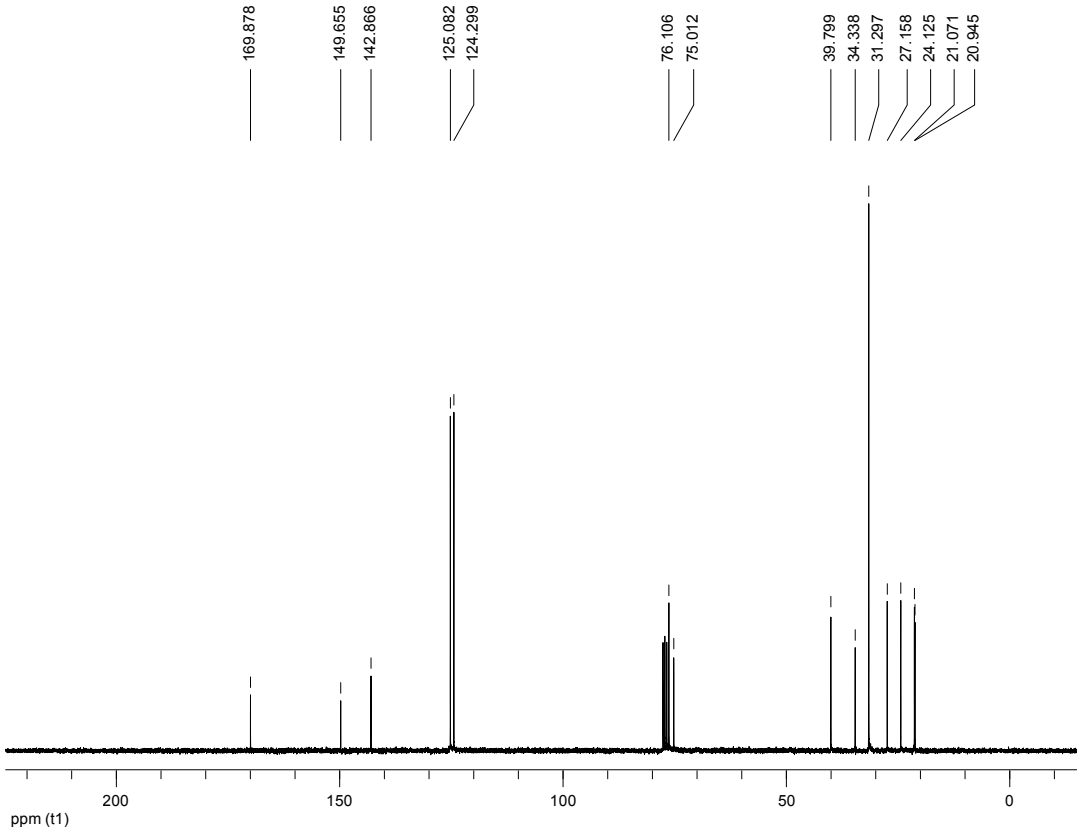

^{1}H NMR in $CDCl_3$

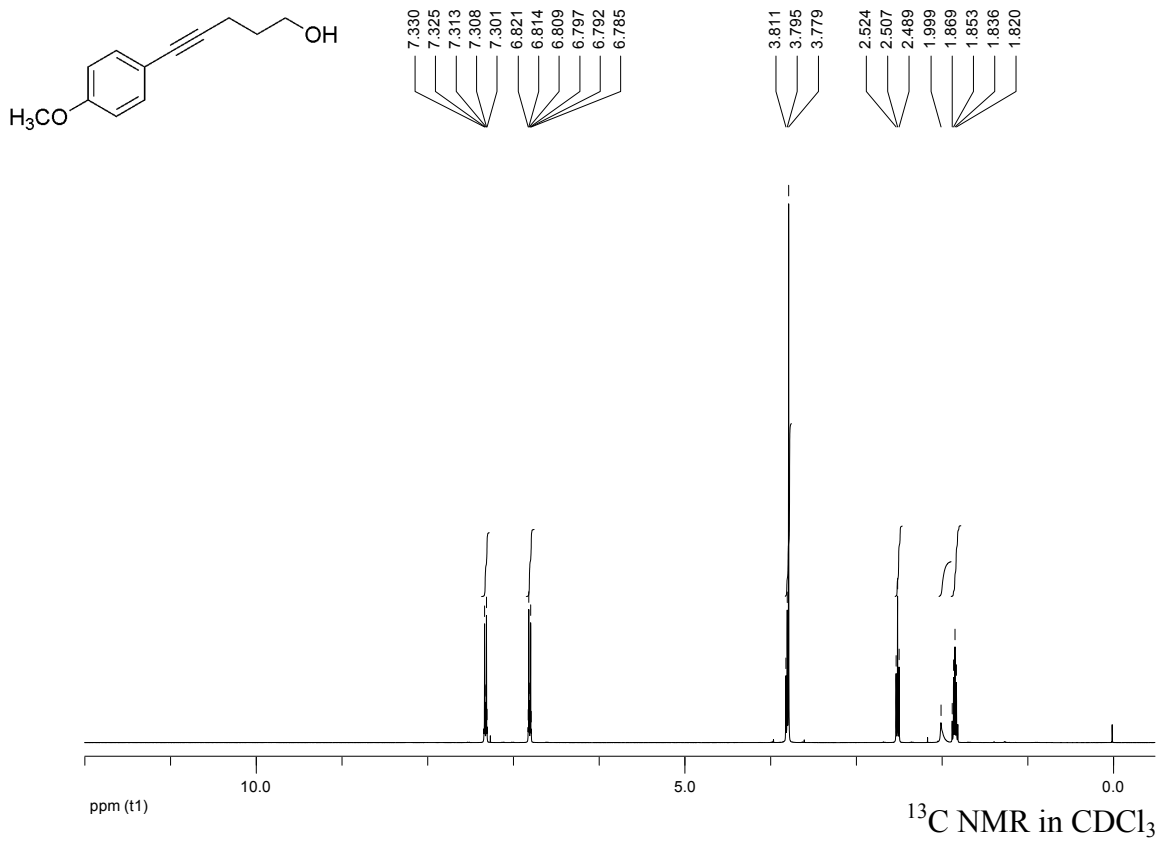

^{13}C NMR in $CDCl_3$

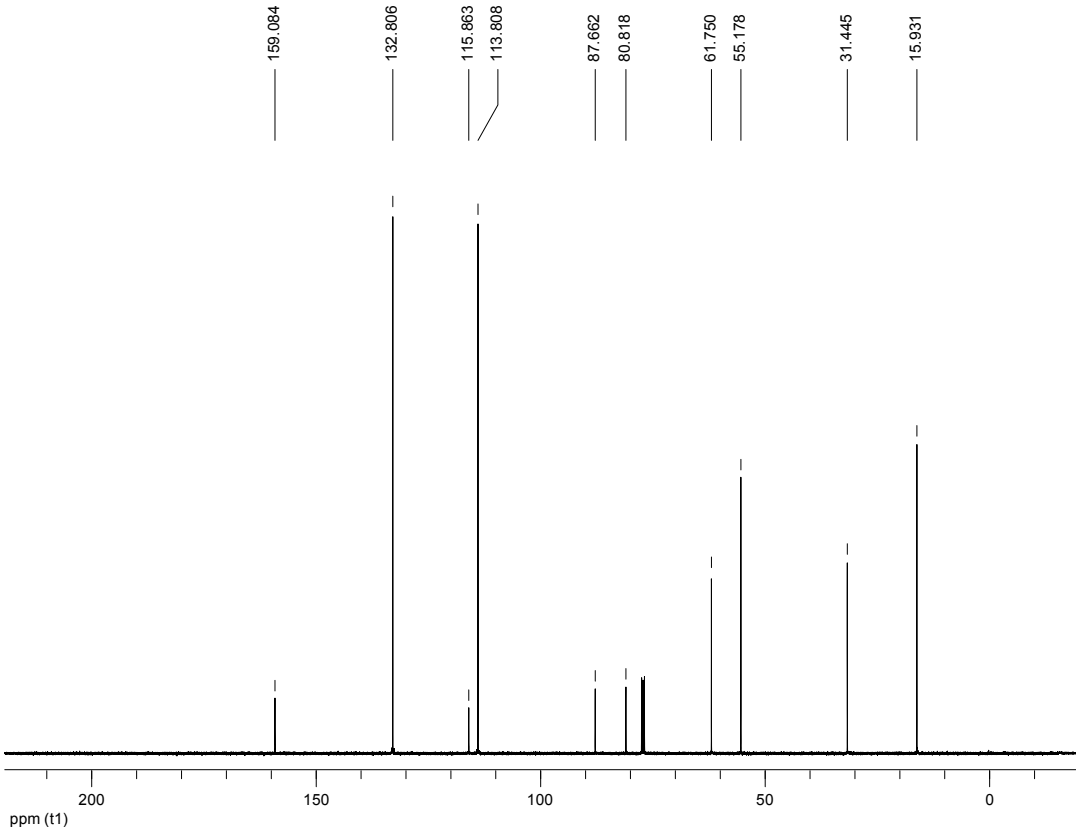

^{1}H NMR in $CDCl_3$

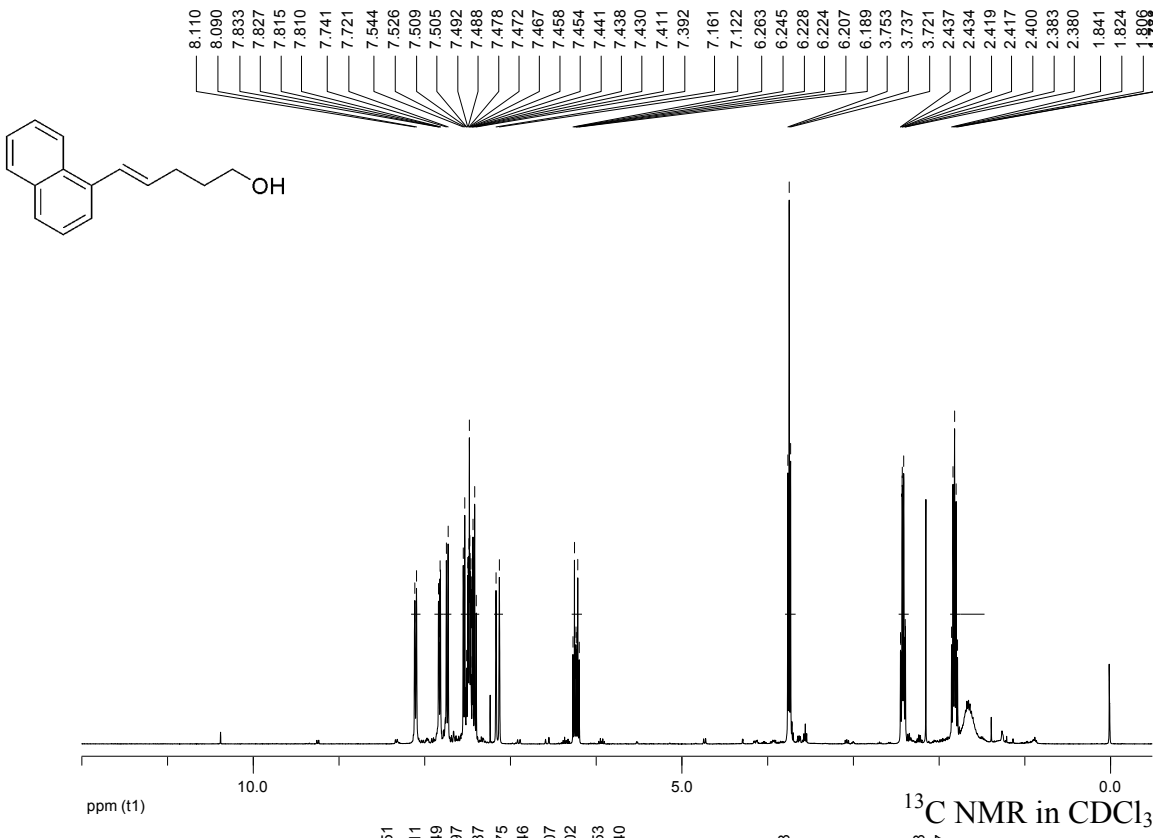

^{13}C NMR in $CDCl_3$

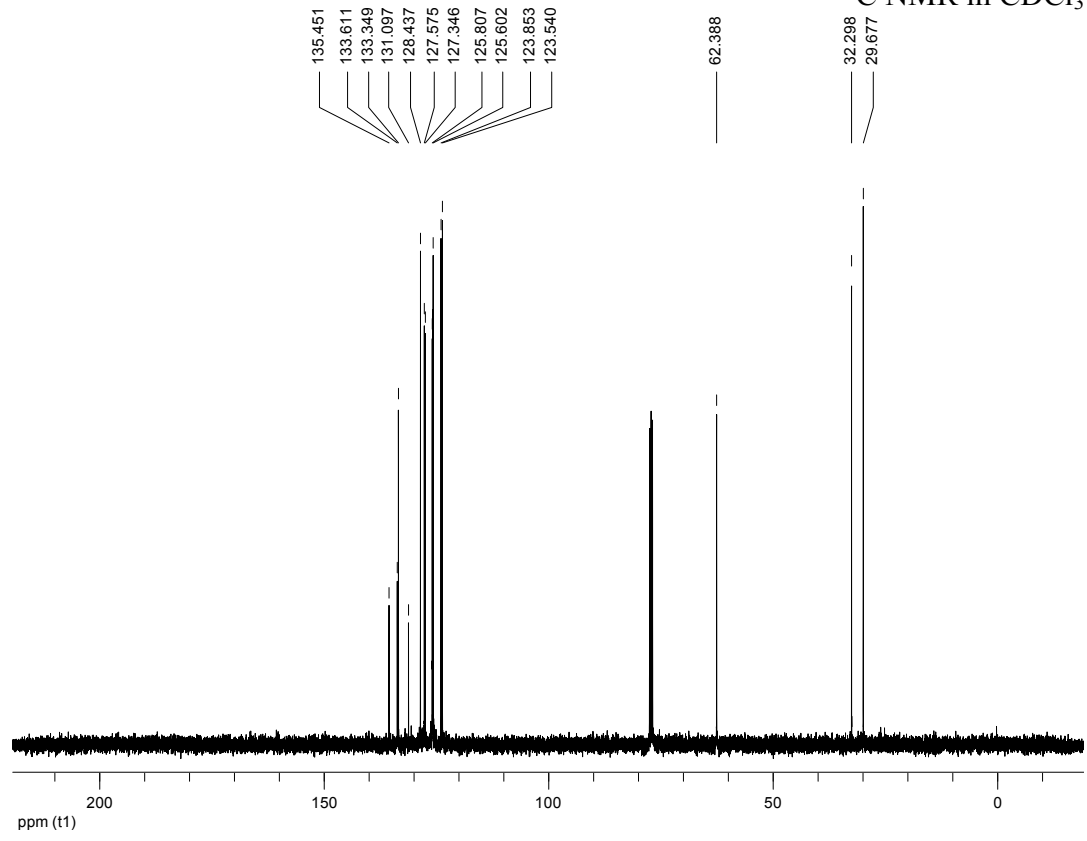

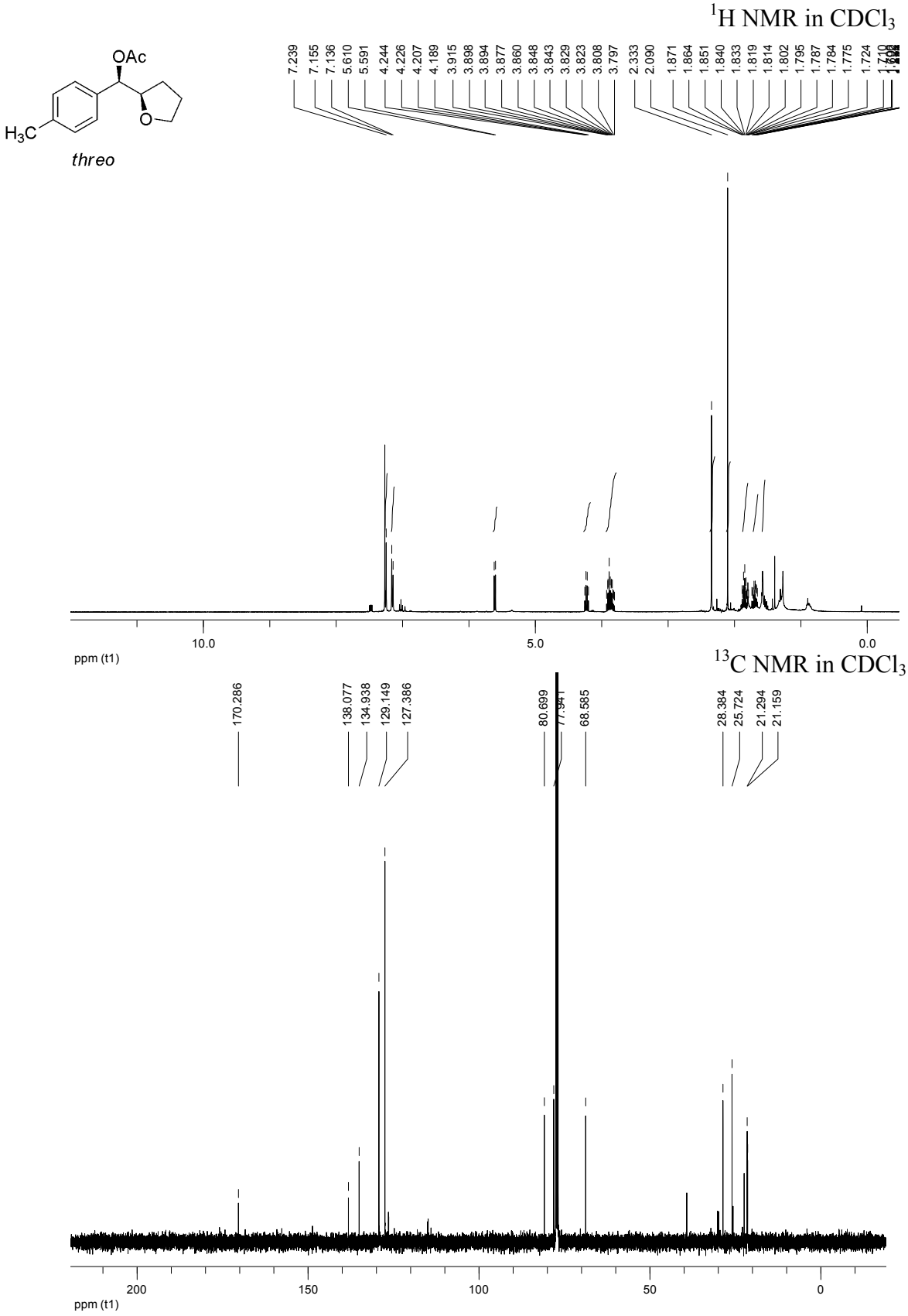
OAc
H3C
O
threo
1H NMR in CDCl3
7.239
7.155
7.136
5.610
5.591
4.244
4.226
4.207
4.189
3.915
3.898
3.894
3.877
3.860
3.848
3.843
3.829
3.823
3.808
3.797
2.333
2.090
1.871
1.864
1.851
1.840
1.833
1.819
1.814
1.802
1.795
1.787
1.784
1.775
1.724
10.0
5.0
0.0
ppm (t1)
13C NMR in CDCl3
170.286
138.077
134.938
129.149
127.386
80.699
77.341
68.585
28.384
25.724
21.294
21.159
200
150
100
50
0
ppm (t1)

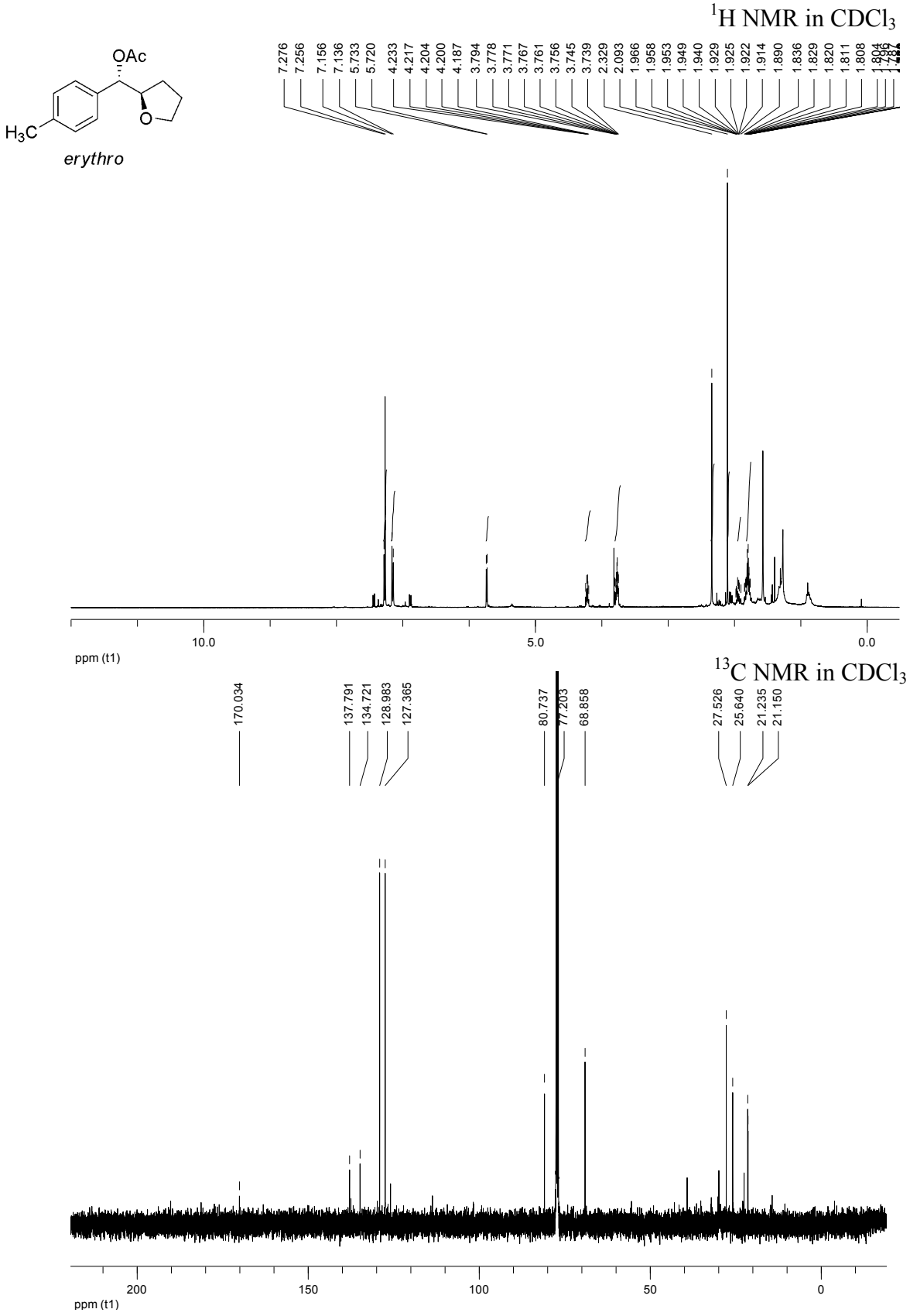
^{1}H NMR in $CDCl_3$
OAc
H_3C
O
erythro
7.276
7.256
7.156
7.136
5.733
5.720
4.233
4.217
4.204
4.200
4.187
3.794
3.778
3.771
3.767
3.761
3.756
3.745
3.739
2.329
2.093
1.966
1.958
1.953
1.949
1.940
1.929
1.925
1.922
1.914
1.890
1.836
1.829
1.820
1.811
1.808
10.0
5.0
0.0
ppm (t1)
^{13}C NMR in $CDCl_3$
170.034
137.791
134.721
128.983
127.365
80.737
77.203
68.858
27.526
25.640
21.235
21.150
200
150
100
50
0
ppm (t1)

^{1}H NMR in $CDCl_3$

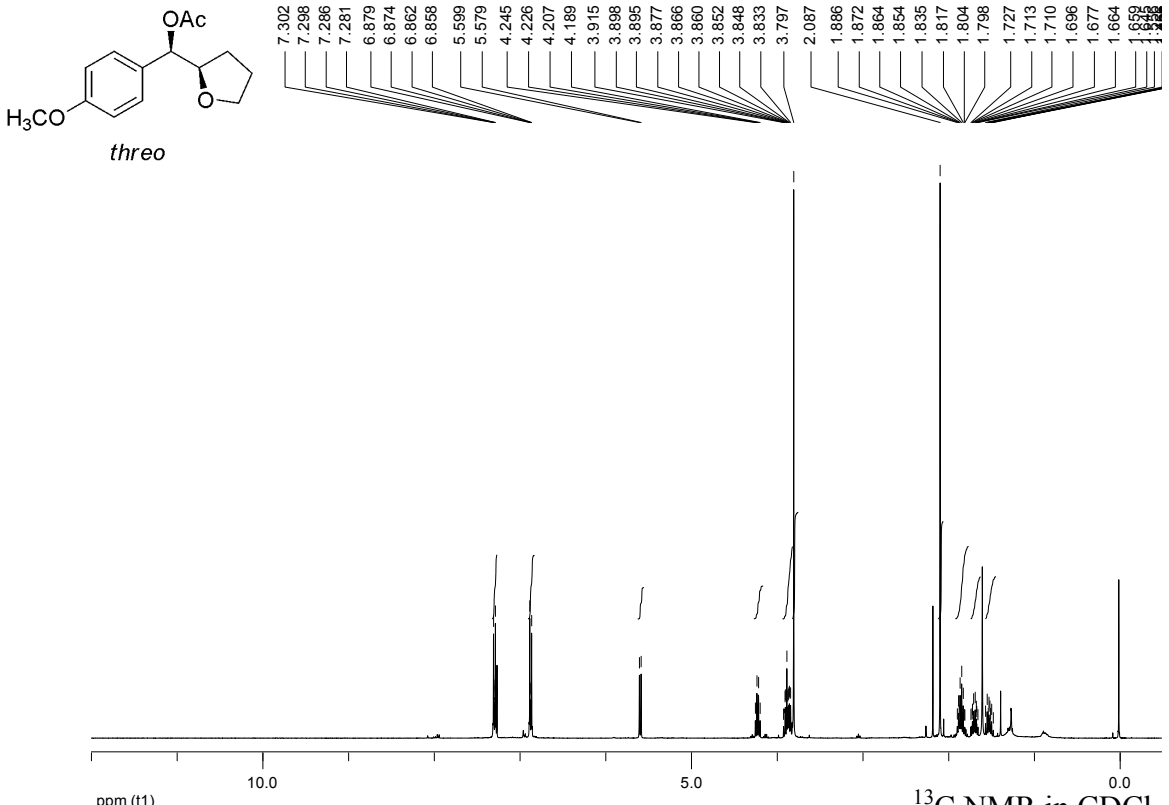

^{13}C NMR in $CDCl_3$

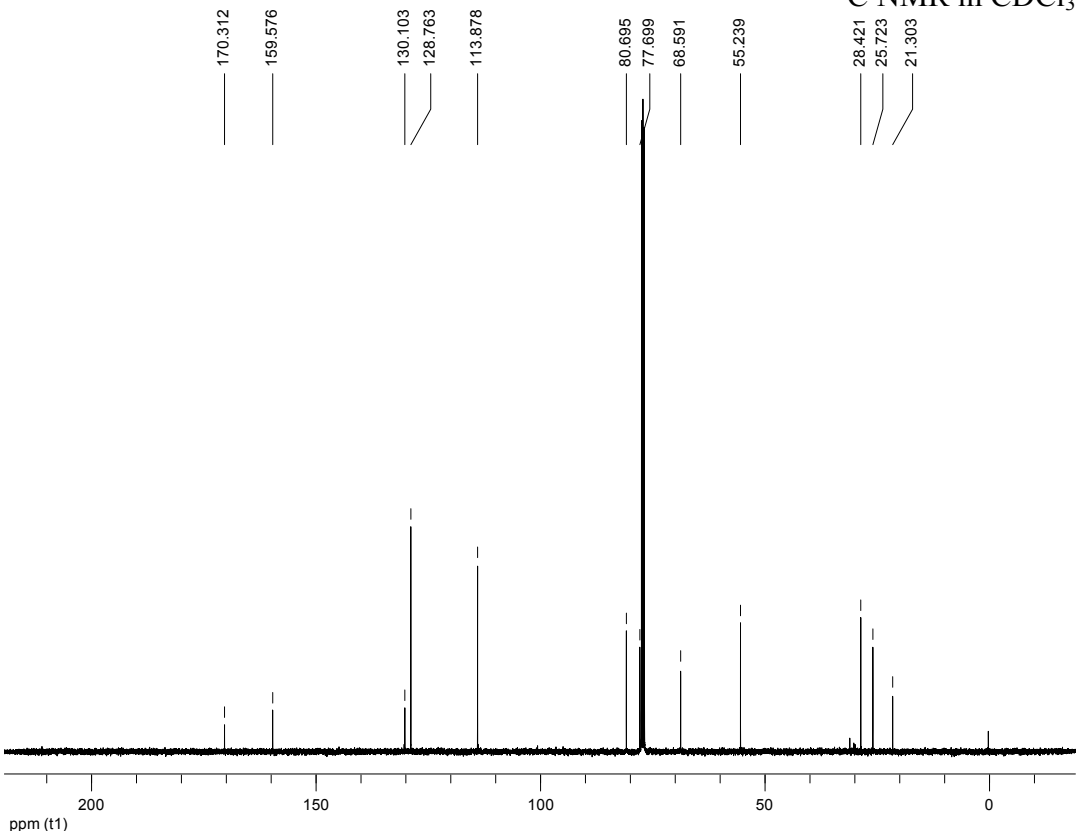

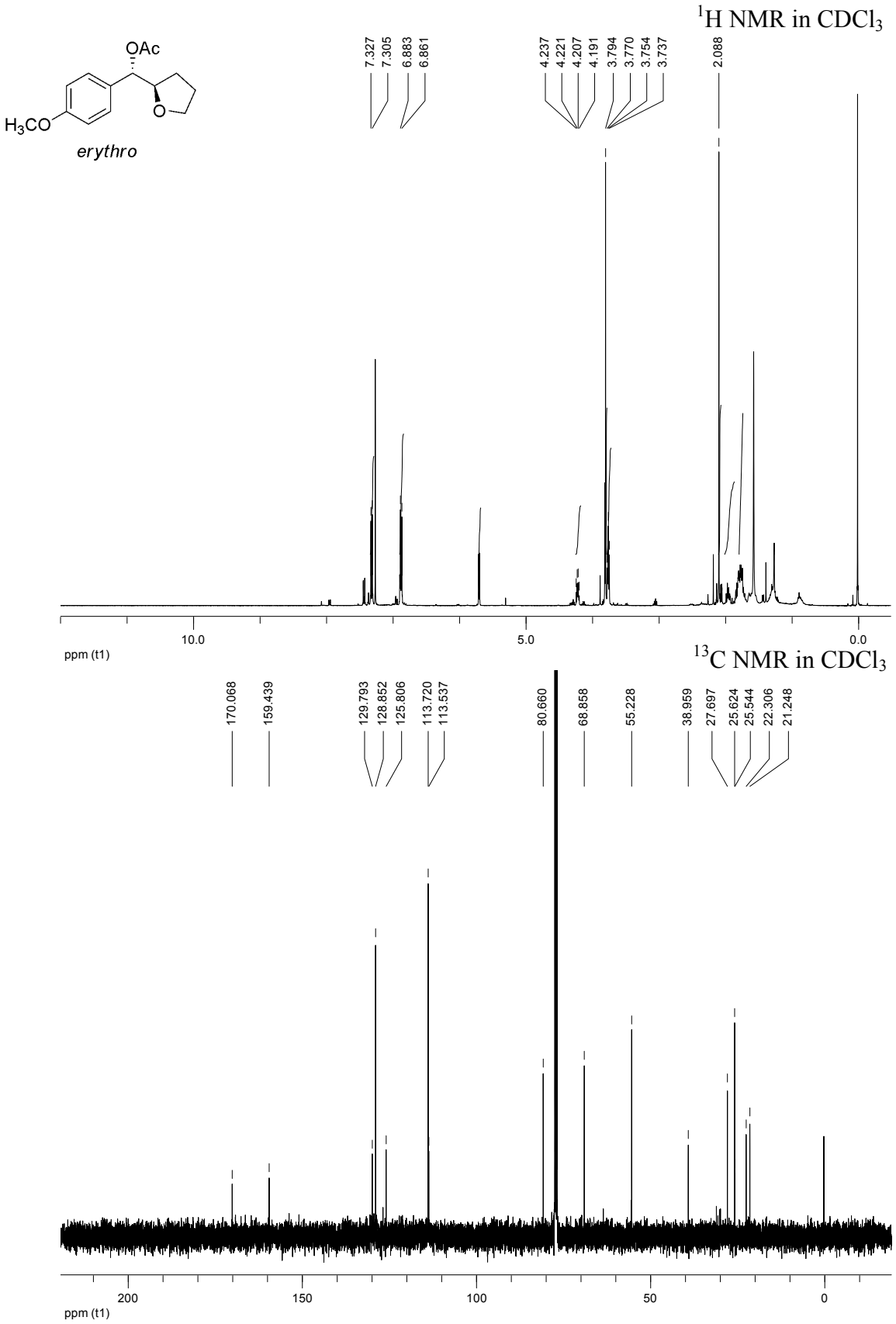
OAc
H3CO
O
erythro
1H NMR in CDCl3
7.327
7.305
6.883
6.861
4.237
4.221
4.207
4.191
3.794
3.770
3.754
3.737
2.088
10.0
5.0
0.0
ppm (t1)
13C NMR in CDCl3
170.068
159.439
129.793
128.852
125.806
113.720
113.537
80.660
68.858
55.228
38.959
27.697
25.624
25.544
22.306
21.248
200
150
100
50
0
ppm (t1)

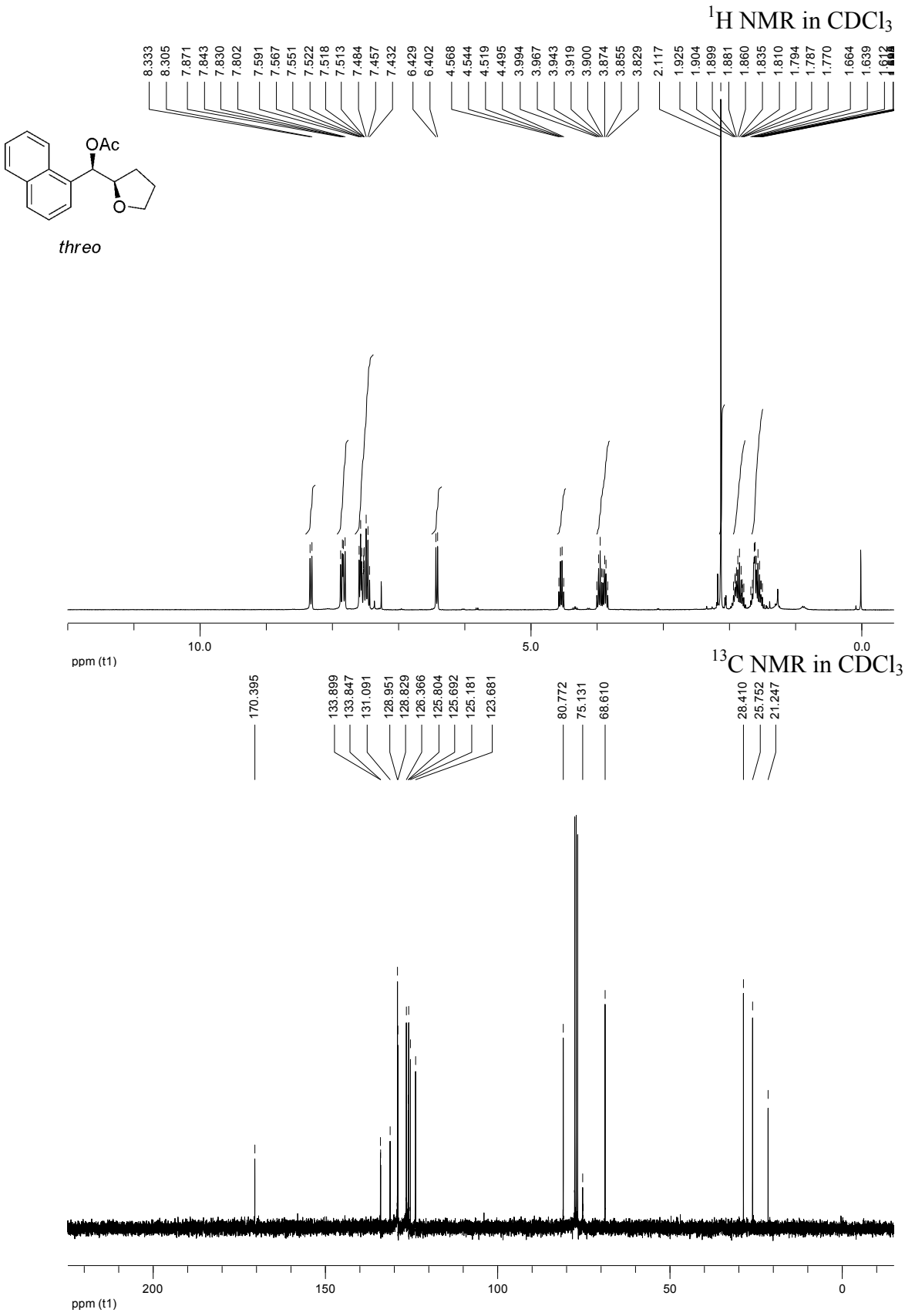
^{1}H NMR in $CDCl_3$
8.333
8.305
7.871
7.843
7.830
7.802
7.591
7.567
7.551
7.522
7.518
7.513
7.484
7.457
7.432
6.429
6.402
4.568
4.544
4.519
4.495
3.994
3.967
3.943
3.919
3.900
3.874
3.855
3.829
2.117
1.925
1.904
1.899
1.881
1.860
1.835
1.810
1.794
1.787
1.770
1.664
1.639
OAc
O
threo
10.0
5.0
0.0
ppm (t1)
^{13}C NMR in $CDCl_3$
170.395
133.899
133.847
131.091
128.951
128.829
126.366
125.804
125.692
125.181
123.681
80.772
75.131
68.610
28.410
25.752
21.247
200
150
100
50
0
ppm (t1)

^{1}H NMR in $CDCl_3$

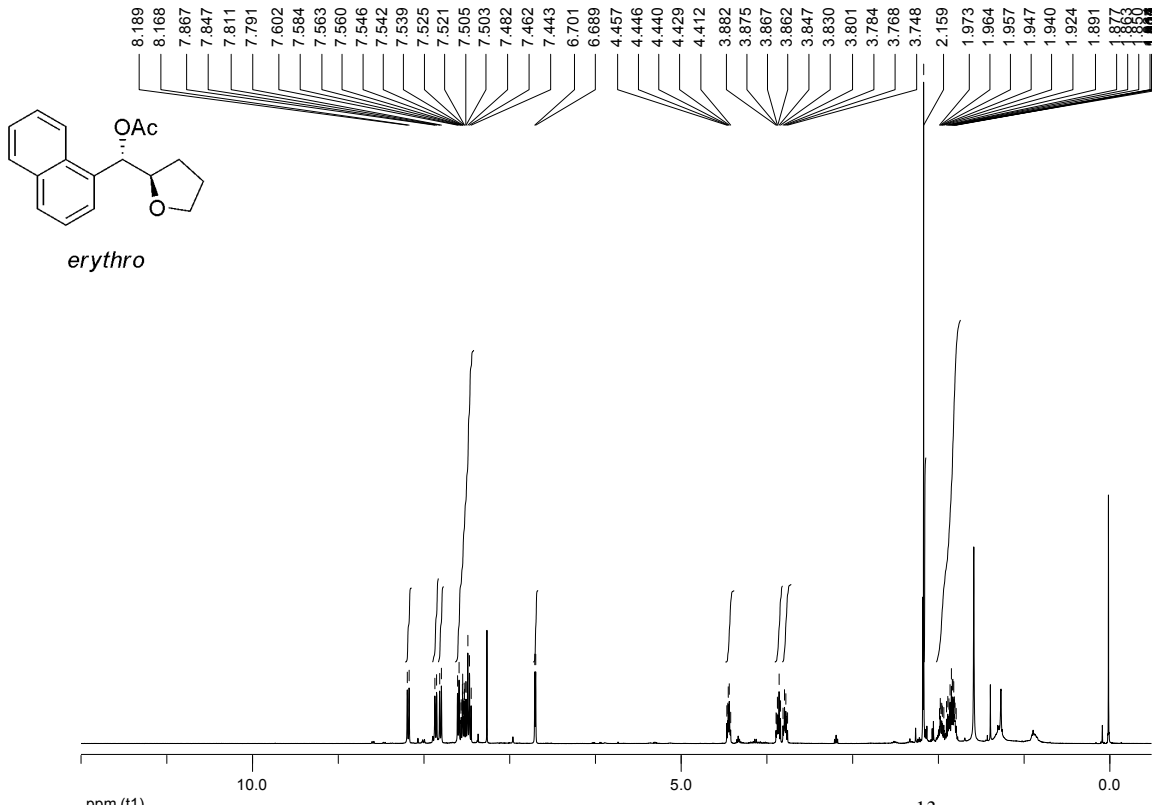

erythro

^{13}C NMR in $CDCl_3$

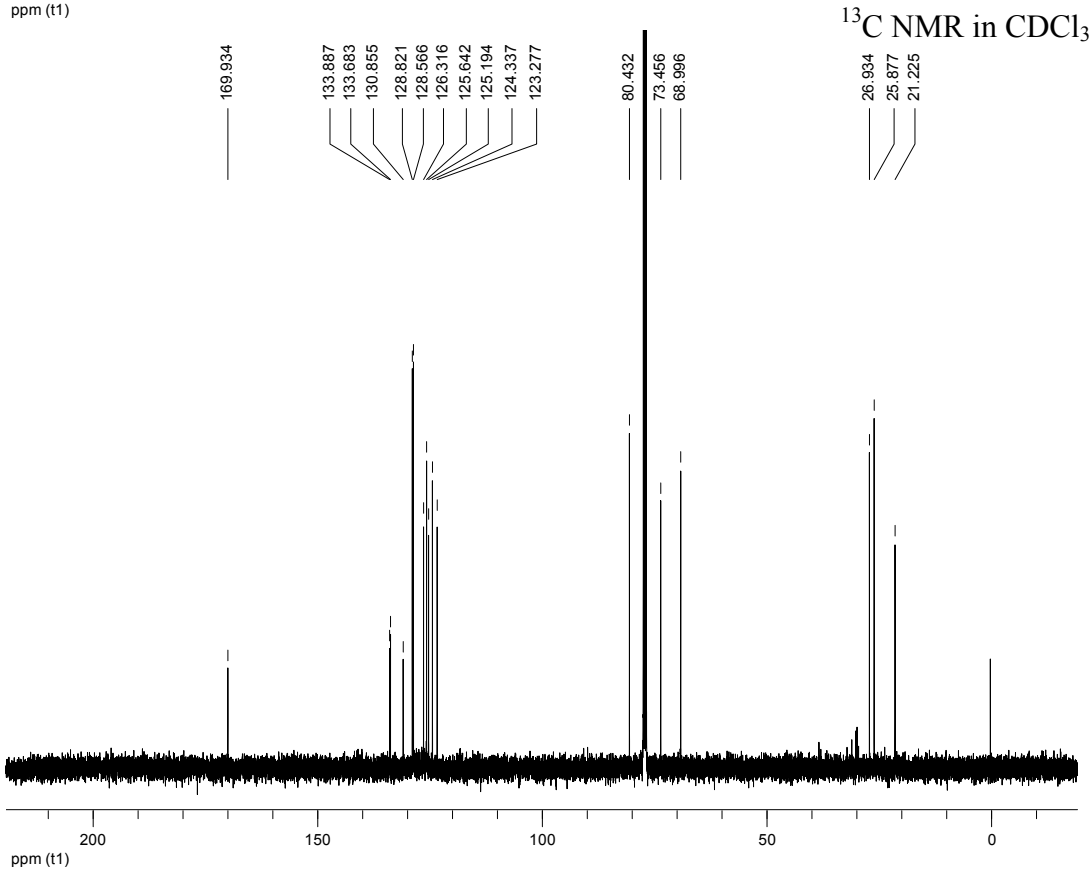

^{1}H NMR in $CDCl_3$

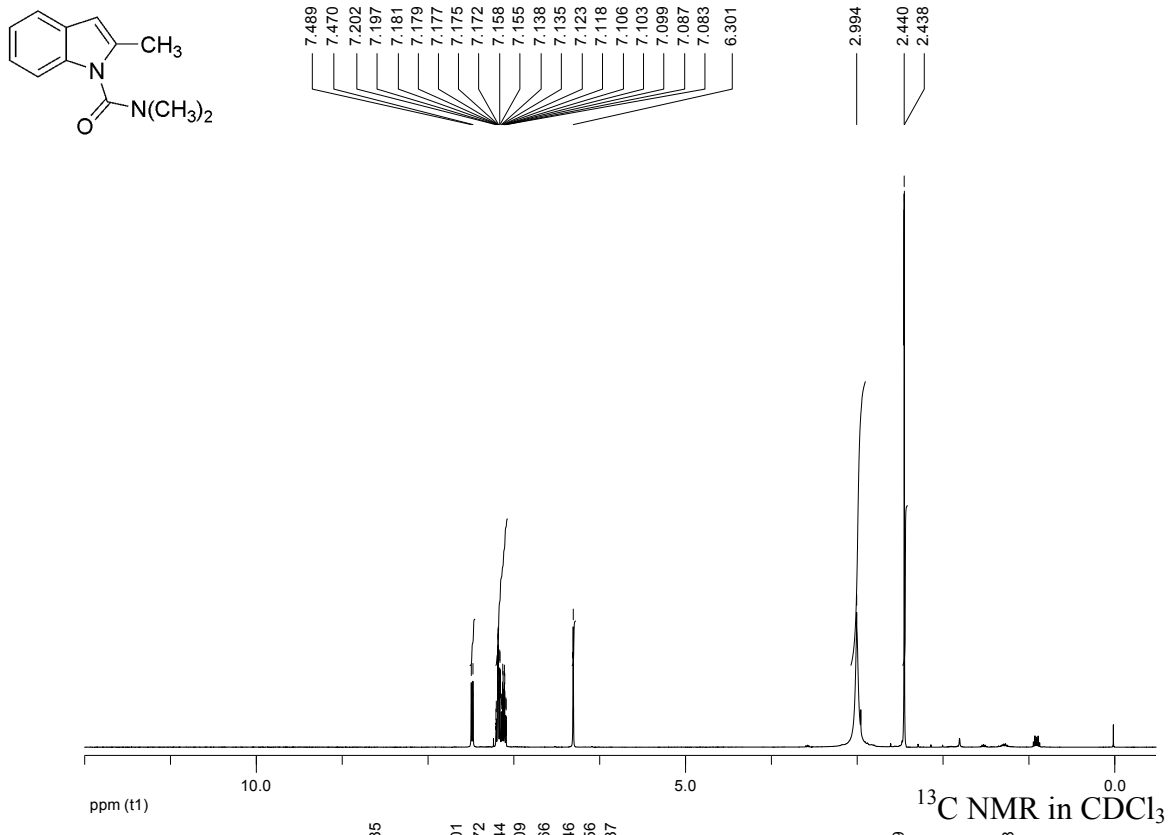

^{13}C NMR in $CDCl_3$

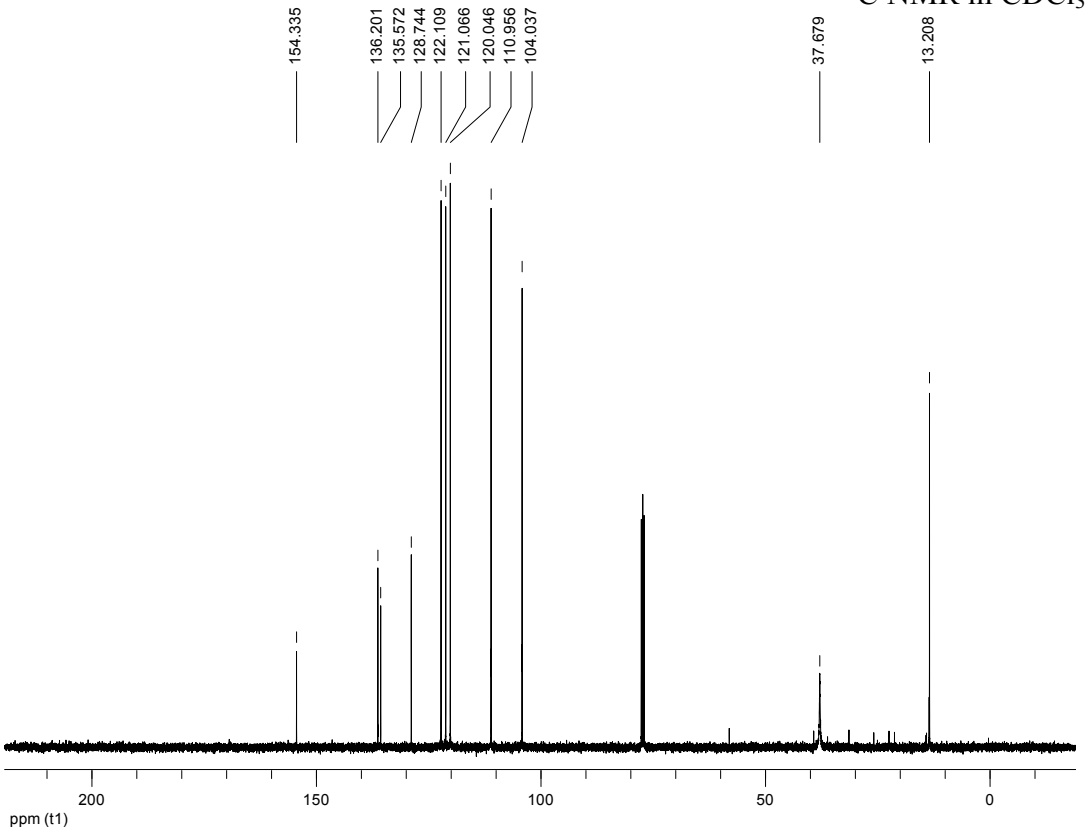

^{1}H NMR in $CDCl_3$

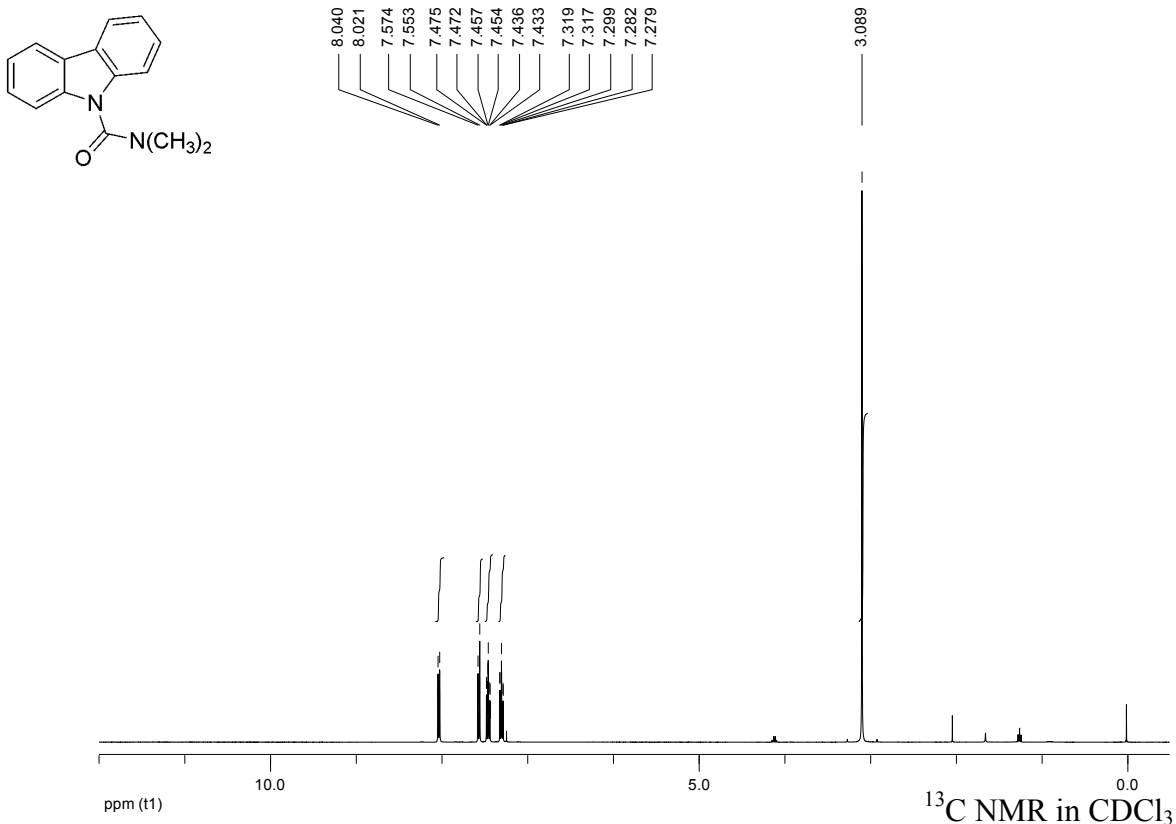

^{13}C NMR in $CDCl_3$

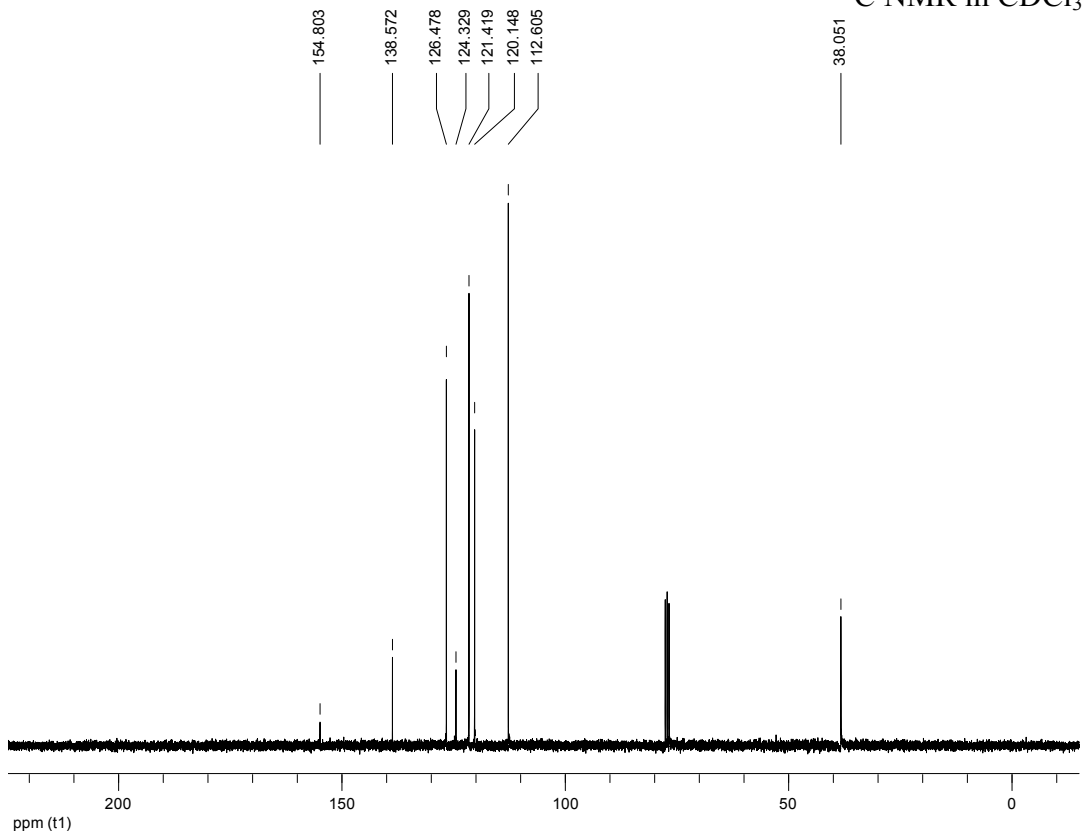

^{1}H NMR in $CDCl_3$

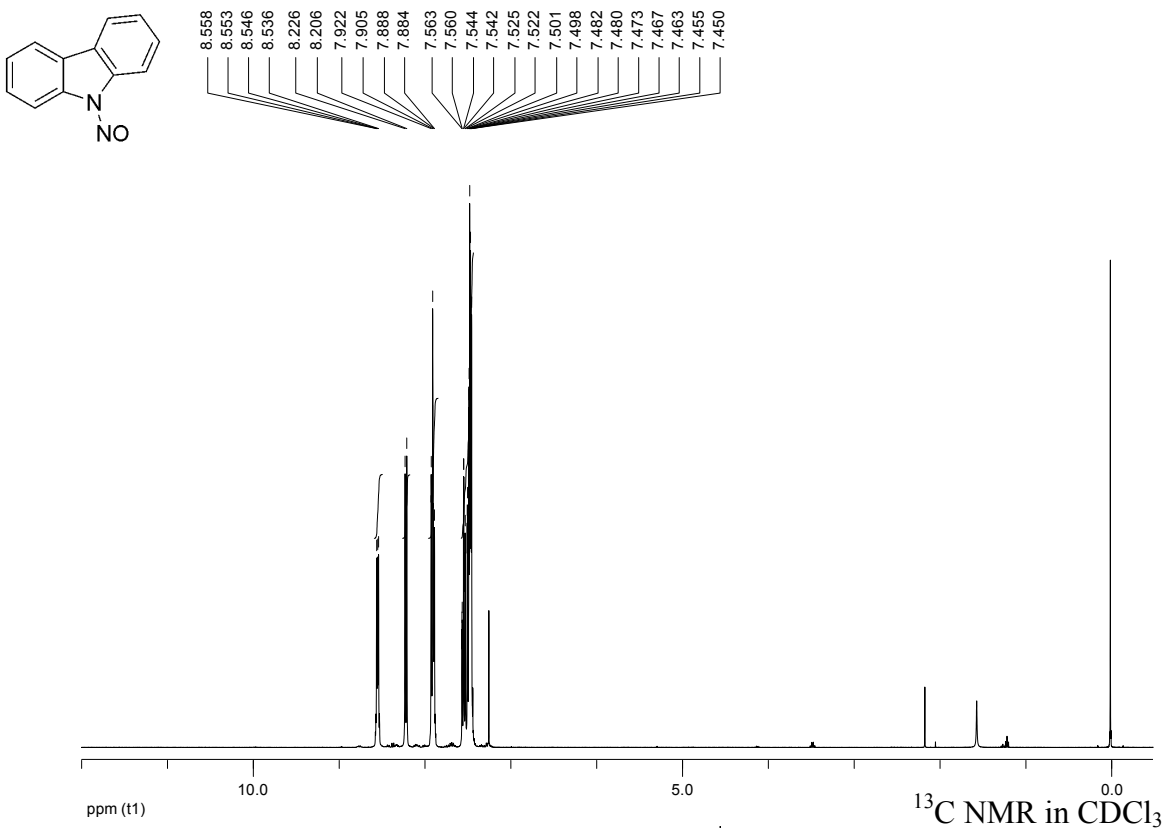

^{13}C NMR in $CDCl_3$

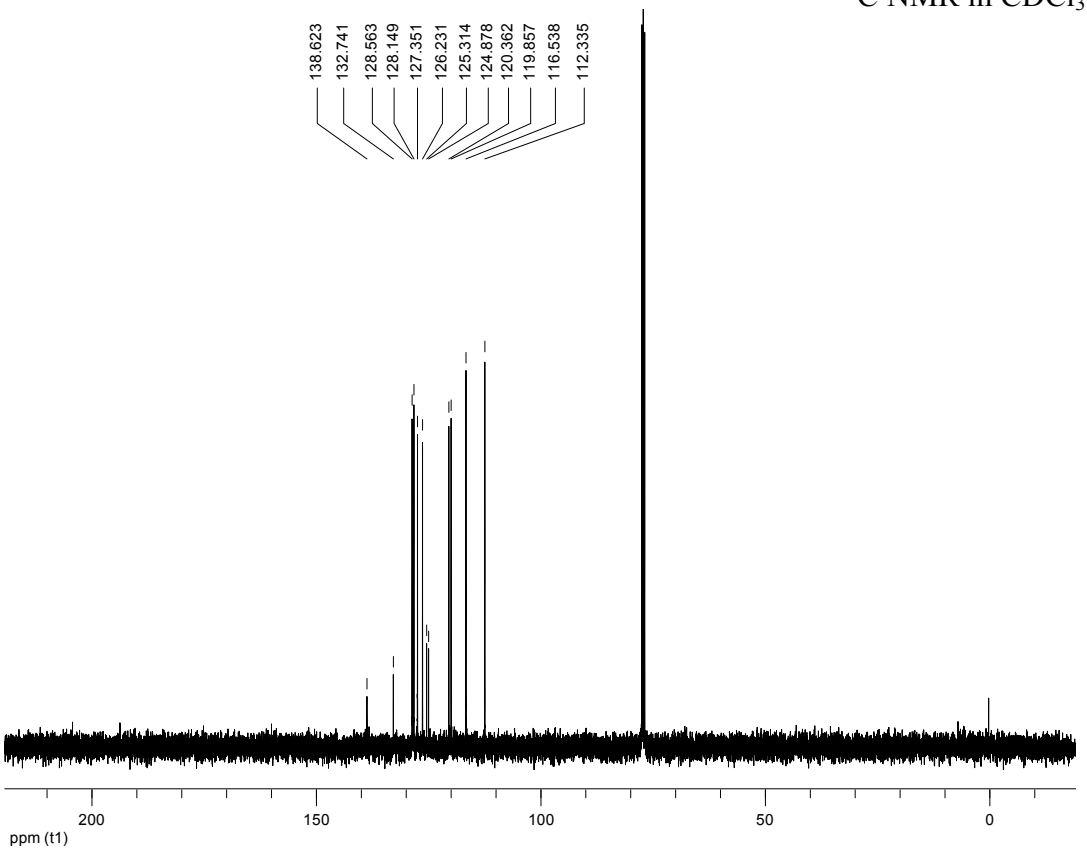

^{1}H NMR in $CDCl_3$

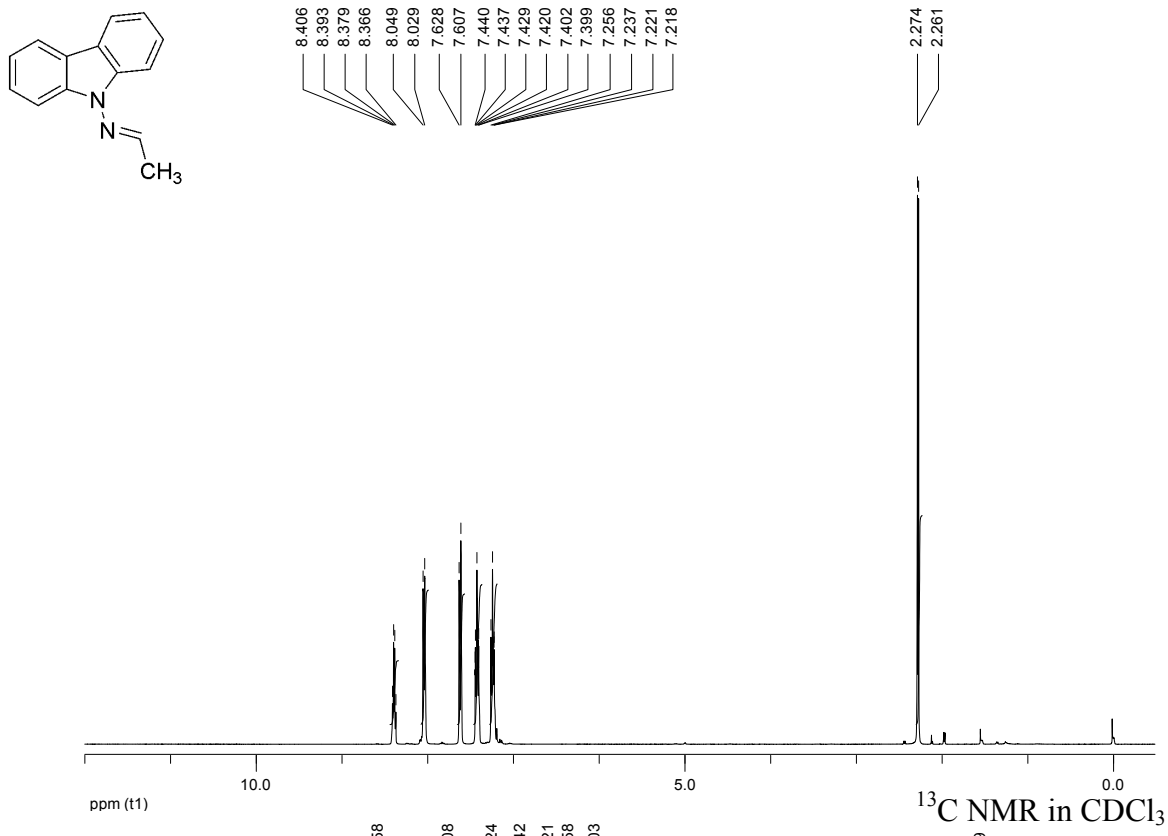

^{13}C NMR in $CDCl_3$

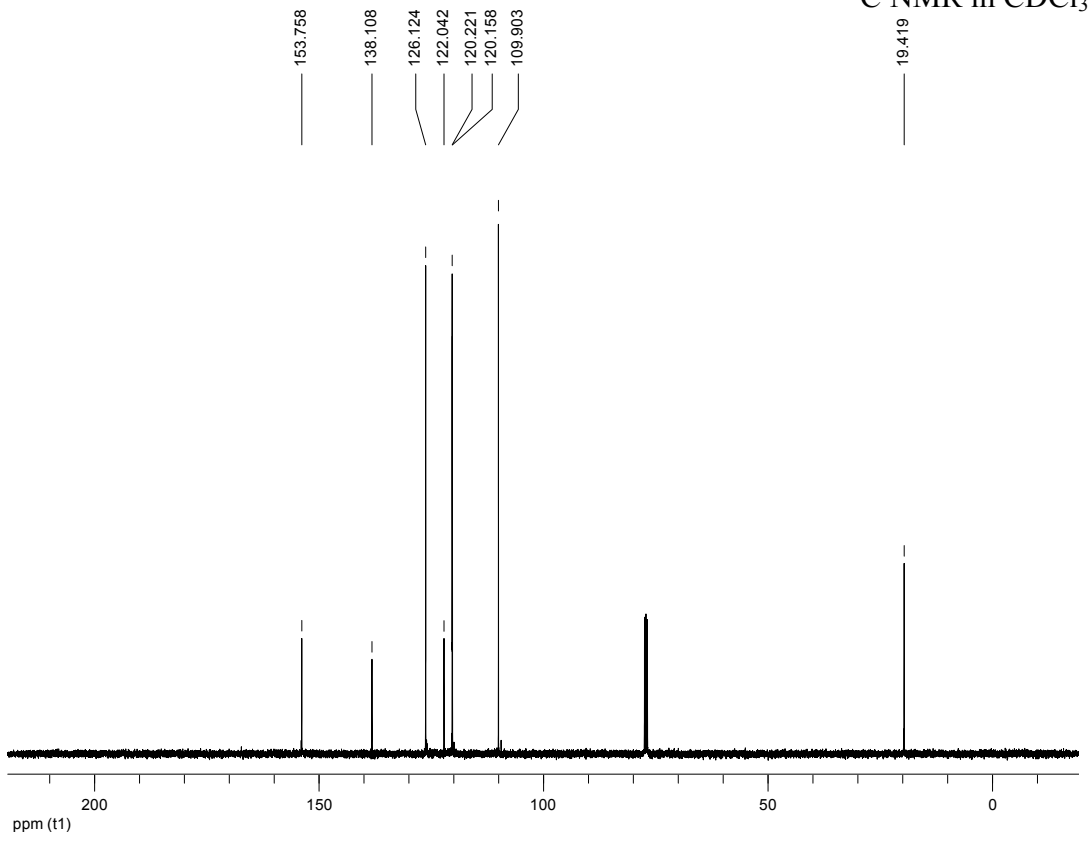

^{1}H NMR in $CDCl_3$

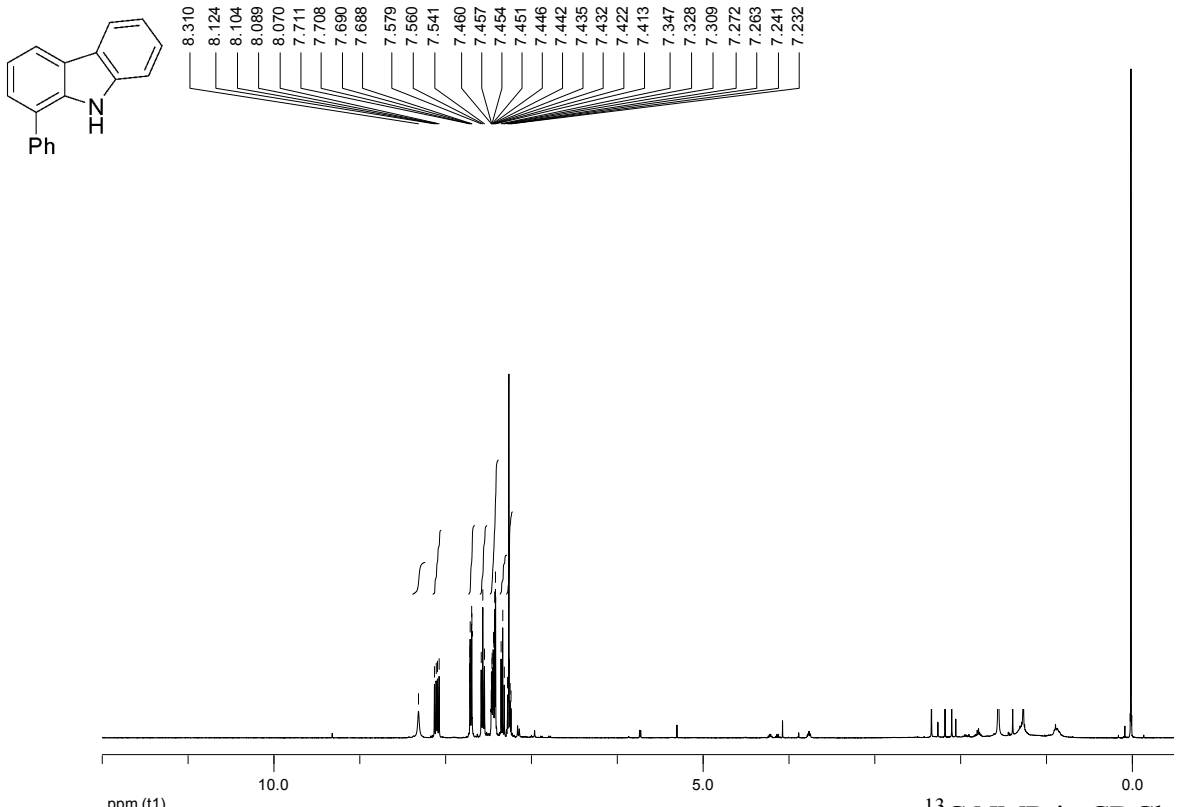

^{13}C NMR in $CDCl_3$

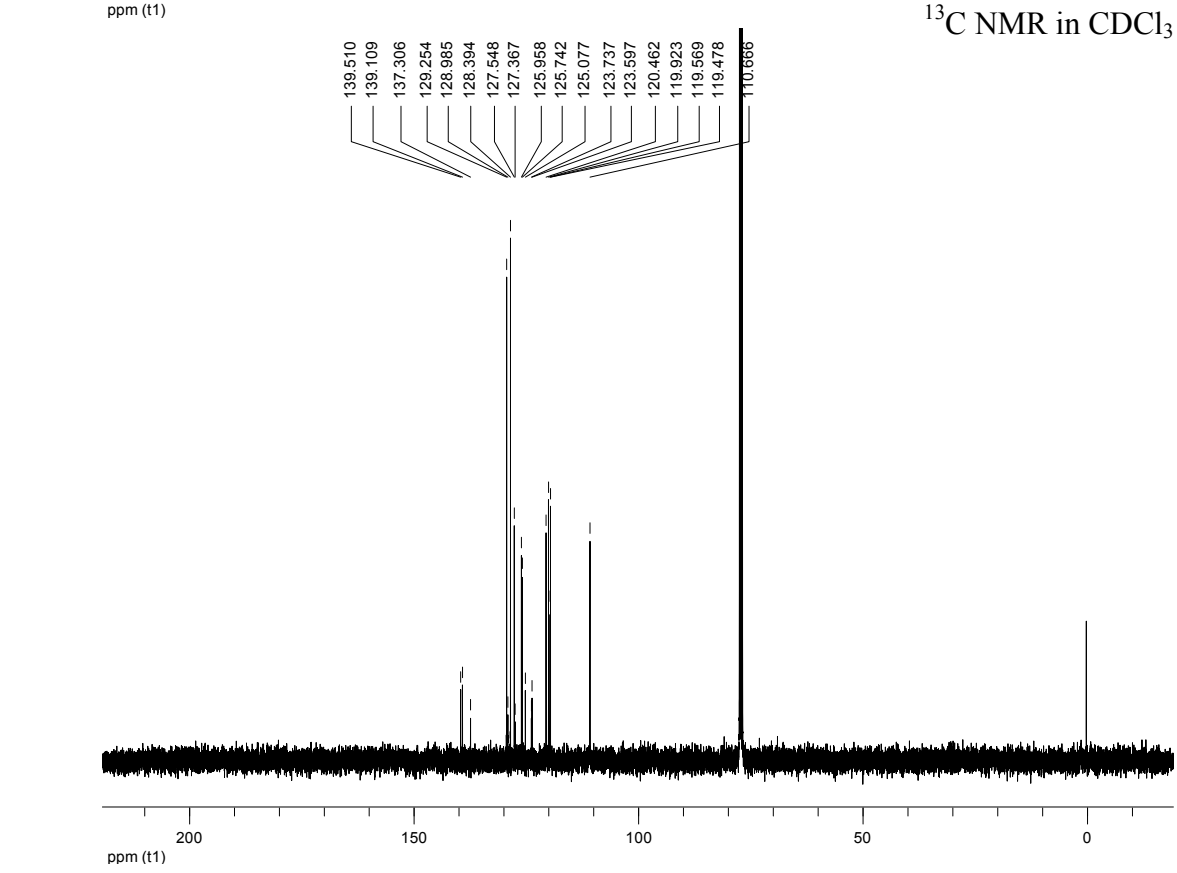

^{1}H NMR in $CDCl_3$

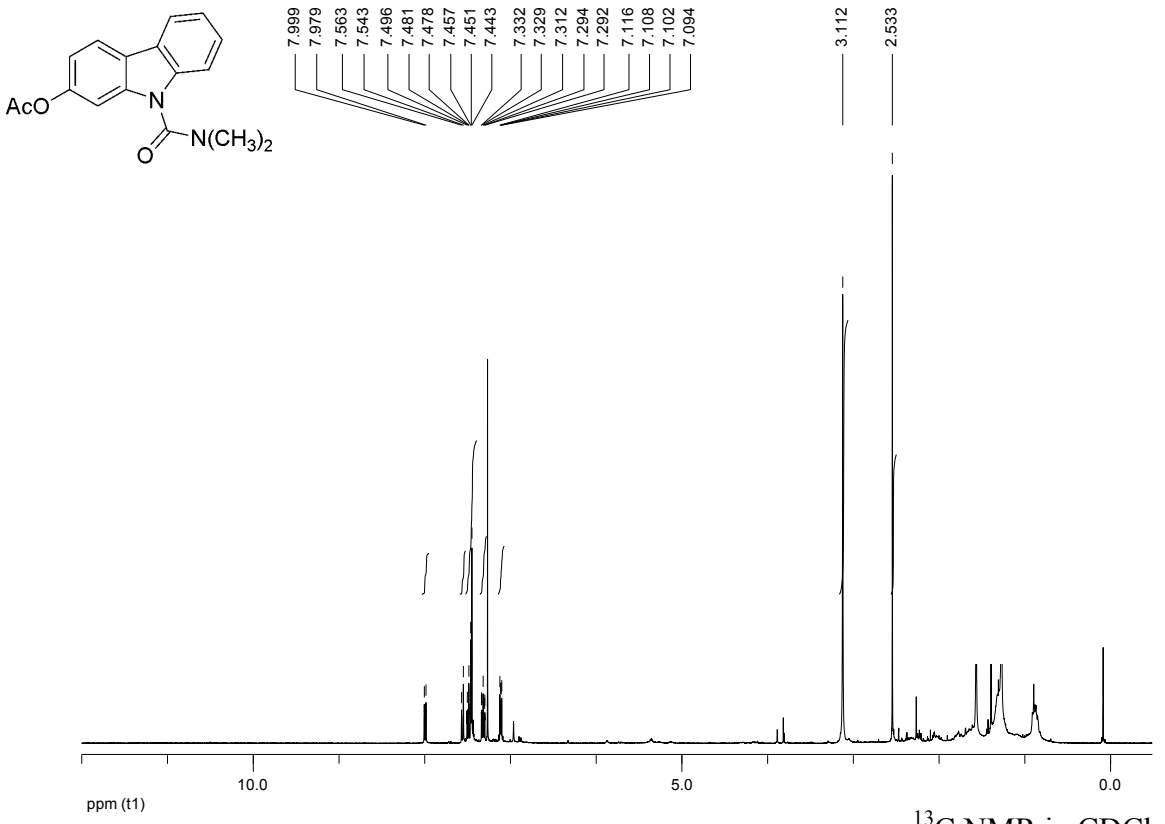

^{13}C NMR in $CDCl_3$

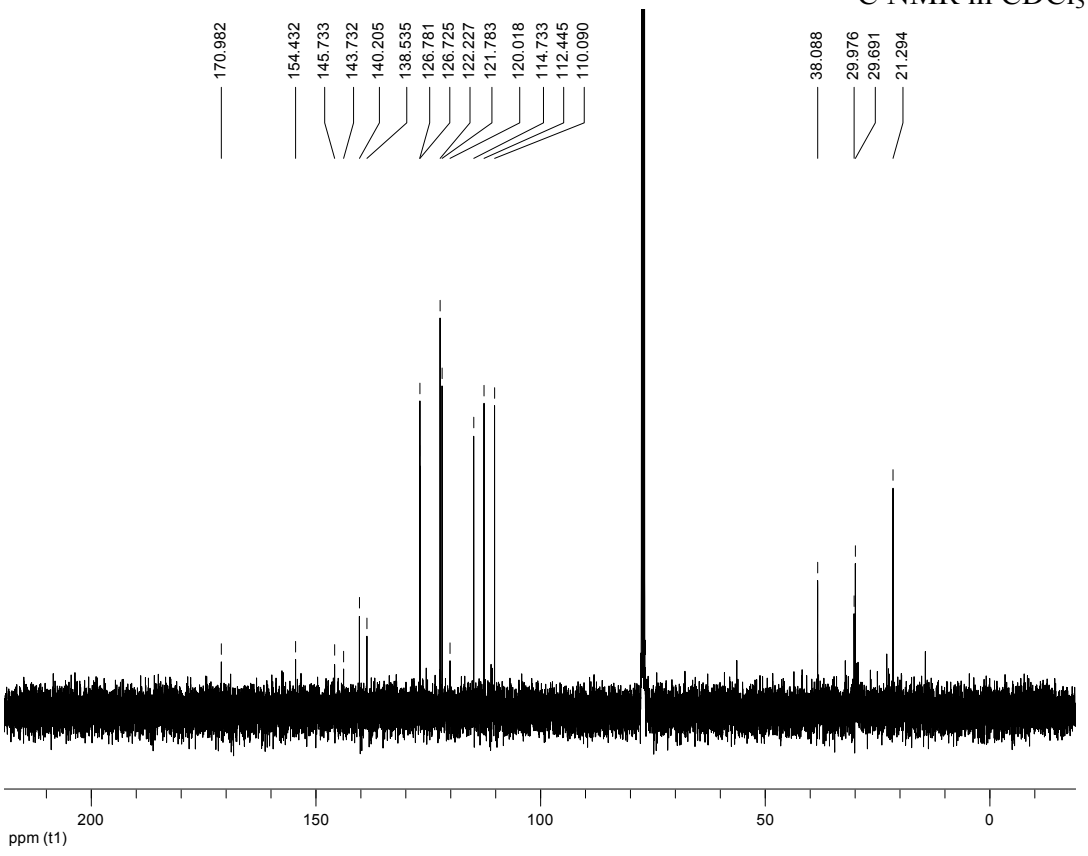

^{1}H NMR in $CDCl_3$

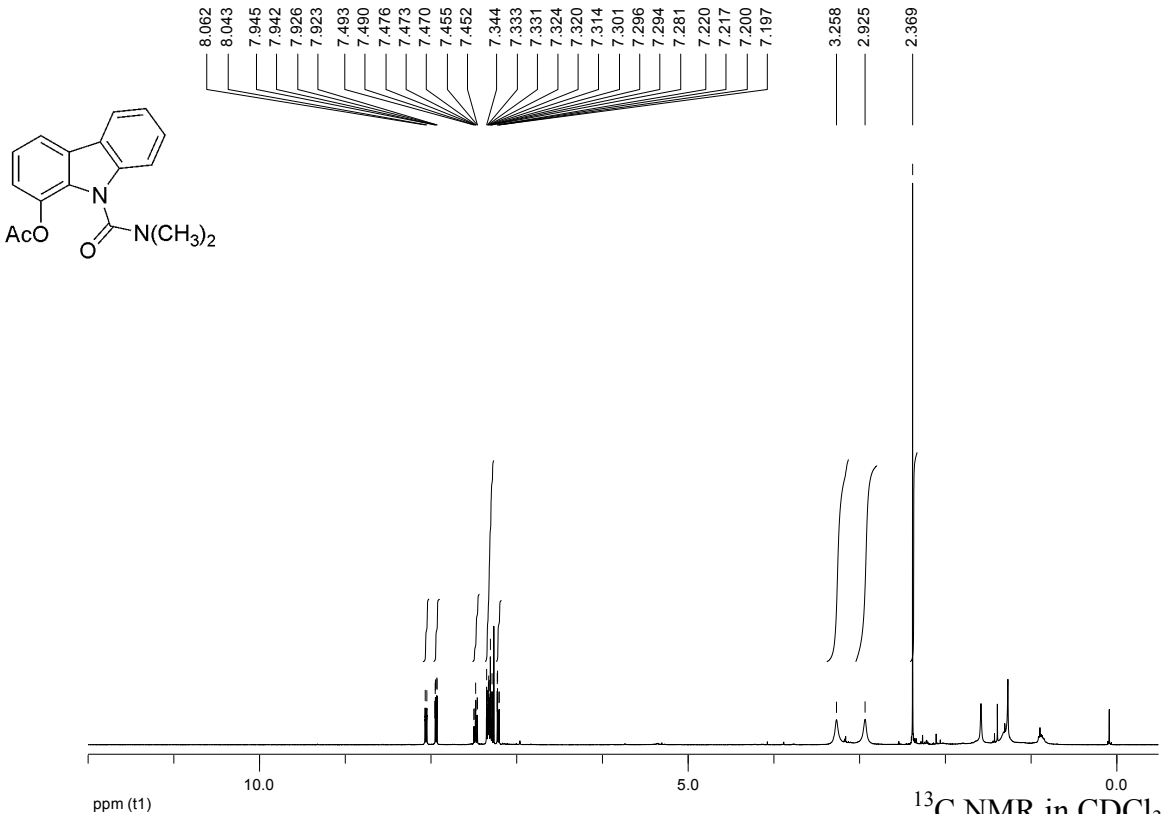

^{13}C NMR in $CDCl_3$

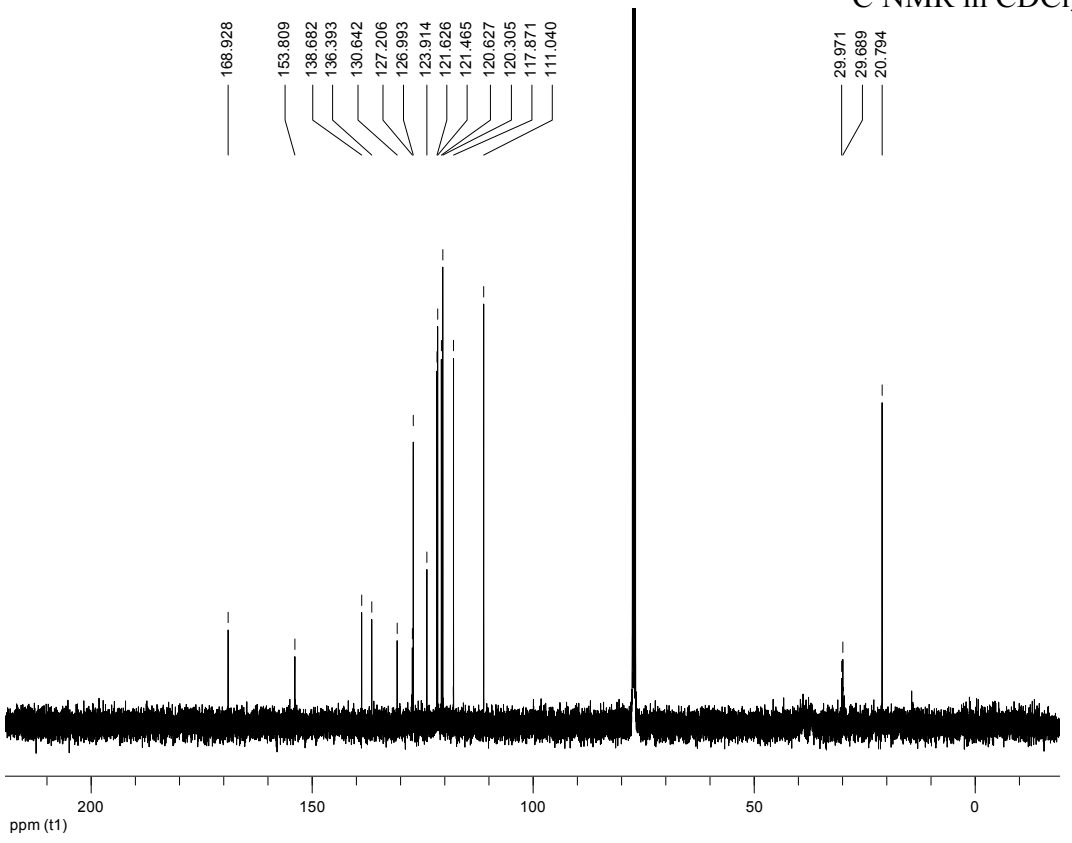

^{1}H NMR in $CDCl_3$

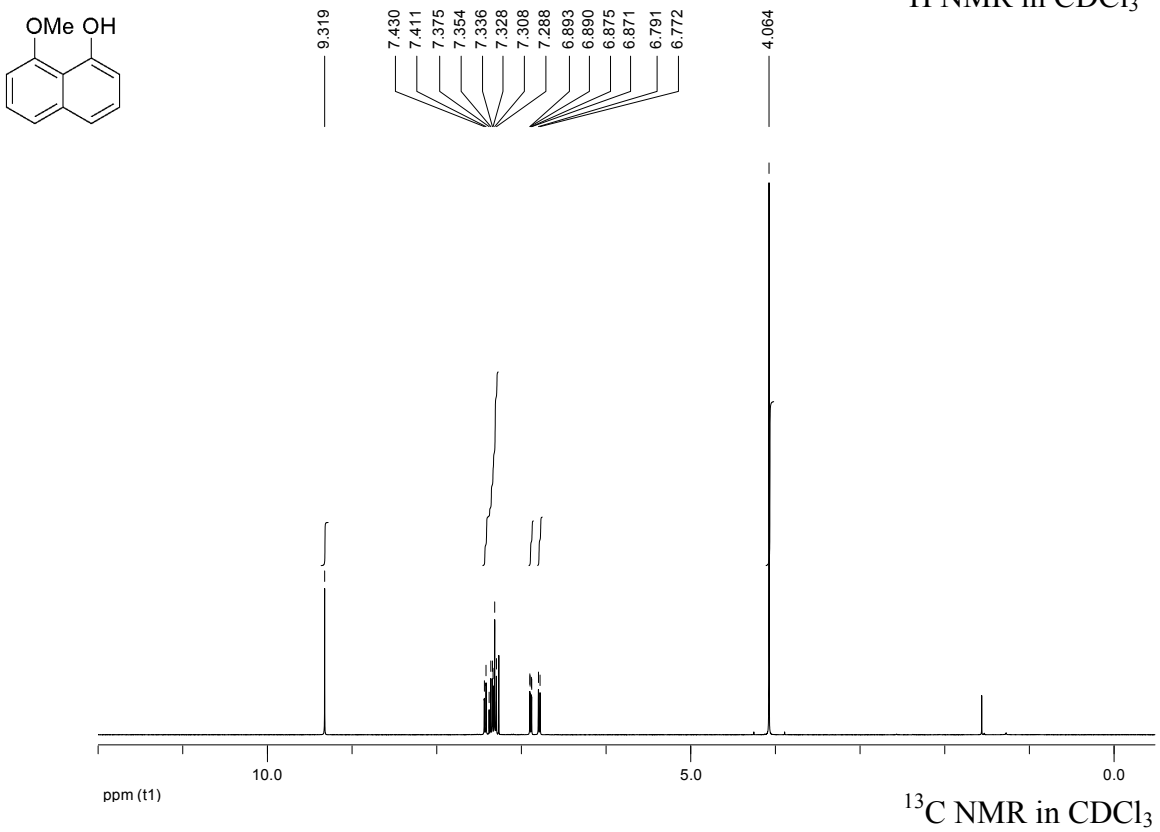

^{13}C NMR in $CDCl_3$

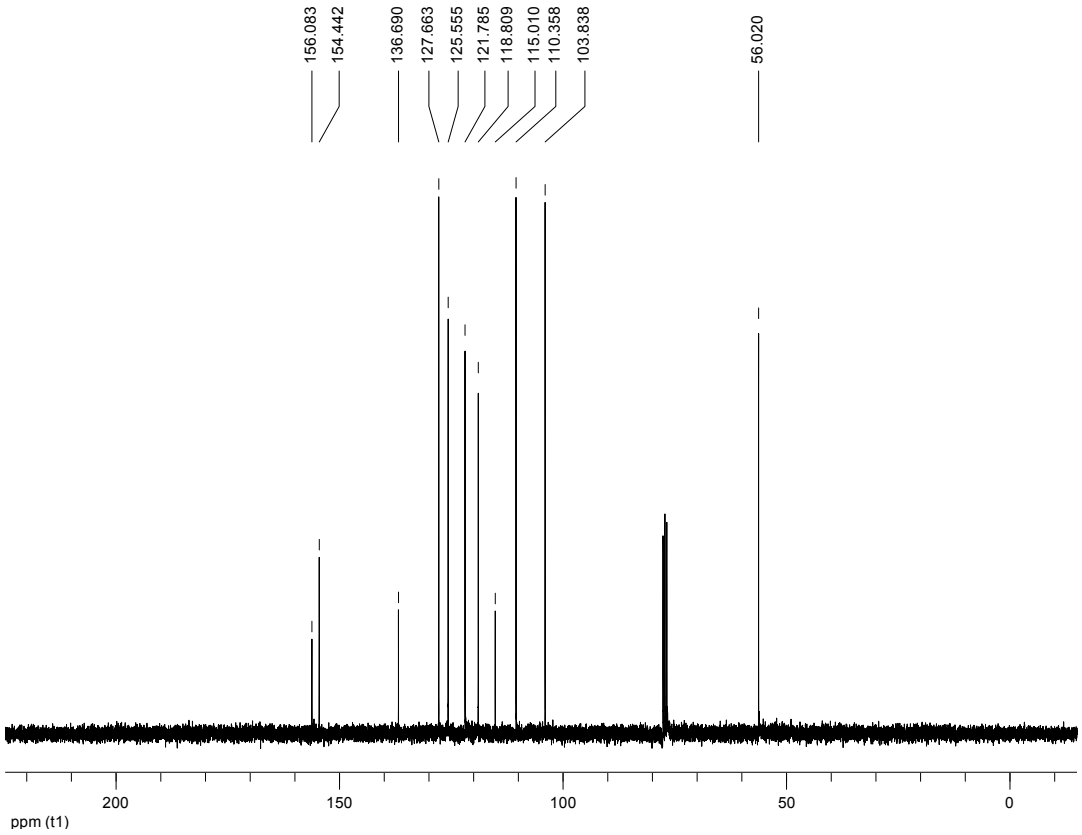

^{1}H NMR in $CDCl_3$

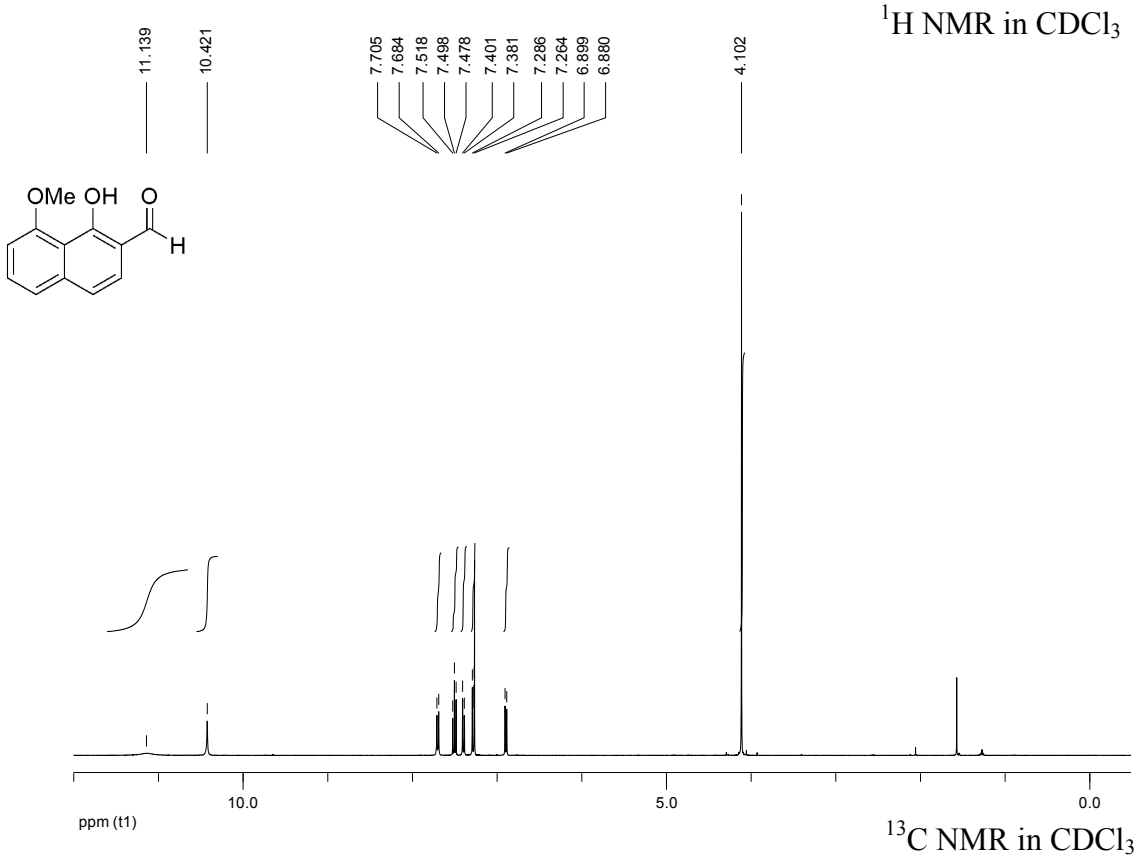

^{13}C NMR in $CDCl_3$

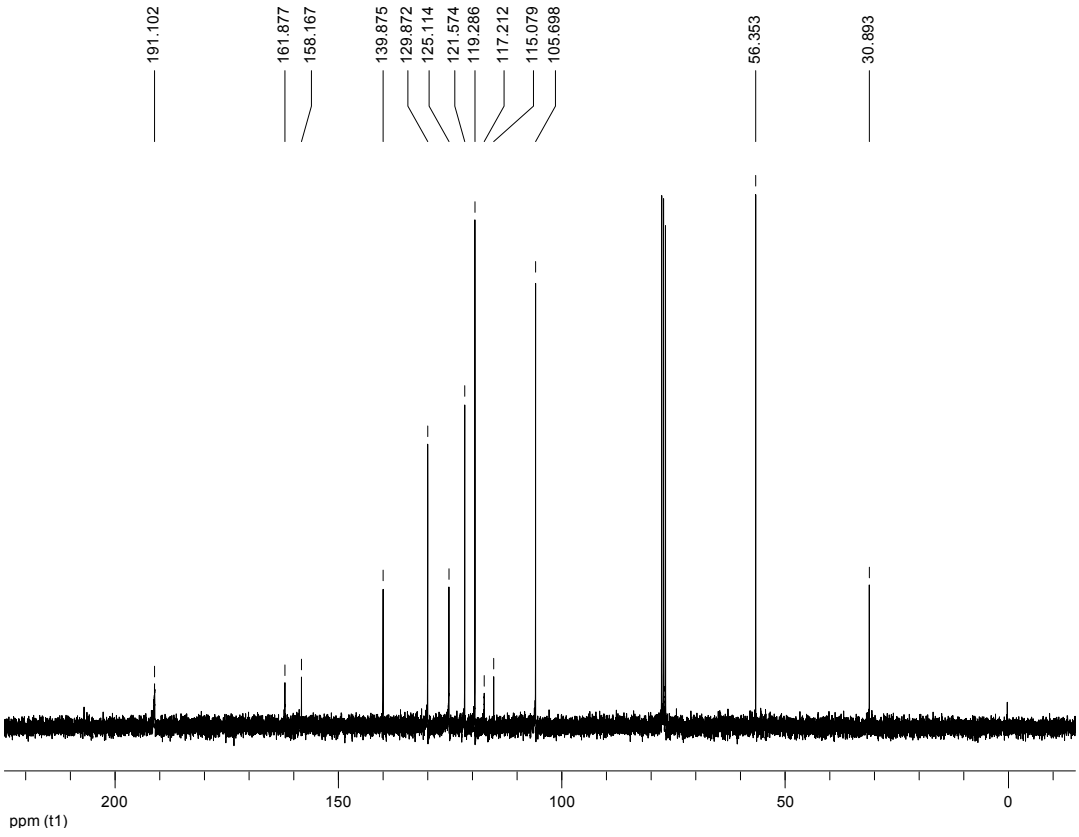

^{1}H NMR in $CDCl_3$

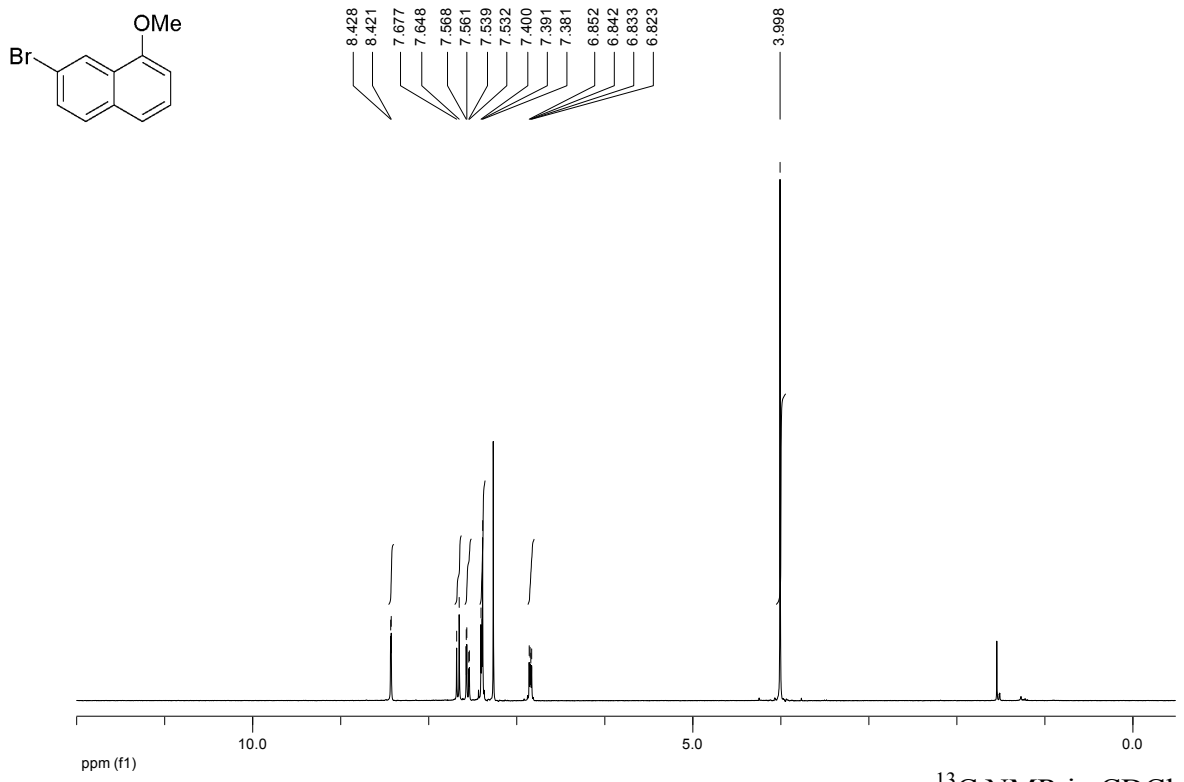

^{13}C NMR in $CDCl_3$

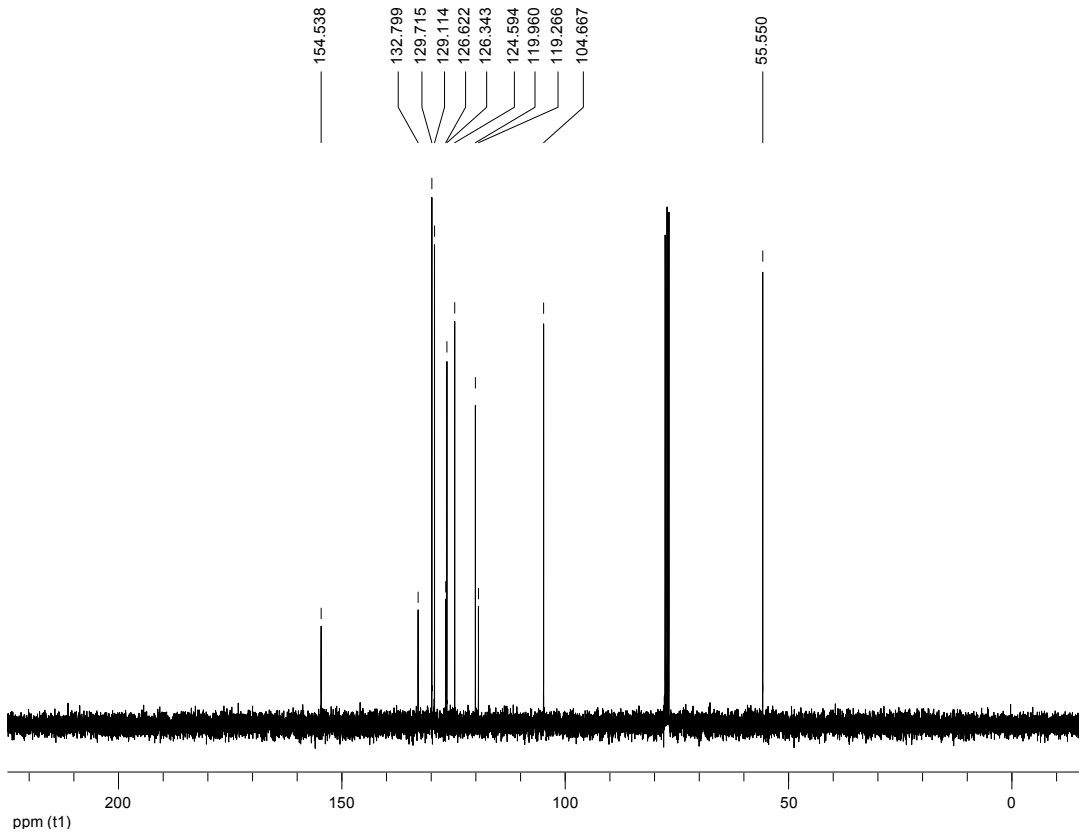

^{1}H NMR in $CDCl_3$

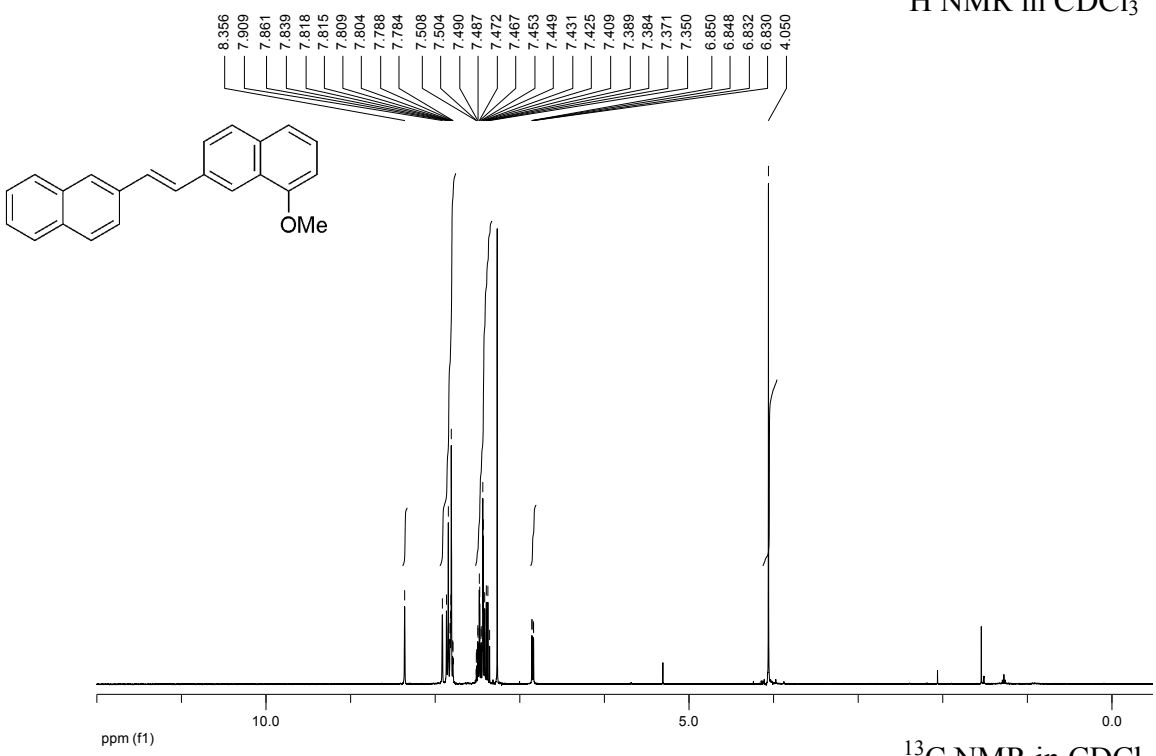

^{13}C NMR in $CDCl_3$